Osteological revision of the holotype of the Middle Jurassic sauropod dinosaur Patagosaurus fariasi (Sauropoda: Cetiosauridae) BONAPARTE 1979

Femke Holwerda, Oliver W.M. Rauhut, Pol Diego

Osteological revision of the holotype of the Middle Jurassic sauropod dinosaur *Patagosaurus fariasi* (Sauropoda: Cetiosauridae) BONAPARTE 1979

Femke M Holwerda[1234], Oliver W M Rauhut[156], Diego Pol[78]

1 Staatliche Naturwissenschaftliche Sammlungen Bayerns (SNSB), Bayerische Staatssamlung für Paläontologie und Geologie, Richard-Wagner-Strasse 10, 80333 München, Germany

2 Department of Geosciences, Utrecht University, Princetonlaan, 3584 CD Utrecht, 10 Netherlands

3 Royal Tyrrell Museum of Palaeontology, Drumheller, AlbertaT0J 0Y0, Canada (current)

4 Fachgruppe Paläoumwelt, GeoZentrum Nordbayern, Friedrich-Alexander-Universität Erlangen-Nürnberg, Loewenichstr. 28, 91054 Erlangen, Germany

5 Department für Umwelt- und Geowissenschaften, Ludwig-Maximilians-Universität München, Richard-Wagner-Str. 10, 80333 München, Germany

6 GeoBioCenter, Ludwig-Maximilians-Universität München, Richard-Wagner-Str. 10, 80333 16 München, Germany

7 Consejo Nacional de Investigaciones Científicas y Técnicas (CONICET), Argentina

8 Museo Paleontológico Egidio Feruglio, Avenida Fontana 140, Trelew, Argentina

ABSTRACT

Middle Jurassic sauropod taxa are poorly known, due to a stratigraphic bias of localities yielding body fossils. One such locality is Cerro Cóndor North, Cañadón Asfalto Formation, Patagonia, Argentina, dated to latest Early–Middle Jurassic. From this locality, the holotype of *Patagosaurus fariasi* Bonaparte 1986 is revised. The material consists of the axial skeleton, the pelvic girdle, and the right femur. *Patagosaurus* is mainly characterised by a combination of features mainly identified on the axial skeleton, including the following: (1) cervical centra with low Elongation Index, (2) high projection of the postzygodiapophyseal lamina, (3) deep anterior pleurocoels that are sometimes compartmentalized in cervicals, (4) high projection of the neural arch and spine in dorsal vertebrae and anterior(most) caudal vertebrae, (5) deep pneumatic foramina in posterior dorsals which connect into an internal pneumatic chamber, (6) anterior caudal vertebrae with 'saddle'shaped neural spines. Diagnostic features on the appendicular skeleton include (7) a transversely wide and anteroposteriorly short femur, (8) a medial placement of the fourth trochanter on the femur, and (9) an anteroposteriorly elongated ilium with a rounded dorsal rim, with hook-shaped anterior lobe. The characters that are diagnostic for *Patagosaurus* are discussed, and the osteology of *Patagosaurus* is compared to that of Early and Middle Jurassic (eu)sauropods from both Laurasia and Gondwana.

Keywords: Sauropoda, Eusauropoda, *Patagosaurus,* Gondwana, Middle Jurassic, pneumaticity

INTRODUCTION

The late Early to Middle Jurassic is an important time window for sauropod evolution, as phylogenetic studies indicate this was the time when most major lineages diversified and spread worldwide. Even though the Late Jurassic shows a diversity peak, the earlier stages of the Jurassic (or perhaps even the latest Triassic) seem to have been the time of the start of

this rise in sauropods (Yates 2003; Barrett & Upchurch2005; Irmis *et al.* 2007; Allain & Aquesbi 2008; Mannion & Upchurch 2010; Yates *et al.* 2010; McPhee *et al.* 2014, 2015, 2016; Xu et al. 2018). Not many terrestrial deposits remain from the specific time window that is the Early - Middle Jurassic, and fewer still contain diagnostic basal sauropod or basal non-neosauropod eusauropod material.

Notable Early Jurassic examples are *Isanosaurus attavipachi* from Thailand Buffetaut et al., 2002, (Laoyumpon et al. 2017); *Sanpasaurus yaoi* McPhee et al., 2016 from China; *Barapasaurus tagorei* Jain et al., 1975*, Kotasaurus yamanpalliensis* Yadagiri, 1988 from India, (Yadagiri 2001; Bandyopadhyay et al. 2010); and indeterminate non-neosauropodan material from Morocco (Nicholl et al. 2018); *Vulcanodon karibaensis* Raath, 1972 from Zimbabwe (Cooper 1984); and the Elliot Formation ?sauropodiform/sauropodomorph fauna from South Africa and Lesotho (McPhee et al. 2017).

Notable Middle Jurassic examples are the cetiosaurs from the UK, e.g. *Cetiosaurus oxoniensis* Phillips, 1871, the Rutland *Cetiosaurus* and cetiosaurid and gravisaurian material from England, Scotland and Germany (von Huene 1927; Upchurch and Martin 2002, 2003; Liston 2004; Galton 2005; Barrett 2006; Buffetaut et al. 2011; Brusatte et al. 2015; Stumpf et al. 2015; Clark and Gavin 2016; Holwerda et al. 2019); *Datousaurus bashanensis* Dong & Tang 1984, *Nebulasaurus taito* Xing et al., 2015*, Lingwulong shenqi* Xu et al., 2018, and the mamenchisaur fauna from China (Young and Zhao 1972; Russell and Zheng 1993; Pi et al. 1996; Moore et al. 2018; Wang et al. 2018); *Tazoudasaurus naimi* Allain et al., 2004*, Spinophorosaurus nigerensis* Remes et al., 2009 and *Chebsaurus algeriensis* Mahammed et al., 2005 from North Africa (Allain and Aquesbi 2008); indeterminate non-neosauropodan material and *Lapparentosaurus madagascariensis* Bonaparte 1986a from Madagascar (Läng 2008; Mannion 2010), and finally, *Patagosaurus fariasi* Bonaparte, 1979, *Volkheimeria*

chubutensis Bonaparte 1979 and *Amygdalodon patagonicus* Cabrera, 1947 (Bonaparte 1986b; Rauhut 2003) from Argentina.

Some sauropods that were traditionally considered to be Middle Jurassic might originate from the Late Jurassic; (*Rhoetosaurus brownei* Longman, 1926 from Australia (Nair and Salisbury 2012; Todd et al. 2019), *Shunosaurus lii* Dong et al., 1983 and *Omeisaurus junghsiensis* Young, 1939 from China (He et al. 1984, 1988; Zhang 1988; Tang et al. 2001; Chatterjee and Zheng 2002; Peng et al. 2005; and see Wang et al. 2018 for refined ages). For a short overview of some of these Early and Middle Jurassic sauropods, see Holwerda and Pol (2018).

In Patagonia, Argentina, the Cañadón Asfalto Formation (Stipanicic et al. 1968; Tasch and Volkheimer 1970), is one of the few geological units worldwide to contain several latest Early to early Middle Jurassic eusauropod fossils. It crops out in west-central Patagonia, Argentina, and has recently been dated as ranging from the Toarcian to the Aalenien/Bajocian (Cúneo et al. 2013). The sauropod fauna of this unit includes *Patagosaurus fariasi*, *Volkheimeria chubutensis* (Bonaparte 1979), and at least two undescribed taxa (Rauhut 2002, 2003; Pol et al. 2009; Holwerda et al. 2015; Becerra et al. 2016; Carballido et al. 2017a).

Patagonia first came under the attention of vertebrate palaeontologists by the discovery of the basal sauropod *Amygdalodon patagonicus* by Cabrera (1947), and later by Casamiquela (1963) from the Pampa de Agnia locality, Cerro Carnerero Formation (Rauhut 2003a). These beds were revisited in 1976, but no further discovery was made, until another excursion in Patagonia, about 50 Km further away in the Cañadón Asfalto Formation, in 1977, was successful. José Bonaparte led numerous additional expeditions to the region between 1977 and 1986, during which *Patagosaurus fariasi*, *Volkheimeria chubutensis* and the theropod *Piatnitzkysaurus floresi* Bonaparte, 1979 were found and described (Bonaparte 1979, 1986b,

1996; Rauhut 2004). Since then, numerous other dinosaurs and other vertebrates have been discovered in the Cañadón Asfalto Formation; see Escapa et al. (2008), Cuneo et al (2013) and Olivera et al. (2015). The MPEF in Trelew has more recently visited the locality of Cerro Cóndor South to uncover more material, of which only one element has been described (Rauhut 2003b).

Thus far*, Patagosaurus* is the only well-known sauropod taxon from this area, and one of the few sauropods from the Middle Jurassic outside of China, known from abundant material. It was coined by Bonaparte in 1979; *Patagosaurus* for Patagonia, and *fariasi* to honour the owners of the Farias farmland, on which it was discovered. It has been included in numerous phylogenetic studies (e.g. Upchurch 1998; Wilson 2002; Upchurch et al. 2004; Harris 2006; Allain and Aquesbi 2008; Wilson and Upchurch 2009; Carballido et al. 2011, 2012; Holwerda and Pol 2018). However, the only description of this taxon published so far (Bonaparte, 1986b) is not only based on the holotype, but also draws information from a selection of associated material, representing several individuals from different localitites, therefore not guaranteeing these are all *Patagosaurus* individuals. Some of the associated material comes partially from the same bonebed as the holotype, but others come from a nearby bonebed (Bonaparte 1979; Bonaparte 1986a). Since this description, new sauropod finds from the Cañadón Asfalto Formation show a higher sauropod diversity for this unit than previously assumed (Pol et al. 2009). Furthermore, recent studies of *Patagosaurus* material revealed the probable presence of another taxon in the associated material (Rauhut 2002; Rauhut 2003). In light of this, a revision of *Patagosaurus* is needed.

MATERIAL AND METHODS

ANATOMICAL ABBREVIATIONS

Terminology: Wilson (1999) is followed for the terminology of vertebral laminae, with some modifications based on Carballido and Sander (2014). The terminology of vertebral fossae follows Wilson *et al.* (2011).

As was already pointed out by Wedel (2003) and Carballido and Sander (2014), the term pleurocoel has not been rigourously defined. The term, however, was used in that paper for a lateral excavation on the vertebral centrum with clearly defined anterior, ventral and dorsal margins, and a usually less clearly defined but still visible posterior margin (Carballido and Sander 2014). As this description is applicable for the lateral pneumatopores found in *Patagosaurus*, it will be used in this sense.

The use of 'anterior' and 'posterior' is preferred instead of 'cranial' and 'caudal'. This is to avoid confusion when describing, for instance, the caudal vertebrae.

Laminae: **acdl**: anterior centrodiapophyseal lamina**; acpl**: anterior centroparapophyseal lamina**; cpol**: centropostzygapophyseal lamina**; cprl**: centroprezygapophyeseal lamina**; pcdl**: posterior centrodiapophyseal lamina**; podl**: postzygadiapophyseal lamina**; posl**: postspinal lamina; **ppdl**: parapodiapophyseal lamina**; prdl:** prezygodiapophyseal lamina; **prsl**: prespinal lamina**; spdl**: spinodiapophyseal lamina**; spol**: spinopostzygapophyseal lamina**; sprl**: spinoprezygapophyseal lamina**; stpol**: single intrapostzygapophyseal lamina; **stprl**: single-intraprezygapophyseal lamina**l; tprl**: intraprezygapophyseal lamina**; tpol**: intrapostzygapophyseal lamina**;**

Fossae: **cdf**, centrodiapophyseal fossa (fenestrae for some posterior dorsals); **cpof**, centropostzygapophyseal fossa; **cprf**, centroprezygapophyseal fossa; **ivf**, intervertebral fossa; **pocdf**, postzygapophyseal centrodiapophyseal fossa; **posdf**, postzygapophyseal spinodiapophyseal fossa; **prcdf**, prezygapophyseal centrodiapophyseal fossa; **prsdf**,

prezygospinodiapophyseal fossa; **sdf**, spinodiapophyseal fossa; **spof**, spinopostzygapophseal fossa; **sprf**, spinoprezygapophseal fossa

Institutional abbreviations: LEICT: New Walk Museum and Art Gallery, Leicester Arts and Museum Service, Leicester, UK. MACN: Museo Argentino de Ciencias Naturales 'Bernardino Rivadavia', Buenos Aires, Argentina. MNHN-MAA: Musee National d'Histoire Naturelle, Paris, France. OUMNH: Oxford University Museum of Natural History, Oxford, UK. PVL: Paleovertebrados, Instituto Miguel Lillo, Tucuman, Argentina.

SYSTEMATIC PALEONTOLOGY

SAURISCHIA SEELEY 1887

SAUROPODA MARSH 1878

EUSAUROPODA UPCHURCH 1995

CETIOSAURIDAE LYDEKKER 1888

PATAGOSAURUS BONAPARTE 1979

PATAGOSAURUS FARIASI BONAPARTE 1979

Holotype: PVL 4170, consisting of several anterior, middle and posterior cervical vertebrae, PVL 4170 1-9, anterior, mid- and posterior dorsals, PVL 4170 10-17, anterior caudals 19-25 and middle to posterior caudals 26-32, sacrum, PVL 4170 18, fused ischia, PVL 4170 36, right ilium, PVL 4170 34, right pubis, PVL 4170 35, and right femur, PVL 4170 37. See Table 1 and 2 for vertebral measurements, and Table 3 for appendicular measurements. The holotype was said to also contain a scapula and coracoid (Bonaparte, 1986a), but these could unfortunately not be located in the collections. In the collections of the MACN we found two elements labelled as MACN-CH 1986 scapula 'A' and coracoid 'B', which might be these holotypic elements; however, at present the association of these bones with the holotype is

uncertain, and the association with another *Patagosaurus* specimen, MACN-CH 935, is also likely, due to close association of these elements with MACN-CH 935 on the excavation map. A large humerus is also indicated in the original quarry map for the holotype, however, the only large humerus retrieved from the PVL collections is from another locality, Cerro Cóndor South. Originally, associated teeth with typical eusauropod wrinkled enamel were mentioned (Bonaparte 1986b). However, no directly associated teeth or tooth-bearing bones are known for the holotype specimen, so that these teeth are not regarded as part of the holotype here and were not used in the diagnosis, even though some are ascribed to *Patagosaurus* (Holwerda et al. 2015). Ribs and chevrons appear on the quarry map of the holotype, but are mixed in with ribs and chevrons of other *Patagosaurus* specimens, and will therefore be omitted from the holotype description.

Original Diagnosis (Bonaparte 1986b): Cetiosaurid of large size, with tall dorsal vertebrae; posterior dorsals with elevated neural arches and well-developed neural spines, formed from 4 divergent laminae and with a massive dorsal region; dorsoventrally-oriented neural spine cavities, more expanded than in *Barapasaurus*. Anterior and lateral regions of the neural arch similar to that of *Cetiosaurus* and *Barapasaurus*. Sacrum with 5 vertebrae, elevated neural spines, and a large dilation of the neural canal forming a neural cavity. Pelvis with pubis showing distal and proximolateral expansions, more developed than in *Barapasaurus*, and a less expanded pubic symphysis than in *Amygdalodon*. Ischium slightly transversely compressed, with a ventromedial ridge of sublaminar type, and with a clear distal expansion. Ratio of tibia-femur lengths from 1:1.5 in juveniles, reaching 1:1.7 in adults. Mandible with weak medial torsion. Spatulate teeth with occlusal traces.

Emended diagnosis: Patagosaurus fariasi is a non-neosauropodan eusauropod dinosaur that can be diagnosed on the basis of the following morphological features, and the following

combination of characters (features with * are tentatively considered autapomorphies): 1) cervical and anterior dorsal vertebrae with marked pleurocoel, which is deep in cervicals but shallower in dorsals. In cervical vertebrae, the pleurocoel is deeper anteriorly with well defined margins, but becomes shallow posteriorly and has only well defined dorsal and ventral margins. 2) In several cervicals, a faint oblique accessory lamina is present, dividing the pleurocoel into an anterior deeper part and a posteriorly shallower part. 3) The cervicals have a relatively high neural spine, accompanied by high dorsal placement of postzygapophyses, which results in a high angle between the postzygodiapophyseal and posterior centrodiapophyseal laminae of about 55°. 4) Posterior dorsal neural arches with a centrodiapopohyseal fossa that extends internally as a pneumatic structure, which is separated by the mirroring structure by a thin septum, and both of which connect into a ventral, oval shaped internal pneumatic chamber, which is dorsal to and well separated from the neural canal*. 5) Posterior dorsals with small round excavations on the posterior side of the distal extremity of the diapophyses*. 6) Posteriormost dorsals have rudimentary aliform processes. 6) All dorsals display an absence of the spinodiapophyseal lamina in all dorsals, with a contact between the lateral spol and podl in posterior-most dorsals instead. 7) Sacrals with dorsoventrally high neural spine. 8) Ilium with round dorsal rim, hooks-shaped anterior lobe and dorsoventrally elongated pubic peduncle. 9) Fused distal ischia with the paired distal shafts creating an angle of 110° to the horizontal, 10) pubis with torsion and kidney-shaped pubic foramen. 11) Femur with posteromedially placed fourth trochanter, and laterally convex surface of femoral shaft.

Horizon, locality and age: Patagosaurus fariasi was found in what are now considered latest Early to early Middle Jurassic beds of the Cañadón Asfálto Formation in west-central Chubut, Patagonia, South Argentina (Cúneo et al., 2013). The Cañadón Asfálto Formation is a continental unit, consisting mainly of lacustrine deposits. *Patagosaurus* was found in the

Cerro Cóndor area. The type locality of the holotype of *Patagosaurus fariasi* is Cerro Cóndor North, which lies approximately 2 Km north-east of the first discovery site of *Patagosaurus* remains: Cerro Cóndor South, close to the village of Cerro Cóndor, near the Chubut river, not far from the town of Paso de Indios (Figure 1).

GEOLOGICAL SETTING

The Cañadon Asfálto Formation (west-central Chubut province, Patagonia, Argentina, see Figure 1) was first studied by Piatnitzky (1936), after which it was formally described and named by Stipanicic et al. (1968) and further described by Nullo (1983). It is part of the sedimentary infill of the eponymous Cañadón Asfalto Basin, which consists of different subunits of Lower Jurassic to Upper Cretaceous sediments. The Cañadon Asfálto Formation is the uppermost unit of the lower megasequence of the Cañadón Asfalto basin, which has sedimentary infill of the Lower Jurassic (Figari *et al.* 2015). This unit is exposed between the Chubut province towns of Paso del Sapo and Paso de Indios (Olivera et al. 2015). The early Middle Jurassic (Toarcian-Bajocian, possibly earliest Bathonian) Cañadón Asfalto Formation conformably overlies the Early Jurassic (Pliensbachian-early Toarcian; Cúneo et al. 2013; Figari et al. 2015; Volkheimer et al. 2015) Lonco Trapial Formation. It has been the subject of numerous geological studies in recent years to determine its sedimentology and age, since the age of the Cañadón Asfálto Formation has long been considered to be Callovian-Oxfordian (and thus the South American equivalent of several other Jurassic beds worldwide, such as the Oxford Clay; Frenguelli 1949; Bonaparte 1979; Bonaparte 1986; Rauhut 2003). However, a recent detailed chronostratigraphic study showed otherwise, using zircon grains from several tuff samples from the Cañadón Asfálto Formation (Cuneo et al. 2013). These were pre-treated by the chemical abrasion, or CA-TIMS technique, in order to constrain radiation-induced Pb loss. This method (using U/PB isotopes) is considered to be one of the most precise dating methods (Mattinson 2005). The U/Pb isotope ratios show

a latest Early (early-mid Toarcian), to early Middle Jurassic age range (Aalenian or Bajocian, Cúneo et al. 2013), although the youngest radiometric age for this formation has been given as Bajocian-Bathonian (Cabaleri et al. 2010a). This much older age of the formation is also consistent with palynological and other radiometric studies (e.g. Volkheimer et al. 2008; Cabaleri et al. 2010; Zavattieri et al. 2010; Olivera et al., 2015; Hauser et al. 2017). Moreover, this new age also puts the vertebrate fossils found in the Cañadón Asfálto Formation in a new light.

Since its discovery, over twenty species of different taxonomic groups (including sauropod, theropod, and ornithischian dinosaurs, pterosaurs, sphenodontians, mammals, fishes, frogs, turtles and crocodiles) have been discovered (Sterli et al. 2010; Olivera et al. 2015). This makes it an important unit for the study of Middle Jurassic tetrapods, and the diversification of Middle Jurassic dinosaurs in particular.

The outcrops of the Cañadón Asfálto Formation are dominated by microbial limestones, often tuffaceous mudstones and shales with conchostracans, and conglomeratic intercalations (Silva Nieto et al. 2002; Tasch and Volkheimer 1970). They provide mainly disarticulated dinosaur remains, as well as a few articulated skeletons, as shown in the quarry map of the sauropod bonebed of Cerro Cóndor North (Figure 1). The Cañadón Asfálto Formation shows evidence of both folding and faulting, which makes correlation of the different localities impossible, until further study is performed.

The region was dominated by a warm and relatively humid climate in the Middle Jurassic, evidenced by palynology (Volkheimer et al. 2001) and by macrofloral remains (e.g. Cheirolepidiaceae and Araucariaceae; Volkheimer et al. 2008, Volkheimer et al. 2015). Lacustrine sedimentation cycles found in paleolakes in the Cañadón Asfálto Formation provide evidence of climatic fluctuations and cyclicity (Cabaleri and Armella 2005; Cabaleri

et al. 2005).

José Bonaparte started excavations in the Cañadón Asfálto Formation with a team of scientists and preparators, and with funding from the National Geographic Society, in 1977. They found bones, on the Farias farm estate close to the river Chubut. After this, in 1978, they found a sauropod skeleton 4-5 km north of Cerro Condor. This site was then dubbed Cerro Cóndor Norte (North), and the original site Cerro Cóndor Sur (South). The Cerro Cóndor North site was excavated until 1982; in 1980, however, most material was uncovered and visible, as demonstrated in the quarry map of Figure 1. From this site, the holotype PVL 4170 originates, as well as at least seven other individuals, most likely of *Patagosaurus*.

The sediments of Cerro Cóndor North are dark grey, and hard. The bones from this quarry are similarly dark grey or dark brown in colour. The sediments of Cerro Cóndor North were interpreted by Bonaparte as fluvial deposits; however, they have more recently been interpreted as mainly lacustrine deposits.
Cerro Cóndor South was thought to be fluvial, but from observations by O.R. is now thought to be originating from an alluvial fan within a shallow lacustrine environment. Sediments from Cerro Cóndor South are fine-grained to paraconglomeratic, light-coloured and contain small freshwater shell fragments of invertebrates. Bonaparte also hinted that this locality consists of multiple layers of sediment with fossils.

RESULTS

AXIAL SKELETON

Cervicals: PVL 4170 has seven cervical vertebrae preserved, ranging from anterior to posterior cervicals. The most anterior cervical preserved (PVL 4170 1) is probably the third or fourth cervical, based on comparisons with the Rutland *Cetiosaurus* (LEICT 468.1968.40; Upchurch and Martin 2002).

Given the incomplete preservation of the neck in *Patagosaurus*, the exact cervical count in this taxon cannot be established. At the very least, the atlas, axis and first one or two postaxial cervicals are missing, given the high projection of the neural spine in the first cervical preserved, and compared to the Rutland *Cetiosaurus,* where neural arches and spines are low in the first 2-3 cervicals after the axis. Only very few non-neosauropodan sauropods with complete cervical series are known, making a comparison of the preserved elements difficult. Of the basal eusauropods with complete cervical series, *Shunosaurus* and *Jobaria tiguidensis* Sereno et al., 1999 have 12 cervicals (Zhang 1988; Sereno et al. 1999), whereas *Spinophorosaurus* has 13 (Remes et al. 2009). The Rutland *Cetiosaurus* was said to have 14 cervicals by Upchurch and Martin (2002), but several of these vertebrae, including the possibly last two cervicals, have only parts of the neural arch preserved, so that it cannot be established with certainty if these two last vertebrae are cervicals or might already be anterior dorsals (Upchurch & Martin 2002). The derived non-neosauropodan mamenchisaurids apomorphically increased the cervical vertebral count to as much as 18 cervicals (Ouyang & Ye 2002). The primitive number of cervicals in basal eusauropods thus seems to be either 12 or 13, and this is the condition we assume for *Patagosaurus*. As the exact position of the different cervicals preserved can thus not be established, the numbering used here starts with the first element preserved, therefore what is actually Cv 3

335 or 4 is numbered cervical 1 in the PVL collections. For convenience we will adhere to this
336 numbering.
337 The cervical centra are longer than high (see Table 1) and opisthocoelous, as in most
338 sauropods. In comparison with other sauropods, cervicals are rather stout, with an average
339 elongation index (aEI; Chure *et al.*, 2010) ranging from 1.9-2 in anterior to 1.2-1.4 in
340 posterior cervicals and the 'traditional' elongation index (EI, Upchurch 1998) ranging from
341 2.1 in anterior to 1.2 in posterior cervicals, compared to ~3.5 on average in
342 *Spinophorosaurus* (Remes et al. 2009b), ~3.1 in the only cervical known from *Amygdalodon*
343 (Rauhut 2003, MLP 46-VIII-21-1/8), and 2,1 in anterior to 5,3 in mid cervicals in an
344 undescribed sauropod from the Bagual site in the Cañadón Asfálto Formation (MPEF-PV
345 'Bagual' C2-4; Pol et al. 2009). This index is thus on average lower if compared to other non-
346 neosauropod eusauropods (see Table 1). The condyle has an anterior protrusion slightly
347 dorsal to its center, and the condyle is 'cupped' by a ca. 1-2 cm thick rugose layer, similar to
348 that in the Rutland *Cetiosaurus* (see Upchurch and Martin 2003, LEICT 468.1968 cervical
349 series). The cotyles are concave; with the deepest concavity slightly dorsal to the midpoint.
350 As in most saurischians, the parapophyses are placed on the anteroventral end of the
351 centra. In lateral view, the centra are ventrally concave posterior to the parapophysis. The
352 posteriormost 1/3rd of the ventral side of the centra is convex, and the dorsoventral height
353 of the centra increases posteriorly. Pleurocoels are developed as large, but only partially
354 well-defined lateral depressions on the centra. In anterior cervicals, the pleurocoel is deeper
355 than in posterior cervicals, and has a well-defined anterior, dorsal and ventral margin. In
356 mid- and posterior cervicals the posterior margin of the pleurocoel is less clearly defined and
357 the depression gradually fades into the lateral surface of the centrum. In some mid- to
358 posterior cervicals, the left and right pleurocoels are only separated by thin septa (which are
359 damaged or broken in some elements), but they do not invade the centrum and ramify
360 within the bone, as is the case in neosauropods, (Wedel et al. 2005). Some cervicals show a

361 faint compartmentalization of anterior and posterior pleurocoels, but they generally lack the
362 oblique lateral lamina that subdivides the cervical pleurocoels in neosauropods and some
363 derived basal eusauropods.
364 In ventral view, the centra are constricted directly posterior to the condyle, as in most
365 sauropods. A prominent ventral keel is present, which extends to about 2/3rd of the length
366 of the ventral axial midline of the cervicals, after which it fades and disappears into the
367 ventral surface of the centrum. It is present in all cervicals preserved (and possibly in the
368 first dorsal as well as a marginally developed keel). The keel is developed as a thin, ventrally
369 protruding ridge, with a very small hypapophysis anteriorly. The latter is developed as a
370 transversely thin, rounded, sail-like ventral protrusion present immediately behind the
371 ventral rim of the condylar 'cup'. This structure is accompanied by elliptical lateral fossae, as
372 in *Amygdalodon* (Rauhut 2003), *Tazoudasaurus* (MNHM To1-64; 81; 112; 354)
373 *Lapparentosaurus* (MNHM MAA 13; 172; 5) and *Spinophorosaurus* (NMB-1699-R), but in
374 contrast to the Rutland *Cetiosaurus* (Leict 468.1968.40; 42; 7) and *Mamenchisaurus*
375 *hochuanensis* (Young and Zhao 1972) and derived sauropods. At the posterior end, the
376 cotyle extends further ventrally than it does dorsally, also seen in *Lapparentosaurus,*
377 *Amygdalodon, Tazoudasaurus*, and *Spinophorosaurus*. The dorsal side of the cotyle shows a
378 U-shaped notch in middle and posterior cervicals.
379 Neurocentral sutures are visible on the lateral side of the centrum in some cervical
380 vertebrae, a possible sign of morphological immaturity in archosaurs (Brochu 1996; Irmis
381 2007). The neural arches of the cervicals are axially elongated, transversely narrow and
382 higher posteriorly than the vertebral centrum, as in most sauropods. The diapophyses are
383 placed on ventrolaterally directed transverse processes, which are attached to the neural
384 arch by bony laminae, which are described in detail below for the individual vertebrae. The
385 prezygapophyses are more prominent than the postzygapophyses, being placed on stout,
386 elongated, beam-like stalks projecting anteriorly from the neural arch. They consistently

project anteriorly beyond the centrum in anterior cervical vertebrae, and show an increasing incline towards posterior cervicals, as in basal sauropods *Tazoudasaurus*, the Rutland *Cetiosaurus*, and in basal neosauropods such as *Haplocanthosaurus priscus* Hatcher, 1903. Well-developed prezygapophyses apparently have a pre-epipophysis, however, a similar structure is mentioned in a basal non-neosauropodan sauropod form the Early Jurassic of Morocco, (Nicholl et al. 2018). The postzygapophyses are less prominent as they do not project much posteriorly from the neural arch. With the increasing height of the neural arch in more posterior cervicals, the postzygodiapophyseal lamina becomes more steeply inclined. A relatively high posterior cervical neural arch is shared with mamenchisaurs (Mannion et al. 2019). In mid cervicals, this inclination of the postzygodiapophyseal lamina is approximately 45-50°, measured from the axial plane, which is larger than in most basal sauropods, but comparable to the situation in diplodocids (see also McPhee et al 2015). At the anterior end of the cervical neural arches the intraprezygapophyseal laminae are separated medially, as in *Tazoudasaurus* (Allain and Aquesbi 2008) and the Rutland *Cetiosaurus* (LEICT 468.1968). The intrapostzygapophyseal laminae (tpol) do meet at the midline. However, there are no centropostzygapophyseal laminae, as in *Tazoudasaurus* (Allain and Aquesbi 2008), but unlike the Rutland *Cetiosaurus* (Leict 468.1968). Cervical vertebra PVL 4170 (7) is the only cervical with a single centropostzygapophyseal lamina (stpol). This lamina is found more commonly in middle and posterior cervicals of neosauropods, *Haplocanthosaurus* and *Cetiosaurus* (Upchurch et al. 2004). As this is the last cervical before the cervico-dorsal transition (which happens at cervical PVL 4170 (8), this could be a feature enabling ligament attachment for stability and strength at the base of the neck, however, this would need more investigation with e.g. biomechanical modeling. The cervical neural spines project higher than in most basal sauropods, especially in the middle and posterior cervicals. The spines are connected to the zygapophyses by well-developed spinopre- and spinopostzygapophyseal laminae. Whereas the summit of the

spine is more or less flush with the spinopostzygapophyseal lamina (spol) in the anteriormost vertebra, it protrudes dorsally beyond that lamina in more posterior elements. The spol are robust in all cervicals, but the sprl is only extensive in anterior elements and becomes short and thin in more posterior cervicals. From cervical 4 onwards the neural spine forms a rounded protrusion which is transversely wider than long anteroposteriorly. The neural spine is slightly anteriorly inclined in anterior cervicals (to at least the fifth preserved element), but becomes more erect towards the end of the cervical series, with a straight anterior margin; this is also seen in *Shunosaurus* (Zhang 1988, T5402).

Cervical vertebra PVL 4170 (1): This is the smallest and anteriormost of the cervical vertebrae preserved. The element is generally complete and well-preserved, but the right prezygapophysis is broken off at the base (see Fig. 2). A lump of sediment is still attached to the anterior part of the neural arch, above the condyle.

The centrum is relatively shorter than in the mid-cervicals, with an EI of 1,55 and an aEI of 1,43. The articular ends are notably offset from each other, with the anterior end facing anteroventrally in respect to the posterior cotyle (Fig. 2E, F). The cotyle is not as concave as in the other cervicals of the series. The ventral keel is strongly developed in the anterior 1/3rd of the centrum, after which it gradually fades into ventral surface. In ventral view, the parapophyses are visible as lateral oval bulges, the articular surfaces of which are confluent with the condyle rim (Figure 2E).

The centrum shows a distinct pleurocoel, present laterally on the vertebral body (Figure 2A, B). It is deeper anteriorly than posteriorly and developed as a rounded concavity that follows the rim of the condyle on the lateral anterior side of the centrum. Posteriorly it extends almost to the posterior end of the centrum; however, it fades gently into the lateral surface from about 2/3rd of the centrum axial length. Within the pleurocoel there appears to be a slight bulge at about the height of the diapophysis, which is similar to the oblique accessory

lamina in neosauropods (Upchurch 1998), dividing the pleurocoel in two subdepressions. This subdivision is also seen to some extent in mamenchisaurids (e.g. Ouyang and Ye 2002; Tang et al. 2001; Young 1939; Young and Zhao 1972; Zhang et al. 1998), and also in the Rutland *Cetiosaurus* (Upchurch and Martin 2003). This incipient subdivision is also present in some other cervicals of *Patagosaurus*, but it is best developed in this element. The parapophysis is positioned anteroventrally on the lateral side of the centrum, and is connected to the rugose rim of the condyle. The dorsal side is excavated, with the recess being confluent with the deep anterior part of the pleurocoel. A stout lamina extends horizontally posteriorly from the parapophysis and forms the ventral border of the pleurocoel and the border between the lateral and the ventral side of the centrum. This lamina becomes less prominent posteriorly (Figure 2A, B).

The posterior region of the neural arch is approximately as high as the posterior end of the centrum. It extends over most of the length of the centrum, but is slightly offset anteriorly from the posterior end of the latter. The neural canal is rather small and round in outline, but only its posterior opening is visible, as the anterior end is still covered in matrix. Despite the anterior position of the vertebrae, lateral neural arch lamination is well-developed, with prominent prdl, podl and pcdl. The diapophysis is developed as a small, lateroventrally projecting process on the anterior third of the neural arch (Figure 2A, C, D). It is connected to the prezygapophysis by a slightly anterodorsally directed prezygadiapophyseal lamina (prdl). The latter is in line with the pcdl, which meets the diapophysis from posteroventral. The postygaydiapophyseal lamina (podl) is steeply anteroventrally inclined and meets the prdl just anterior to the diapophysis. A short and stout acdl is present, but hidden in lateral view by the diapophysis.

The prezygapophysis is placed on a stout, anteriorly and slightly dorsally directed process that slightly overhangs the anterior condyle of the centrum (Figure 2A, C). The base of this process is connected to the centrum by a short and almost vertical centroprezygapophyseal

lamina (cprl), which here meets the prdl in an acute angle; from this point onwards only a single, very robust lateroventral lamina continues anteriorly onto the stall and braces the prezygapophysis from lateroventral. The prezygapophyseal articular suface is flat, triangular to elliptic in shape and measures about 3 by 3 cm. It is inclined dorsomedially at an angle of approximately 30-40° from the horizontal. The intraprezygapophyseal lamina is very short and widely separated from its counterpart in the middle of the anterior surface of the neural arch.

A slightly asymmetrical centroprezygapophyseal fossa (cprf) is present below the intraprezygapophyseal (tprl) and centroprezygapophyseal laminae on either side of the neural arch, with the right fossa being hidden by sediment (Figure 2C). Anteroventral to the diapophysis an axially elongated prezygapophyseal centrodiapophyseal fossa (prcdf) is visible, contra Upchurch and Martin (2003), who reported this to be absent in *Patagosaurus*. A slightly larger centrodiapophyseal fossa (cdf) is present posteroventral to the diapophysis, and a very large, triangular pocdf is present between the pcdl and podl.

The postzygapophysis is placed on the posterodorsal edge of the neural arch, above the posterior end of the centrum, which it does not overhang it posteriorly. It is developed as a large, lateroventrally facing facet which is dorsally bordered by the slightly curved podl and dorsally braced by the stout spinopostzygapophyseal lamina (spol). The stout and almost vertical cpol connects the centrum to the medial margin of the postzagypophysis. The intrapostzygapophyseal lamina (tpol) is directed ventromedially and connects the medial side of the postzygapophysis to the dorsal margin of the neural canal, where it is separated from its counterpart.

The neural spine is relatively low, barely extending dorsally beyond the postzygapophysis, but it is anteroposteriorly elongate and robust, becoming wider transversely posteriorly (Figure 2A, B, C, D). It is placed more over the anterior side of the centrum and is almost 2/3 of the length of the latter. Its anterior margin is inclined anterodorsally. The spine is

491 connected to the medial side of the prezygapophyseal process by a short
492 spinoprezygapophyseal lamina (sprl), which meets its counterpart at about one third of the
493 height of the neural spine, thus defining a small sprf. The spol is robust, but also short and
494 connects the posterior end of the spine with the dorsal surface of the postzygapophysis. A
495 large, diamond-shaped spof is bordered by the spols and tpols, with the latter being longer
496 than the former. The entire dorsal surface of the neural spine is rugose.
497
498 *Cervical vertebra PVL 4170 (2):* This anterior cervical vertebra is the second element
499 preserved after the anteriormost cervical, and appears to be directly sequential based on
500 the size similarity in cotylar and condylar size between PVL 4170 (1) and (3). It is incomplete,
501 missing the neural arch and neural spine, which are broken off (Fig 3). The centrum,
502 prezygapophyses and the right postzygapophysis, however, are complete. The left
503 postzygapophysis is also broken. The vertebra is slightly flattened/displaced towards the
504 right lateral side, most likely due to compression.
505 The centrum is stout and robust, although slightly more elongated than that of the previous
506 cervical PVL 4170 (1). Its EI is 1,64 and its aEI is 1,97. The overall shape is not as curved as in
507 PVL 4170 (1), but rather straight along the axial plane, with a slight concave curvature of the
508 ventral side of the centrum. The condyle is convex, although slightly more dorsoventrally
509 flattened than in the previous cervical. In lateral view it shows a slightly pointy 'nose', i.e. a
510 pointed protrusion, on its dorsal side (Fig. 3A, B). The cotyle is slightly flattened
511 dorsoventrally as well, and it is wider transversely than dorsoventrally. Because the condyle
512 and cotyle show a high amount of osteological detail, this flattening might be natural, and
513 not caused by compression. On the ventral side of the cotyle, a lateral flange extends on the
514 left side but not on the right (Fig. 3E). This flange extends further posteriorly than the dorsal
515 rim of the cotyle, extending posteriorly and laterally. The dorsal side of the rim of the cotyle
516 shows a U-shaped indentation in dorsal and posterior view, posterior to the neural canal. As

517 in the first preserved cervical, the parapophyses are placed at the anteroventral end of the
518 centrum and extend from the thick condylar rim to the lateral and posterior sides of the
519 condyle. They are generally conical in shape and elongated towards the rest of the centrum.
520 The parapophyseal articular surfaces are more elongated axially than in the previous cervical
521 (PVL 4170 1). In ventral view, the ventral keel on the centrum is clearly present anteriorly on
522 the vertebral body, but fades after about 2/3rd of the vertebral length towards the posterior
523 side where it is not clearly visible (Fig. 3E).
524 On the lateral sides of the centrum, pleurocoels are clearly visible as deep round anterior
525 depressions, directly behind the rim of the anterior condyle (Fig. 3A, C). These depressions
526 fade into the lateral side of the centrum posteriorly. In this cervical, as in the first preserved
527 cervical, the right pleurocoel slightly ramifies anteriorly near the right parapophysis;
528 however, this is not visible on the left side of the centrum. As in the previous cervical, the
529 ventrolateral side of the centrum and ventral border of the pleurocoel is formed by a stout
530 lamina that extends from the posterior edge of the parapophyses to the posterior end of the
531 cotyle.
532 The neural arch is only partially preserved (Fig. 3A, B). Its height is similar to the height of
533 the cotyle. The neural arch in this element is limited to the middle/posterior end of the
534 vertebra; however, this is probably due to the fact that the neural spine is missing. The
535 neural canal, however, is clearly visible in this vertebra, being round to oval in anterior view
536 and more rounded triangular in posterior view. As in the previous vertebra, the lateral
537 neural arch lamination is well-developed, with the stoutest laminae being the prdl, the
538 posterior centrodiapophyseal lamina (pcdl), and the right podl. The anterior
539 centrodiapophyseal lamina (acdl) is also visible; however, it is smaller and shorter than the
540 pcdl. Both diapophyses are present on the neural arch, and are positioned dorsal and slightly
541 posterior to the parapophyses. The diapophyses are developed as small, lateroventrally
542 projecting protrusions of bone, being oval in shape in lateral view and conical in anterior

543 view. The left diapophysis is flexed more towards the centrum than the right, this is probably
544 due to deformation. The right prdl runs straight in a slight anterodorsal slope from the
545 diapophysis towards the prezygapophysis, where it meets with the cprl. Similarly, the right
546 sprl runs more or less parallel to the prdl. The left prdl, however, forms a much steeper
547 angle from the left diapophysis to the left prezygapophysis, due to the taphonomical
548 deformation. Towards the posterior end of the neural arch, the pcdl is in alignment with the
549 prdl. However, the former is directed slightly posteroventrally. The right podl is visible but is
550 damaged. It is a stout lamina and it forms a steep angle of 50° from the horizontal axis in its
551 course from the right diapophysis towards the right postzygapophysis.
552
553 The prezygapophyses are much more elongated than in the previous cervical PVL 4170 (1),
554 (Fig. 3B, C). They project further anteriorly from the vertebral condyle than PVL 4170 (1) by
555 about 9 cm. Moreover, unlike in PVL 4170 (1), they project mostly anteriorly and only slightly
556 dorsally from the neural arch. Once more the taphonomical deformation of this cervical is
557 apparent, as the left prezygapophysis is displaced and bent towards the vertebral body,
558 while the right projects more lateral and away from the vertebral body. The
559 prezygapophyses are supported by very stout stalks, which are formed by the prdl on the
560 dorsolateral side, the cprl on the lateral, and, partially, the sprl on their dorsal side. The prdl
561 meets the cprl in an acute angle, which is obscured from view by the prezygapophyseal
562 articular surfaces. A small, short, pair of tprl is present, which meet in a wide acute angle,
563 dorsal to the neural canal (Fig. 3C). Lateral to these laminae, small, paired, rounded to oval
564 prcdfs are visible underneath the prezygapophyses. They are also transversely convex.
565 The only preserved, right postzygapophysis is flexed slightly medially in dorsal view, and has
566 its articular surface directed dorsally and tipped slightly anteriorly and laterally (Figure 3B,
567 D). It is supported by the stout podl and an acutely angled, thin cpol, which together with
568 the pcdl creates a triangular, wing-like structure, which is offset from the neural arch

dorsally and posteriorly. The thin sheet of bone between the podl and the pcdl is pierced. The distal end of the postzygapophysis is rounded to triangular in shape. A relatively deep right pocdf is visible between the cpol and the podl. No tpol is visible here.

Cervical vertebra PVL 4170 (3): This is the third cervical preserved in the series; it probably corresponds to the 5-6th cervical (compared to the Rutland *Cetiosaurus* Leict LEICT 468.1968). It is well-preserved, but lacks both diapophyses, see Figure 4. The cervical is stout, and is similar to PVL 4170 (2) in that the centrum is generally straight, and the anterior and posterior ends are not as offset from each other as in the first preserved cervical. Nevertheless, the cotyle is slightly offset to the ventral side, and the condyle bends slightly ventrally from the relatively straight vertebral body (Fig. 4A, B). The prezygapophyses are slightly displaced, the right projects further laterally than the left; this might be caused by deformation.

Both the condyle and cotyle are larger in this cervical than in the previous two (Fig. 4A, B). The condyle is oval in shape, and is transversely wider than dorsoventrally. It has a small rounded protrusion, visible slightly dorsal to the midpoint of the condyle (Fig. 4E). A thick rugose rim surrounds the condyle, from which the parapophyses protrude at the lateroventral sides. The cotyle is more or less equally wide transversely as high dorsoventrally. It has its deepest depression slightly dorsal to the midpoint. The cotyle does not have a rugose rim; however, its ventral rim projects further posterior and slightly lateral than its dorsal rim. In ventral view, (as well as in lateral view) the parapophyses are clearly visible as rugose, oval structures that protrude from behind the condylar rim to the posterior and lateral sides. Also emerging from this condylar rim is the ventral keel, which is prominently visible for about 2/3rds of the length of the centrum, after which it fades into the ventral body of the centrum. At the onset of the keel, a small round hypapophysis

protrudes ventrally from the centrum. Two oval depressions are visible on the lateral sides of the hypapophysis.

In lateral view, the centrum shows neurocentral sutures between the lower part of the centrum and the upper part of the vertebral body (Fig. 4A, B). The suture is better preserved on the right side than on the left side of the centrum. On both lateral sides of the centrum, a prominent pleurocoel is visible as a deep oval depression, which becomes shallower posteriorly but spans almost the entire length of the vertebral body. Unlike in the previous two cervicals, no compartmentalization of the pleurocoel is visible in this element. The dorsal and ventral rim of the pleurocoels are marked by two stout laminae that define the ventral and dorsal sides of the centrum.

The neural arch becomes more dorsoventrally elevated in this cervical, with the neural arch being slightly higher than the dorsoventral height of the cotyle (Fig. 4A, B). The neural canal is triangular to slightly teardrop-shaped in anterior view, in contrast to the previous two cervicals. In posterior view, the neural canal is oval, with a flat ventral surface. Because the diapophyses are damaged, the lamination underneath the diapophyses is clearly visible in lateral view. The acdl is developed as a short lamina, running anteroventrally in an oblique slope towards the anterodorsal end of the pleurocoel. The pcdl is a very stout, elongated lamina in this cervical. It runs from directly underneath the diapophysis to the posterior end of the vertebral body, but fades into the centrum shortly before the rim of the cotyle. The acdl and pcdl delimit a small triangular centrodiapophyseal fossa (cdf), while a much wider postzygapophyseal centrodiapophyseal fossa (pocdf) is bordered by the slightly convex, stout podl (Figure 4A, B, C). This lamina runs at an oblique angle of about 40 degrees to the horizontal from the diapophysis to the postzygapophysis. Shortly before reaching the postzygapophysis, the curvature of the lamina changes from straight to slightly concave (ventrally), giving the podl a slight sinusoidal appearance. The prdl runs from the diapophyses to the prezygapophyses in an oblique angle similar to the podl. The four major

621 laminae on this cervical, prdl, acdl, pcdl, and podl, together create an X shape (in near
622 symmetrical oblique angles) on the midpoint of this cervical.
623 The prezygapophyses project anteriorly, dorsally, and slightly laterally, with the angle
624 between each prezygapophyseal summit being about 110-120° (Fig. 4D). They project
625 asymmetrically; this is probably due to taphonomical deformation. The stout stalks
626 supporting the prezygapophyses are concave ventrally, and convex dorsally, and project 9
627 cm anterior from the vertebral body (Fig. 4A, B, D). The articular surfaces are triangular in
628 shape. The prezygapophyses are supported by the prdl from the dorsolateral side, and by
629 the cprls ventrally. The cprls extend in a near vertical axis from the ventral side of the neural
630 arch, but at about the height of the neural canal project laterally towards the
631 prezygapophyseal articular surface in an angle of about 30°. In anterior view, the stout,
632 sinusoidal tprl join together from the medial articular surface of the prezygapophyses to the
633 ventral side of the prezygapophyses, just dorsal to the neural canal. Here a very short, stout,
634 single intraprezygapophyseal lamina (stprl) is present. The paired prcdfs, seen as triangular
635 depressions, bordered by the tprls and the cprls, are larger than in previous cervicals PVL
636 4170 (1) and (2).
637 The postzygapophyses are triangular in shape in posterior view, and their articular surfaces
638 in posterior/ventral view are rounded to triangular in shape (Fig. 4C). There is a slight V-
639 shaped indentation on the medial side of each postzygapophysis between the posterior
640 termination of the podl and the cpol at the postzygapophyses. The cpols run in a curved,
641 oblique angle of about 55° to the horizontal, from the postzygapophyseal articular surfaces
642 to the dorsal rim of the posterior neural canal. No stpol is visible here. On each lateral side
643 of the paired cpols, large triangular paired pocdf are visible, bordered by the vertically
644 aligned podls.
645 The neural spine is already prominent in this cervical, more so than in PVL 4170 (1) and (2)
646 (Fig. 4A, B, F). In dorsal view, the neural spine appears solid, and is rounded in shape, and

the anterior, posterior and lateral rims are clearly visible and protrude slightly dorsally (Figure 4F). The dorsalmost part shows rugosities, probably for ligament attachment. In anterior view, the neural spine is kite-shaped, and shows rugosities on the anterior surface. Relatively thin, paired sprl curve down from the anterior lateral sides of the neural spine, where they extend in an inverted V-shape to the lateral sides of the prezygapophyses. Medial to these laminae, an oval sprf is visible, ventrally bordered by the tprls. Similarly, in posterior view, the spols form an inverted V towards the postzygapophyses, dorsally bordering the spof, which is clearly visible as a deep and large fossa, which in turn is bordered laterally by the paired cpols. The neural spine in lateral view as well as in posterior view is seen to incline anteriorly, making the neural spine summit less prominent in posterior view (Fig. 4A, B, C).

Cervical vertebrae PVL 4170 (4): The fourth preserved cervical is generally well-preserved. However, the left diapophysis and part of the neural arch are missing, and the right neural arch, between the neural spine and the diapophysis, is partially reconstructed, see Figure 5. The left prezygapophysis, and the articular surface of the postzygapophysis are also partially missing. This cervical could have been more robust than the next one, and the neural spine could have projected further dorsally, making this cervical in fact cervical (5), however, as it is reconstructed, this cannot be ascertained for certain.

The centrum is more elongated then that of the previous cervical (Fig. 5A, B). The centrum only shows a mild curvature, and the cotyle and condyle are not offset from one another; the condyle bends slightly ventrally and the cotyle also mildly curves ventrally. The lateroventral rims of the cotyle flare out slightly laterally and posteriorly, and are more enlongated ventrally than dorsally. In anterior view, the condyle is oval and slightly dorsoventrally flattened (Fig. 5D). It has a thick, prominent rim surrounding it, from which the parapophyses are offset in anterior view. In posterior view, the cotyle is larger than the

674 condyle, and more or less equally wide transversely as dorsoventrally. In ventral view, the
675 thick rim that cups the condyle is clearly visible (Fig. 5E). From this rim, the hypapophysis
676 protrudes ventrally as a small rounded bulge. The ventral keel is prominently visible, and
677 runs along the ventral surface of the centrum until it fades into the posterior 1/3rd of the
678 centrum, where it widens transversely towards its posterior end. This is also seen to some
679 extent in *Lapparentosaurus* (MNHM MAA 13; 172; 5), although this fanning includes a
680 dichotomous branching of the posterior end of the ventral keel in the latter taxon. In lateral
681 view, the ventral keel protrudes slightly more ventrally than the stout lamina that defines
682 the ventral lateral end of the centrum. In lateral view, the pleurocoels are visible as deep
683 depressions on the lateral side of the centrum, being deepest behind the rim of the condyle,
684 and fading into the posterior 1/3rd of the lateral centrum. Interestingly, this cervical shows
685 pleurocoels with well-defined posterior margins (as well as anterior, dorsal and ventral),
686 which differs from the pleurocoels in the previous cervicals (Fig. 5A, B). Moreover, the
687 pleurocoels in this element are slightly compartmentalized (a deeper depression of the
688 pleurocoel is visible anteriorly and posteriorly, while the mid section is less deep in the
689 lateral body of the centrum), as in the first two cervicals.
690 As in the previous three cervicals, the neural arch extends over most of the length of the
691 centrum, but ends a short way anterior to the posterior end of the centrum. The neural
692 canal is rounded to teardrop-shaped in anterior view, and oval to triangular in posterior
693 view, with an abrupt transverse ventral rim, as in PVL 4170 (3). The configuration of the four
694 prominent laminae on the lateral neural arch is similar to that of PVL 4170 (3) in that pcdl,
695 prdl, podl and acdl form an X-shaped structure. However, the right diapophysis (the left is
696 missing) of this element is larger than in the previous cervicals. The right diapophyis is
697 developed as a ventrolaterally projecting process, which is supported posteriorly by the very
698 stout pcdl, and anteriorly by a smaller, shorter acdl. The diapophysis is oval in shape and is
699 axially shorter than dorsoventrally.

The right prezygapophysis is supported laterally and dorsally by the stout prdl, which extends from the anterodorsal side of the diapophysis to approximately 2/3rds of the length of the stalk of the prezygapophysis (Fig. 5B, D). Ventrally, the prezygapophysis is supported by the cprl, which is nearly vertically positioned on the neural arch. The prezygapophysis has a triangular articular surface. As in the previous cervicals, the cprl and tprl meet at the distal end of the prezygapophysis in an acute angle of approximately 30 degrees. The paired tprls slope steeply down and meet on the dorsal rim of the anterior neural canal. The cprl and tprls enclose paired, rhomboid prcdf.

In posterior view, the left postzygapophysis is only partially preserved, as the articular surface is missing, but the right structure is present, showing a flattened articular surface (Fig. 5C). The intrapostzygapophyseal laminae form a V shape with an angle of about 55° from the sagittal plane of the centrum, which is similar to PVL 4170 (3). They meet only on the dorsal rim of the posterior neural canal. The paired, triangular pocdfs, which are demarcated by the cpols and the podls, are also similar to the third preserved cervical.

The neural spine is robust in anterior view (Fig. 5D). It is narrower at the base (at the onset of the spinoprezygapophyseal lamina) and expands transversely towards the summit, which in anterior view is shaped like a rounded hexagon. The right sprl is a near-vertically positioned, prominent structure that extends from about 1/3rd under the neural spine summit to the ventral pairing of the tprls. In lateral view, the neural spine is anteroposteriorly shorter, with respect to the length of the centrum, than in previous cervicals. Its anterior margin is slightly inclined anteriorly. In posterior view, the neural spine summit has a more rounded, rectangular shape, and is clearly inclined towards the anterior side of the cervical. The (only preserved) right spol curves concavely towards the postzygapophysis (Figure 5A,B,C). The spinopostzygapophyseal fossa is deep and triangular in shape.

In dorsal view, the neural spine summit is roughly quadrangular in outline, although it is slightly wider transversely than long anteroposteriorly (Figure 5F). On the anterior rim of the summit, the spine slightly bulges out convexly, with an indent on the midline, rendering the anterior rim slightly heart-shaped. The posterior side of the neural spine summit is slightly concave in dorsal view, with the spol sharply protruding from each lateral side.

Cervical vertebra PVL 4170 (5): This is a mid-posterior cervical, which is well-preserved, with all zygapophyses and diapophyses intact, although the neural spine is slightly taphonomically deformed, and the diapophyses are slightly asymmetrical, also probably due to deformation. The left parapophysis is also missing (Fig. 6A).

The centrum is different from the previous cervicals in that it is more robust, less axially elongated and the condyle, cotyle and neural spine are dorsoventrally larger (Fig. 6A, B). The anterior condyle is rounded, robust and slightly dorsoventrally flattened. The anterior end of the condyle has a rounded protrusion on the midpart. The rim of the condyle is clearly visible and protrudes slightly dorsally (Fig. 6C). Posteriorly, the cotyle is deeply concave and is larger transversely and dorsoventrally than the condyle. The posterior end of the centrum, ventral to the cotyle, flares out laterally, however, it shows a U-shaped indent in the midpart, seen in posterior view (Fig. 6D). In lateral view, the centrum is concavely constricted anteriorly, directly posterior to the rim of the condyle. As in the other cervicals, the dorsal end of the posterior cotyle extends a little further posteriorly from the neural canal in lateral and ventral view. The right parapophysis is visible in lateral view at the ventrolateral end of the condylar rim (Fig. 6B). It is oval in shape and protrudes ventrally and posteriorly. The pleurocoel on the lateral side of the centrum is deeper anteriorly than posteriorly, and spans almost the entire lateral side of the condyle anteriorly (Fig. 6A, B). Posteriorly it fades into the centrum. In ventral view, the ventral keel is clearly visible, and

stretches over the entire length of the centrum, but flattens in the posteriormost part (Fig. 6E). The hypapophysis protrudes less in this cervical than in the previous ones. The parapophysis is more elongated axially than transversely in ventral view, and less rounded than in the previous cervicals; rather than having a rounded rectangular shape in ventral view, it is more elliptical in shape, and is slightly more offset to the lateral sides of the centrum (Fig. 6E). Both posterior centroparapophyseal laminae are clearly visible in this element as short but strong laminae that are confluent with the ventrolateral edges of the vertebral body.

The neural arch is higher dorsoventrally in this element than in the previous ones. In lateral view, the neural arch spans almost the entire axial length of the centrum, however, as in the previous cervicals, it is slightly offset from the anterior dorsal end of the centrum (Fig. 6A, B). In anterior view, the neural canal is slightly teardrop-shaped, and dorsoventrally is more elongated than transversely. In posterior view, the neural canal is also teardrop-shaped, however here it is more dorsoventrally flattened and transversely widened at the base. The diapophyses, in lateral view, appear as rounded appendices, which are offset from the vertebral body as ventral and lateral projection. They are transversely thin and flattened. In anterior view they are more complex in shape, created by a conjoining of the acdl, pcdl and prdl in a triangular shape, which shows a ventral hook-shaped distal protrusion. In posterior view the diapophyses are enclosed in sheets of bone. The prezygapophyses on this cervical rest on more dorsoventrally elongate stalks than in previous cervicals (Fig. 6A, B, C). These stalks have a pedestal-like appearance, and show lateral rounded bulges at their base, dorsal and lateral to the thick condylar rim. The prezygapophyses project anteriorly and slightly medially and dorsally, and are anteriorly triangular in shape. There are deep rhomboid prcdfs visible as dorsoventrally narrow, slit-like fossae, ventral to the prezygapophyses. The centroprezygapophyseal laminae form an oblique angle towards the centrum. The prezygodiapophyseal laminae run ventrally from the prezygapophyses in a sharp angle.

These laminae meet dorsally in an acute angle. The tprl meet dorsal to the neural canal in a wider angle than in the previous cervicals, showing a widening of the space between the prezygapophyses towards more posterior cervicals in *Patagosaurus*.

The postzygapophyses and prezygapophyses are both more aligned with the axial column than in previous cervicals (Fig. 6F). In lateral view, the articular surface of the postzygapophyses is aligned with the horizontal axis, and in dorsal and posterior view the articular surfaces are triangular in shape (Fig. 6A, B). In lateral view, the podl form a wide angle with the axial column, owing to the further elongation of the cpol (producing more elevated postzygapophyses). The cpols show an acute angle from the postzygapophyses to the anterior and ventral side, and are slightly ragged in appearance. They meet the centrum anteriorly to the dorsal rim of the cotyle. In posterior view, the cpol run at an acute angle, and in a slightly concave way, to the ventral side of the postzygapophysis (Figure 6D). This angle is smaller than in previous cervicals, being about 35°, due to the elongation of the neural arch and higher dorsal position of the postzygapophyses. Between the cpol and podl, large, triangular pocdf are visible.

The neural spine in anterior view is slightly sinusoidal, probably due to taphonomic deformation (Fig. 6C). In lateral view, the neural spine is further reduced in its axial length compared to the previous cervicals (Fig. 6A, B). The spine summit is prominent; it is seen to protrude dorsally and anteriorly, clearly separated from the vertebral body as a rounded rectangular bony mass. In dorsal view, the neural spine summit is wider than the neural spine body, and is of a teardrop-shaped protuberant shape (Fig. 6F). It is also expanded transversely. Anteriorly on the neural spine, a prominent protuberance is visible anteriorly, possibly an attachment site for ligaments. The sprls are seen, in dorsal view, to protrude from the anterior side of the neural spine summit (Fig. 6C). They run nearly vertically towards the dorsal base of the prezygapophyseal stalks. At the base of the neural spine they

802 are slightly transversely constricted. The spol are positioned as near-horizontally aligned
803 with the axial plane of the cervical. They are thin, prominent laminae.
804
805 *Cervical vertebrae PVL 4170 (6):* This is a well-preserved posterior cervical with some
806 damaged/broken thin septa. The centrum is robust, as in PVL 4170 (5), but unlike the more
807 elongated anterior cervicals. The cervical is further distinguished by having an axially more
808 elongated neural arch than in the previous cervical, see Figure 7.
809 The centrum is shorter than in previous cervicals, and stouter, with a transversely flattened
810 condyle with a small rounded protrusion slightly higher than the midpoint (Fig. 7A, B). The
811 cotyle is slightly larger and higher dorsoventrally than the condyle, as in the other cervicals.
812 In ventral view, the ventral keel is developed as a protruding ridge between two concavities,
813 which are flanked by the ventrolateral ridges of the centrum (Fig. 7E). This keel flattens
814 towards the caudal end into a bulge and is no longer visible at the posterior end of the
815 ventral side of the centrum. Instead there is a slight depression on the distal end of the keel.
816 The centrum is constricted directly posterior to the parapophyses, which shows a deep
817 concavity of the centrum in lateral view, after which the centrum curves more gently
818 towards a convex posterior end of the centrum (Fig. 7A, B). The pleurocoel is anteriorly
819 deep, and the thin septum that separated it from its mirroring pleurocoel is broken, creating
820 an anterior fenestra. On the left side of the centrum the neurocentral suture is visible. In
821 anterior view, the neural canal is oval, being higher dorsoventrally than wide transversely,
822 and in posterior view, the neural canal is subcircular with a pointed dorsal side.
823 In anterior view, the prezygapophyses are a triangular shape, due to the tapering of both
824 cprl and prdl towards the dorsal tip of the prezygapophyses, where they meet in an inverted
825 V-shape, as in PVL 4170 (5), see Fig. 7C. The cprf are not as deep as in the previous cervicals.
826 The dorsal end of the prezygapophyses is not as convex as in the previous cervicals. In
827 ventral and posterior view, the postzygapophyseal articular surfaces are triangular (Fig. 7D,

E). In lateral view, the sprl is positioned less vertical than in PVL 4170 5, and instead slopes in a gentle curve towards the prezygapophyses (Fig. 7A, B). In posterior view, the thick cpols and the spols support the laterally canted, 'wing-tip'-shaped sheet of bones that are supported by the podl and pcdl on the lateral side (Fig. 7D). The cpol do not meet, while there is no tpol. In dorsal view, the postzygapophyses and spol expand further beyond the centrum than the prezygapophyses overhang the centrum anteriorly, which is the reversed condition compared to the more anterior cervicals in PVL 4170. The spinopostzygapophyseal lamina is also less oblique than in previous cervicals, and curves gently concavely towards the postzygapophyses (Fig. 7D).

The neural spine is craniocaudally flattened but transversely broader than PVL 4170 (5). The base of the neural spine is only supported by a rather thin bony sheet, both anteriorly and posteriorly, as can be seen due to a break. The dorsal end and summit of the neural spine, however, are formed by solid bone. In anterior view, the spine is not as teardrop-shaped as in PVL 4170 (5), but is more rectangular, and widens towards its summit. The neural spine does not tilt notably forward as in PVL 4170 (5), but cants only slightly anteriorly. The neural spine summit extends dorsally beyond the spol as an oval to rhomboid protuberance. The neural spine and the postzygapophyses, together with the podl are more axially elongated and dorsally elevated in this cervical than in the previous ones. In dorsal view, the neural spine summit is a stout, transverse strut. It is slightly transversely expanded, and thicker at the lateral ends.

Cervical vertebra PVL 4170 (7): This is a partially reconstructed posterior cervical, with the left diapophysis missing (Fig. 8). The vertebra is shorter axially and higher dorsoventrally than previous cervicals (Fig. 8A, B). The centrum is stout. In anterior view, the condyle is dorsoventrally compressed and transversely widened (Fig. 8 F). The 'cup' is very distinct. The cotyle is larger than the condyle, more rounded, and shows an indentation dorsally for the

855 neural canal, making the cotyle slightly heart-shaped (Fig. 8E). In ventral view, this centrum
856 is less elongated and transversely wider than previous cervicals. The keel is still well
857 developed, as are the lateral concavities coinciding with the hypapophysis, which is present
858 as a sharp ridge (Fig. 8C). The posterior ventral side of the centrum is ventrally offset from
859 the anterior ventral side, due to the larger size of the cotyle in this specimen, and due to the
860 ventral bulge of the distal half of the centrum. The parapophyses are more aligned with the
861 centrum, in that they do not project ventrolaterally, but more posteriorly, in contrast to
862 previous cervicals (Fig. 8C). The parapophyses are oval in ventral view and more triangular in
863 lateral view. The neural canal is dorsoventrally flattened and teardrop-shaped (Fig. 8E, F).
864 The prezygapophyses differ from previous cervicals in that they form a more accute angle
865 with the vertebral body and have a flat, dorsally directed articular surface in lateral view
866 (Fig. 8A, B). The beams supporting the prezygapophyseal articular surface are stout, as in the
867 previous cervicals. The prezygapophyses are inverted V-shaped in anterior view (Fig. 8F).
868 However, this structure is wider transversely than in previous cervicals. The
869 intraprezygapophyseal laminae tilt ventromedially, whereas the distal tips of the
870 prezygadiapophyseal laminae tilt ventrolaterally, creating an inverted V-shape in anterior
871 view of each prezygapophysis, as in the previous cervical. The stprl is not present (see Table
872 2). In dorsal view, the articular surface of the prezygapophysis is more rounded than in
873 previous cervicals. The postzygapophyses are supported from the lateral and ventral sides
874 by the prominent podl, which project in a wide angle of about 70 degrees from the posterior
875 side of the diapophysis to the postzygapophyses; this lamina curves gently convexly (Figure
876 8A, B, E). In lateral view, the postzygapophyses are present as triangular structures at the
877 distal end of the thick podl. Dorsal to the postzygapophyses, triangular epipophyses are
878 visible (Fig. 8A, B, E). Also, in lateral view, the tpols run ventral to the postzygadiapophyses
879 in a vertical line towards a U-shaped recess, formed by the stpol. In posterior view, the
880 intrapostzygapophyseal laminae form a V-shape. The tpol are much shorter than in PVL 4170

881 (6), which also limits the size of the spinopostzygapophyseal fossa (spof). The stpol is
882 present as a thin lamina that recedes towards the neural arch (Figure 8E). This is the only
883 cervical that has an stpol that is longer than 1 cm. It separates paired rhomboid cpof. These
884 are flanked by the thick podl, which are more elongated in this vertebra than in cervical PLV
885 4170 (6). The right diapophysis expands from the lateral side of the neural arch, and shows a
886 strong ventral bend towards its distal end. This strong bend could be the product of
887 deformation. The left diapophysis also bends ventrally and laterally, but not as strongly as
888 the right one (Fig. 8A, B, E, F). The diapophyses are clearly visible both in anterior and
889 posterior view. Ventrally and anteriorly they are concave, with elongated but axially short
890 prcdfs. They are dorsally supported by the convergence of the prdl and the podl, which form
891 a thick rugose, rounded plate of bone on the dorsal tips of the diapophyses.
892 The neural spine is transversely broad and axially short, and rectangular in shape (Fig. 8F). In
893 dorsal view, it fans out transversely at the apex, but, together with the sprl, becomes
894 constricted ventrally (Fig. 8D). This cervical is further distinguished from the previous
895 cervicals by the dorsoventral elongation of the neural spine, and the accompanying
896 elongation of the tpol in lateral view (Fig. 8A, B).
897
898 *Cervicodorsal PVL 4170 (8):* The neural arch is dorsoventrally elongated in this transitional
899 vertebra between cervicals and dorsals; a trend that persists throughout the anterior and
900 posterior dorsals. The posterior articular surface (cotyle) is dorsoventrally higher than the
901 anterior condyle, (Fig. 9).

902 The condyle is of similar shape to that in PVL 4170 (7) (Fig. 9A, B, C). The cotyle of this
903 vertebra is well-preserved and has an oval, slightly dorsoventrally flattened shape, with a
904 small concave recess at the base of the neural canal (Fig. 9D).

On the ventral side of the centrum, the ventral keel and adjacent fossae are still clearly visible (Fig. 9F). In lateral view, the ventral margin of the centrum is strongly concave in the first half of its length (slightly damaged but still visible) and in the posterior part becomes more convex and robust (Fig. 9F). The ventral keel extends over the first 1/3 of the length, as in the other vertebrae, and then becomes a bulge, adding to the convexity of the posterior ventral end of the centrum. In lateral view, the pleurocoels of either side show a cut through the centrum, creating a foramen (Fig. 9A, B). This supports the observation that the pleurocoels are very deep in the cervicals of *Patagosaurus*, and that they are normally only separated from the adjacent pleurocoel by a very thin midline septum (Carballido and Sander 2014), which in this vertebra is not preserved. The parapophyses are present as rounded to triangular extensions on the lateral sides of the condylar rim (Fig. 9F). They are not clearly visible in anterior or lateral view, but are visible in ventral view. At the base of the prezygapophyseal stalks, however, similar triangular protrusions exist (Fig. 9C).

The cprl project slightly laterally from the centrum (Figure 9A, B). The prdcf are larger than in previous vertebrae, due to the wider lateral projection of the diapophyses. These fossae are triangular in shape (Figure 9C). The prezygapophyses are roughly square with rounded edges in dorsal view. The spinoprezygapophyseal fossa (sprf) is very deep. The prdl are prominently developed as sinusoidal thick laminae, supporting the prdl from below and from the lateral side, and supporting the diapophyses anteriorly. The prezygapophyseal articular surfaces are flat and axially longer than in previous vertebrae (Fig. 9E). The angle of lateral expansion of the sprl however, is greater than in previous vertebrae.

In posterior view, the postzygapophyses project to the lateral side (Fig. 9D). The tpols do not meet, but run down parallel in the dorsoventral plane to the neural canal. A faint right cpol seems to be present in this vertebra, however, it could also be an anomaly of the pocdf. This elongates the spof. The podl project dorsally and posteriorly in a high angle. Towards about

930 2/3rd of the total vertebral height. These project in a straight line, after which they bend in a
931 convex curve to the posterior side. The pcdl make a similar bending curve towards the
932 centrum, due to the elongation of the posterior neural arch. Prominent pocdf are present as
933 shallow triangular fossae.

934 In dorsal view, as in PVL 4170 (7), the neural spine is transversely wide and axially short (Fig.
935 9E). It is constricted towards the postzygapophyses so that it 'folds' posteriorly. In anterior
936 view, the neural spine is ventrally more constricted than in the previous vertebra (Fig. 9C). It
937 is more elongated dorsoventrally, and the neural spine is transversely overall less wide than
938 the previous vertebra.

939

940 *Dorsals:* the holotype specimen has nine dorsals preserved, including a transitional
941 cervicodorsal vertebra. Dorsals are numbered PVL 4170 (9) – (17). Most of the anterior and
942 mid-dorsals are preserved, however, some may be missing, seen in the sudden transition
943 from anterior-mid dorsals PVL 4170 (10) – (11) and mid-posterior dorsals PVL 4170 (12) –
944 (13). Most neural arches and spines are relatively complete; except dorsal PVL 4170 (15) has
945 only the centrum preserved. The number of missing dorsals can only be estimated. The
946 Rutland *Cetiosaurus*, thus far morphologically the closest sauropod to *Patagosaurus* (see
947 Holwerda and Pol 2018), shows the disappearance of the acdl at around vertebra nr 15. As
948 the acdl seems to disappear in anteriormost dorsals of *Patagosaurus*, assuming the
949 anteriormost dorsal is preserved, both sauropods could have had as few as 10 dorsal
950 vertebrae (see Table 2). However, (approximately) contemporaneous non-neosauropodan
951 eusauropods are reported to have 12 dorsals (*Jobaria*, mamenchisaurs) or 13 (*Shunosaurus*).
952 *Barapasaurus* is estimated to have had even 14 dorsal vertebrae. Diplodocids *Apatosaurus*
953 Marsh, 1877*, Diplodocus* Marsh, 1878, and *Barosaurus* Marsh, 1890 all had 10 dorsal

954 vertebrae, and basal neosauropod *Haplocanthosaurus* 13-14 (Hatcher 1903; Carballido et al.
955 2017).

956 The dorsal centra in PVL 4170 become axially shorter and dorsoventrally higher towards the
957 posterior dorsals, with mediolateral width increasing proportionally with height towards
958 posterior dorsals. Anterior-mid dorsal centra are therefore more rectangular in anterior and
959 posterior view, and the posteriormost dorsals more round with a higher mediolateral width.
960 The centra also change from being opisthocoelous to amphicoelous between anterior-mid
961 dorsals PVL 4170 (11)-(13), see Fig. 12 - 14. Opisthocoelus anterior dorsals are shared with
962 *Cetiosaurus*, *Tazoudasaurus*, and diplodocids (Tschopp et al. 2015). The pleurocoel on dorsal
963 vertebral centra in *Patagosaurus* remains visible on the lateral side of the centrum
964 throughout the dorsal series, but does gradually become more of an oval depression. The
965 ventral surface of the centra in anterior dorsals is similar to posterior cervicals in that there
966 is a vestigial ventral keel in anteriormost dorsals, but also in the constriction of the centrum
967 anteriorly, right behind the condyle. The cotyle flares out laterally. Towards mid and
968 posterior dorsals, the centrum in ventral view becomes more symmetrical, with a
969 constriction at the midpoint and flaring out of the centrum towards anterior and posterior
970 articular surfaces. In lateral view, the posterior dorsal centra show a strong curving inwards
971 more anteriorly than posteriorly. Towards the posterior end of the dorsal column, the neural
972 arches increase in height to twice that of the posterior cervicals. The neural spines become
973 axially shorter and transversely broader, however, the posteriormost dorsals have
974 protuberant neural spines that are nearly as high as the combined length of the neural arch
975 and centrum. The neural canal becomes elongated dorsoventrally in the elongated neural
976 arches, and is oval.

977 Anteriormost dorsals (PVL 4170 9-10) are already more elongated dorsoventrally than the
978 cervicals, however, they are still opisthocoelous, and are morphologically distinct from the

posterior dorsals, in that they have transversely wide neural spines, which are flattened axially. The neural canal is transversely wide and oval. The diapophyses are bent ventrally as in the cervicals, and the prezygapophyses are placed higher dorsally than the diapophyses. Prezygapophyses are also directed obliquely dorsally. The spol flare out ventrally, giving the neural spine a broad exterior. As in the cervicals, the angle made between the podl and the pcdl is high.

Middle dorsals (PVL 4170 11-12) become more transversely slender in the neural arch, and the prezygapophyses have a more horizontally positioned articular surface. The transverse processes are also more elongated than the anterior dorsals. The pedicels become more elevated, and the neural spine more elongated dorsoventrally. spol still flare out, but less posteriorly than in anterior dorsals, creating a more 'compact' neural spine complex.

At the transition from middle to posterior dorsals, anteriorly, cprl lengthen as the neural arch and the pedicels elongate. Posteriorly, first the intrapostzygapophyseal laminae meet, then the centropostzygapophyseal laminae disappear, and instead an stpol appears (see Table 2).

The posterior dorsals (PVL 4170 13-17) possess the most discriminating combination of features for *Patagosaurus*. The holotype posterior dorsals show an extensive elongation of the neural arch, both at the pedicels as well as at the neural spine. Elongation of the neural spine towards posterior dorsals is common for sauropods (e.g. *Cetiosaurus*, *Barapasaurus*, *Haplocanthosaurus, Omeisaurus,* (Hatcher 1903; He et al. 1984; Upchurch and Martin 2003; Bandyopadhyay et al. 2010), however this in combination with the elevation of the pedicels is not seen to this degree, save for *Cetiosaurus*, and then the elongation is still higher in *Patagosaurus*. The elongation of the neural arch and pedicels is only seen in *Mamenchisaurus youngi* (Pi et al. 1996). The lateral elongation of the transverse processes is reduced. Next to being elongated, the pedicels also show a lateral, ragged sheet of bone that stretches from the base of the prezygapophyses to the ventral end of the cprl. This is

1005 seen in a more rudimentary form in *Cetiosaurus oxoniensis* (Upchurch and Martin 2003,
1006 OUMNH J13644/2). The relatively horizontal lateral projection of the transverse processes
1007 also distinguishes *Patagosaurus* from many (more or less) contemporary basal non-
1008 neosauropodan eusauropods, as these tend to project more dorsally in *Cetiosaurus*,
1009 *Mamenchisaurus*, *Omeisaurus*, and also in the basal neosauropod *Haplocanthosaurus*
1010 (Hatcher 1903; Young and Zhao 1972; Pi et al. 1996; Tang et al. 2001; Upchurch and Martin
1011 2002, 2003). In anterior view, the neural arch is characterized by two dorsoventrally
1012 elongated oval excavations; the cprf, which are separated by a stprl. The stprl runs down to
1013 the dorsal rim of the neural canal. This is also seen in *Cetiosaurus oxoniensis* OUMNH
1014 J13644/2, and to some extent in *Tazoudasaurus* (Allain and Aquesbi 2008), and
1015 *Spinophorosaurus* (Remes et al. 2009). However, in these taxa, this lamina is shorter, as the
1016 neural arch is less dorsoventrally elongated. In *Patagosaurus* dorsals, the neural canal itself
1017 is also dorsoventrally elongated and oval, this is also seen in *Cetiosaurus oxoniensis* OUMNH
1018 J13644/2, although not to the extent of *Patagosaurus*. It is not slit-like, as seen in
1019 *Amygdalodon* (Rauhut 2003a; Carballido et al. 2011) and *Barapasaurus* ISIR 700
1020 (Bandyopadhyay et al. 2010). In posterior view, the spol remain close to the body of the
1021 neural spine, i.e. they do not flare out laterally as in the anterior and mid-dorsals. The
1022 hyposphene appears here as a small, rhomboid structure, accompanied by very faint
1023 centropostzygapophyseal laminae which are embedded in the posterior neural arch. The
1024 hyposphene is a few cm more dorsal to the neural canal (about 5 cm). It is prominently
1025 visible below the postzygapophyses, which now are aligned at 90° with the neural spine, and
1026 have a horizontal articular surface. Posteriorly, during the transition from mid- to posterior
1027 dorsals, the tpol becomes shorter, and eventually dissapears as the postzygapophyses
1028 approach each other medially. Instead, the stpol split into the medial and lateral
1029 spinopostzygapophyseal laminae (m.spol and l.spol, see Table 2). The podl include the l.spol.

The stpol continues to run down to the hyposphene. Posterior dorsals have a very rudimentary aliform process, sensu Carballido and Sander (2014).

The most noted autapomorphy of *Patagosaurus* is the presence of paired cdf, or fenestrae, which appear from dorsals PVL 4170 13 onwards. It was long thought that these were connected to the neural canal, however, recent CT data reveals that a thin septum which separates the adjacent fenestrae from each other, and from the neural canal. Ventrally these fenestrae form a central chamber, still well above the neural canal (see PVL 4170 13).

The cpof is present in posterior dorsals of *Patagosaurus*, however it is only weakly developed. It is more developed in *Cetiosaurus*.

Dorsal PVL 4170 (9): Anterior-mid dorsal with the centrum drastically reduced in anteroposterior length, making it stouter than the cervicals, but still clearly opisthocoelous., see Fig. 10. The left diapophysis, neural arch and part of the neural spine are partially reconstructed. The condyle has a slightly pointed protrusion on the midpoint, as in the cervicals (See Fig. 10A, B, F). Ventrally, the centrum constricts strongly immediately posterior to the anterior condyle (Fig. 10F). The ventral keel marginally visible, and exists more as a scar running down the midline from the small hypapophysis. The ventral side of the posterior cotyle is slightly deformed, with the left lateral end projecting further than the right. As in the other ventral posterior surfaces of the vertebrae, the lateral ends flare out slightly further posteriorly than the axial midpart (Fig. 10 A, B, F).

The neural canal in anterior view is subtriangular in shape, and transversely wider than dorsoventrally high (Fig. 10C). Directly above it, there is a small protrusion present of the hypapophysis. In posterior view, the shape of the neural canal is similar, however, the posterior opening is less triangular and more rounded (Fig. 10D).

The neural arch of this vertebra is still transversely wide, as in the cervicals. However, it is also becoming dorsoventrally higher (see Fig. 10A, B, C, D). Because of this, the

centroprezygapophyseal fossae, which are placed medially to the prezygapophyseal stalks, are not as deep as in the cervicals (Fig. 10C). In lateral view, the prezygapophyseal pedestals are directed nearly vertically in the dorsoventral plane (Fig. 10A, B).

The prezygapophyses are leaning slightly medially and ventrally towards the single intraprezygapophyseal lamina that runs along the midline of the vertebral neural arch on the anterior side (Fig. 10C). In dorsal view, the prezygapophyses are subtriangular in shape and are widely spaced apart, with about 1/3rd of the spinal summit width between them (Fig. 10E).

The postzygapophyses are raised even higher dorsally in this anterior dorsal than in the cervicals, at about 2/3rd of the height of the neural spine (Fig. 10A, B, D). Consequently, the podl are more elongated and makes a high angle, of about 130°, with respect to the axial plane and to the pcdl. Both podl's are slightly arched towards the postzygapophyses (Figure 10A, B). Because of the extension of the podl, the posdf takes in a large portion of the posterior lateral surface of the vertebra (Fig. 10A, B). The tpols in posterior view are prominent, convexely curving laminae, which meet right above the posterior neural canal. In lateral view, the tpols show a triangular recess below the postzygapophyses, after which the tpols expand posteriorly before meeting the hypopshene dorsal to the neural canal (Fig. 10D).

In this vertebra, the cpol's are no longer clearly visible, and indeed, only the left cpol is seen as a thin lamina on the neural arch, lateral and ventral to the left tpol (Fig. 10D). Here, a rudimentary hyposphene is present as a small teardrop-shape ventral to the ventral fusion of the tpols. The fusion of the tpols and the hyposphene are also visible as a triangular protruding complex in dorsal view.

The right diapophysis is prominent in anterior, posterior and lateral view as a stout, lateroventrally positioned element (Figure 10A, B, C, D). It is transversely broader than in the cervicals. In anterior view, the prdl and acdl/pcdl are all positioned in an inverted V-shape

with oblique angles of about 45° to the horizontal. In anterior view, the cprl divides the cprf neatly from the prcdf, which is similarly inverted V-shaped as the outline of the diapophyseal laminae (Fig. 10C). In posterior view, the pocdf is confluent with the posterior flat surface of the diapophysis (Fig. 10D). The posterior centrodiapophyseal lamina in posterior view, curves convexly towards the ventral side of the vertebra.

The articular surface of the diapophysis is flat to concave, and rounded to rectangular in shape. Posteriorly, they show small, elliptic depressions, on the distal end of the diapophyses (Fig. 10D).

Note that the sprl are reconstructed, and will not be discussed here. The spol are clearly seen in anterior view; they flare out transversely in a steep sloping line (Fig. 10C). The spol are rugose, and the tpol as well, these appear ragged in lateral view. In this anterior dorsal, the spinopostzygapophyseal fossae (spof) are more rectangular than in the cervicals, and also deeper (Fig. 10D).

The neural spine is constricted transversely around the dorsoventral midlength, and fans out transversely towards the summit. The spine summit consists of a thick transverse ridge, which folds posteriorly on each lateral side, before smoothly transitioning to the spols (Fig. 10E). The neural spine summit is positioned higher dorsally in this anterior dorsal than in the cervicals (so that the spol are consequently more elongated).

Dorsal PVL 4170 (10): This partially reconstructed anterior-middle dorsal (Fig. 11) is slightly taphonomically distorted, in that the right transverse process is bent slightly more ventrally, and the neural spine is slightly tilted to the left side (see Fig. 11). Parts of the centrum, the middle anterior part of the neural arch, and ventral parts of the diapophyses are partially reconstructed.

The centrum is still slightly opisthocoelous in lateral view, as in PVL 4170 (9), and as in the cervicals, with the characteristic stout rim cupping the anterior condyle (Fig. 11A, B). It is noteworthy however, that the centrum and neural arch do not entirely match, possibly due to this vertebra being partially reconstructed. The centrum in ventral view is transversely constricted posterior to the rim that cups the condyle (Fig. 11F). The rim stands out transversely from the centrum body. The parapophyses are located dorsal to this this expansion, as triangular protrusions. The cotyle in posterior view is concave, and is slightly transversely wider than dorsoventrally high.

The neural arch transversely narrows slightly, dorsal to the parapophyses (both at its anterior and posterior side; Fig. 11C). The anterior neural canal is embedded in this narrowing, and is rounded to rectangular in shape. It is less wide transversely as in the posterior cervicals (Fig. 11C). The posterior neural canal is equally rectangular to rounded in shape. About 5 cm dorsal to it, the hyposphene is present as a rhomboid, small structure (Fig. 11D).

The diapophyses in this dorsal are creating a wider angle with respect to the horizontal than in the last dorsal PVL 4170 (9), see Fig. 11C, D. The prdl, the acdl, and posteriorly, the pcdl, all arch into a less oblique angle, creating an inverted V-shape of about 50° (note that the right diapophysis is slightly distorted due to taphonomical damage). The diapophyseal articular surface is triangular, with the tip pointing ventrally, and the flat surface pointing dorsally, in lateral view (Fig. 11A, B). Ventral to the diapophyses, in lateral view, the anterior and pcdl are more or less equally distributed in length and spacing on the lateral surface of the neural arch. A roughly triangular but deep cdf can be seen between these laminae.

The prezygapophyses in dorsal view make a wide wing-like structure together with the diapophyses and the prdls (Fig. 11E). There is a U-shaped, wide recess between the prezygapophyses. In anterior view, the prezygapophyses stand widely apart from one another, and are supported by stout cprl, creating thick pedicels that expand laterally above

the centrum, dorsal to a slight recess right above the centrum (Fig. 11C). The articular surface of the prezygapophyses is rounded to rectangular in shape, and in anterior view is tilted ventrally towards the midline of the vertebra (Fig. 11C, E). The prezygapophyseal spinodiapophyseal fossae (prsdf) are present between the prezygapophyseal pedicels, on the neural arch. They are rounded to rectangular in shape, dorsoventrally elongated, and shallow, the deepest point being near the onset of the sprl (Fig. 11C).

The postzygapophyseal articular surfaces are obliquely offset from the hyposphene. The articular surfaces are roughly triangular in shape (Fig. 11D). In posterior view, the tpol are distinctly flaring out from the dorsal end of the hyposphene to the postzygapophyses. The cpols are present only as very faint, low ridges embedding the hyposphene on the lateral side (Fig. 11D). The postzygodiapophyseal lamina is short and stout, therefore dramatically reduced in length and angle compared to dorsal PVL 4170 (9), (Fig. 11A, B), leading to believe at least one dorsal between PVL 4170 (9) and (10) should have existed. The spof is deeply excavated, occupying about 1/3rd of the transverse length of the neural spine (Figure 11D,E). The postzygapophyseal centrodiapophyseal fossae (pocdf) are shallow, and only a bit more excavated near the ventral rim of the postzygapophyseal pedicels.

The sprl run from the top of the spine to the prezygapophyses in an oblique angle of about 40°. They flank the entire length of the neural spine, creating roughly a V-shape (Fig. 11C, E). The spol are clearly visible in anterior view in this vertebra, as they flare out laterally from the neural spine, giving the neural arch and spine a triangular appearance.

In anterior view, the neural spine is roughtly V-shaped, with a transversely broad dorsalmost rim (Fig. 11C). In posterior view, the neural spine combined with spol and postzygapophyses are slightly bell-shaped. The neural spine tapers dorsally to a point, exposing a stout rim. In dorsal view, the neural spine summit is clearly seen as an anteroposteriorly thin rim, transversely wide, reaching to the level of the onset of the postzygapophyses (Fig. 11E).

Dorsal PVL 4170 (11): Partially reconstructed dorsal; the centrum is a replica, which will not be described. The neural arch and spine and transverse processes, however, are original, see Figure 12. The diapophyses of this vertebra are elongated laterally compared to the other dorsals, and the transition between this and the previous and next vertebrae, leads to believe a transitional dorsal could have existed originally.

The neural arch is mainly shaped by the acdl in anterior view, and the pcdl in posterior view. It is about as long and wide, as PVL 4170 (10), see Fig. 12A, B. The neural canal in anterior view is rounded to rectangular in shape, with a dorsoventral elongation (Fig. 12C). The posterior neural canal is more flattened, and triangular to round in shape. The hyposphene is seen as a small rhomboid structure, about 5 cm dorsal to the posterior neural canal (Fig. 12D).

In this dorsal, the diapophyses are more prominent and extend wider transversely than in previous dorsals (Fig. 12C, D). Their shape in anterior and posterior view is near rectangular. They are directed laterally and slightly ventrally in anterior view (Fig. 12C). The articular surface of the diapophyses is more rounded than triangular (Fig. 12A, B). The diapophyses in posterior view are slightly expanded towards their extremities (Fig. 12D). The pcdl are slightly damaged and have a frayed appearance, but arch convexly towards the transverse processes.

The prezygapophyses are more or less perpendicularly placed towards the neural spine, and slightly canted medially in anterior view (Fig. 12C). Their articular surface lies in the dorsal plane. The articular surface of the prezygapophyses is roughly square in shape (Fig. 12E). In dorsal view, a U-shaped recess is seen between the prezygapophyseal articular surfaces. The prdl are stout and run in a convex arch transversely to the diapophyses. In this vertebra, the single intraprezygapophyseal lamina (stprl) is visible, as the interprezygapophyseal laminae (tprl) run down in a curved V-shape towards the neural canal (Fig. 12C). The paired cprf,

positioned laterally to the stprl, are more excavated than in previous dorsals, and also have a more defined rim.

The postzygapophyses are more pronounced in this vertebra than in previous dorsals, and also protrude posteriorly more than in previous dorsals (Fig. 12D). Their articular surface is triangular in shape. There is a similar U-shaped recess between the postzygapophyses, though not as wide, as with the prezygapophyses (Fig. 12C, D). The tpols are shorter in this vertebra, as they do not reach as far down ventrally to reach the hyposphene. Below the tpols, two cpols are seen to strut the hyposphene on lateral sides. The triangular and shallow pocdf's are positioned on each lateral side of the cpols, and ventral to the tpols (Fig. 12D).

The neural spine is transversely wide and anteroposteriorly short, but protrudes out posteriorly at both lateral sides and on the midline (Fig. 12D). This midline could be a rudimentary scar of a postspinal lamina (posl), but that is not clearly visible. In anterior view, the neural spine resembles that of PVL 4170 10, however the neural spine is more dorsoventrally elongated, and the spol are more dented than straight as they run down to the postzygapophyses. The morphology of the neural spine posteriorly, towards the postzygapophyses is similar to PVL 4170 10 in that the composition looks bell-shaped in posterior view, and the posterior half contains a deep V-shaped spof. The neural spine is more dorsally elevated however, and the summit is less transversely broad than in the previous dorsal (Fig. 12E).

Dorsal PVL 4170 (12): Mid-posterior dorsal with partially reconstructed neural spine (which will therefore be omitted from description). The transition from middle to posterior dorsals is perhaps the most drastic morphological transition in *Patagosaurus,* and hints at missing vertebrae (Fig. 13).

The centrum is clearly opisthocoelous, though the condyle is not as convex as in previous anterior dorsals (Fig. 13A, B). The centrum is posteriorly still wider transversely than anteriorly. The condyle still has a rugose rim, as in the cervicals. The parapophyses are positioned on the dorsolateral side of this rim, and are visible as rounded rugose protrusions. The pleurocoel is still clearly visible, and has a deep, rounded dorsal rim, and a clear rectangular posterior rim. The ventral side of the cotyle extends further posteriorly than the dorsal side (Fig. 13E). The cotyle is heart-shaped in posterior view, with a rounded 'trench' below the neural canal (Fig. 13D). In ventral view, the centrum is not as constricted as in previous vertebrae; even though there is still a slight constriction posterior to the rim of the condyle. The ventral keel is no longer present.

The neural canal in anterior view is elongated to an oval to teardrop shape, which is dorsoventrally longer than transversely wide (Fig. 13C). The neural canal in posterior view is oval to rectangular in shape, and is also dorsoventrally elongated.

The neural arch in this dorsal is rather rectangular and straight in anterior and posterior view, widens axially in lateral view, towards the prezygapophyses (Figure 13 A, B, C, D). A fenestra is formed instead of the cdf. The centrodiapophyseal laminae run smoothly in a convex curve towards the centrum.

The pedicels of the prezygapophyses are stout, and expand laterally towards the ventral side of the prezygapophyses (Fig. 13C). The tprl meet ventrally and at the midpoint between the prezygapophyses, where a rudimentary hypantrum is formed, below which a stprl runs down to the dorsal roof of the neural canal. This lamina separates two parallel, rhomboid, deep cprf.

In posterior view, the postzygapophyses form a wide V-shape, and the tpols meet dorsal to a small diamond-shaped possible rudimentary hyposphene, below which a stpol runs down to the neural canal, which is oval and dorsoventrally elongated (Fig. 13D). The podl is a sharply curved, short lamina, not to be confused with the spdl, which is not present in this vertebra

(Fig. 13A, B). Two parallel cpols might be present, but this is not entirely clear as the posterior part of this vertebra is partially reconstructed (Fig. 13D).

In anterior view, the diapophyses are no longer ventrally and laterally positioned, but dorsally and laterally, in an oblique angle dorsally (Figure 13C). In lateral view, pcdl runs in a sinusoidal shape down from the diapophysis to the neural arch, while the prdl is convex (Fig. 13A, B). The diapophyses extend a bit further ventrally in a subtriangular protrusion. The diapophyses are slightly excavated between the podl and the pcdl. In dorsal view, the diapophyses are seen to extend to nearly the entire width of the centrum (Fig. 13F). They are slightly pointed posteriorly as well.

Dorsal PVL 4170 (13): This is the most complete posterior dorsal of the holotype (Fig. 14, 15). It has consequently been scanned in order to elucidate on the pneumatic features present in the holotype (Fig. 14). The pneumatic opening ventral to the diapophyses, on the lateral surface of the neural arch, opens into an internal pneumatic chamber (Fig. 14 B, C), but is separated from the opening on the opposite neural arch by a thin septum (Fig. 14 I, J). The pneumatic chamber is situated ventral to this septum, and is round to squared in shape. It remains separated from the neural canal (see Discussion).

The anterior articular surface of the centrum is oval in anterior view, with a slight constriction at about two-thirds of the dorsoventral height (Fig. 15C). Consequently, the ventral side is transversely wider than the dorsal side. In posterior view, the posterior articular surface of the centrum is heart-shaped at its dorsal side, and flattened on its ventral side. The articular surface itself is slightly oval, and is constricted towards the upper 1/3rd as in the anterior side. In ventral view, the centrum is more or less equally flaring out at each articular surface, and slightly constricted in the midpoint. No keel is visible, but on the anterior ventral side of the centrum, a small triangular 'lip' is seen. In lateral view, the centrum is ventrally concave, with the posterior ventral side expanding further ventrally

than the anterior side (Fig. 15A, B). There is a slight depression on the lateral side of each centrum.

The dorsal anterior side of the centrum is expanding a bit further anteriorly beyond the pedicels of the neural arch, but the dorsal posterior side of the centrum expands considerably further posteriorly from the neural arch.

The parapophyses are not clearly visible in anterior view, however, they are visible in lateral and ventral view as rugose oval protrusions on the rugose lateral sides of the cprls.

In anterior view, the neural canal is clearly visible in this specimen. It is oval and dorsoventrally much more elongated than in the previous vertebrae (Fig. 15A). It is transversely narrow, and slightly above the midpoint is constricted, so that the neural canal looks like a figure 8-shape. The neural canal is not clearly visible in posterior view; however, the neural arch is excavated in a triangular shape around the neural canal (Figure 15D). It is surrounded by stout centropostzygapophyseal laminae. Dorsal to this depression, the stpol supports the rhomboid hyposphene from below (see description of postzygapophyses).

The neural arch itself is ventrally restricted transversely. The pedicels of the neural arch are equally dorsoventrally elongated and transversely narrow. The anterior side of the neural arch is characterised by a dorsoventrally oriented, long stprl, dividing two mirrored, shallow, oval to bean-shaped cprf. The lateral sides of the neural arch tilt towards the midline in posterior view, giving the neural arch a constricted look towards its dorsal end. On the lateral side of the neural arch, the centrodiapophyseal fossa (or more foramen in this vertebra) is visible as a dorsoventrally elongated oval, opening slightly posterior to the midpoint of the neural arch.

The diapophyses project laterally in a near perpendicular angle from the neural arch (Fig. 15A, D). They are ventrally excavated, with the prdl running concavely from the lateral side of the prezygapophyses to the diapophyses. In dorsal view, the diapophyses are seen to bend slightly posteriorly as well as laterally. The tips point sharply to the posterior side. The

diapophyseal articular surfaces are triangular, with a rounded posterior rim, in lateral view. The dorsal distal ends of the diapophyses have a small triangular protrusion, projecting dorsally, in anterior view. The diapophyses show round excavations on the posterior side of their distal ends. The ventral side of the diapophyses is also concavely curved with a concave paradiapophyseal lamina (ppdl) running parallel to the prdl. The pcdl curve concavely from the diapophyses down to the ventralmost side of the neural arch. These sustain a thin sheet of bone that holds the diapophyses on each lateral side in posterior view.

The prezygapophyses are transversely shorter than in previous dorsals, and are stout; almost as thick dorsoventrally as transversely (Fig. 15A, B, C). They tilt at an oblique angle anteriorly and dorsally from this narrow arch. The prezygapophyseal articular surfaces are horizontally aligned in the axial plane, and are near perpendicular to the neural spine. In dorsal view, prezygapophyses are directed mostly anteriorly, and there is a deep U-shaped recess between them. On the lateral side of the prezygapophyses, running from the lateral ends of the cdf, the cprl are characterized by laterally flaring, rugose, rugged bony flanges, that spread anteriorly as well as laterally. In anterior and lateral view, prdl and the ppdl run parallel in a convex arch at the ventral end of the neural spine. They are equally thin and dorsoventrally flattened.

The postzygapophyses are triangular in shape, and are positioned slightly more dorsally on the neural arch than the prezygapophyses (Fig. 15D). The postzygapophyses are flat to slightly convex on articular surface, seen from lateral and ventral view. The stpol tapers dorsally and posteriorly in an oblique angle from the rhomboid hyposphene to the neural arch. The postzygapophyses are not visible in lateral view as they are obscured by the diapophyses. The postzygapophyses connect with the diapophyses through a strongly bending podl, which is often mistaken for a spinodiapophyseal lamina (spdl; Wilson, 2011a, Carballido and Sander, 2014).

In this dorsal, the prdl and the podl are seen to support wide, but thin plates of bone between the prezyga- dia- and postzygapophyses.

The neural spine is roughly cone-shaped, and is constricted toward the summit both anteriorly and posteriorly. In anterior view, the sprl flare out towards the ventral contact of the prezygapophyses. The sprls are seen as sharply protruding thin laminae. The sprdfs, bordered by the sprls, are visible as deep triangular depressions in dorsal view. The neural spine shows a triangular excavated prezygospinodiapophyseal fossa (prsdf) on each lateral side, which have clear posterior rims.

Similar to the sprls, in posterior view, the spol are seen to flare out towards the ventral side of the neural spine. In this dorsal, the spol has divided into a lateral spol and medial spol (l. spol and m. spol), visible as running from the ventral one-third of the neural spine to the postzygapophyses. On the midline between these laminae, a deep but transversely narrow rudimentary spof is present. The lateral spols flare out on the lateral sides, giving the spine a 'rocket-shape' in posterior view. A slight transverse thickening of this stout lateral spol is visible at about two-thirds of the spinal dorsoventral length.

On the dorsoventral midline of the spine, in posterior view, a rough scar is visible, which could be a very rudimentary postspinal (posl) lamina.

The spine itself tilts very slightly posteriorly, especially the most distal one-third part. This distal end is solid, and cone-shaped, with a rounded summit. The spine summit has a slight bulge on each lateral side, which might be a rudimentary aliform process (see Carballido and Sander, 2014), and the summit is more rounded than flattened. The summit of the neural spine in dorsal view is rounded, but has a constricted anterior end, where it points towards the sprls. The posterior end projects more posteriorly and is round, though with a slightly pointed end at the posterior midline.

Dorsal PVL 4170 (14): Posterior dorsal with preserved neural arch, spine and centrum. Because of its fragile state, a ventral image could not be obtained. Parts of the diapophyses and neural arch are damaged.

In anterior view, the anterior articular surface of the centrum is oval, and dorsoventrally flattened, so that the transverse width is greater than the dorsoventral height (Fig. 16D). The dorsal end is slightly heart-shaped. The anterior articular surface of the centrum is dorsoventrally longer than the posterior side. The posterior dorsal rim of the articular surface of the centrum extends further posteriorly than the ventral side. The extension is rounded and is visible on both lateral sides of this dorsal vertebra (Fig. 16A, B). The width of the centrum extends beyond the width of the pedicels of the neural arch. In posterior view, the centrum is dorsoventrally flattened and expands a little transversely on the midline (Fig.16C). The dorsal end of the posterior articular surface is slightly excavated dorsally, as are posterior surfaces of the pedicels surrounding the neural canal, embedding the neural canal. In lateral view, the centrum is ventrally concave. It is slightly reconstructed however, so there might not be more original curvature preserved. There are shallow, elliptical depressions visible on each lateral side of the centrum.

The anterior side of the neural canal is oval and dorsoventrally elongated, and narrows in the upper one-third towards its dorsal end (Fig. 16D). The posterior side is more triangular in shape, but overall roughly similar to the anterior side (Fig. 16C). The medial sides of the pedicels of the neural arch are excavated, forming an oval excavation around the neural canal.

The anterior central part of the neural arch is damaged, thereby revealing the pneumatic centrodiapophyseal fenestra, which connects to each lateral side of the neural arch below the diapophyses (Fig. 16A, B). These openings perforate the neural arch to the posterior side, indicating there must have been only a thin sheet of bone covering them. The neural arch tapers towards the midpoint on both the anterior and posterior sides in lateral view,

however, the anterior end expands towards the posterior side again together with the parapophysis and the base of the prezygapophysis (Fig. 16A, B). The neural arch constricts around the central part of the vertebra in posterior view. On the right lateral neural arch, a neurocentral suture is present. Posteriorly, the hyposphene is visible as a clear triangular protrusion below the postzygapophyses. The hyposphene is smaller than in the previous dorsals (Fig. 16C).

The left lateral side of this dorsal is missing the diapophyses, however, this does give a good view of the proximal bases of the diapophyseal laminae; the prdl is a relatively delicate and short lamina that runs obliquely to the ventral anterior base of the prezygapophysis; the podl lies on the same oblique sagittal plane and projects dorsally and posteriorly towards the postzygapophysis (Fig. 16B). The right lateral side in lateral view shows the partial right diapophysis, of which the distal end is broken, revealing two laminae, the distal side of the prdl and the distal side of the pcdl (Fig. 16A). Also, a thin short lamina runs from the posterior end of the diapophysis to the postzygapophyses; this lamina connects also to the lateral spol, therefore is the podl+lspol complex. On both lateral sides, ventral to the diapophyseal base, the centrodiapophyseal fenestra is clearly visible and perforates the neural arch completely; however, there would probably have been a thin septum separating them.

The right diapophysis is partially preserved; it is shorter than in the previous dorsals, and stout. It projects laterally, slightly dorsally and posteriorly, unlike the diapophyses of the previous dorsals (Fig. 16A, B, C, D). The diapophysis is wing-shaped in posterior view; the pcdl encircles a wide sheet of bone on its posterior side. The prezygodiapophyseal lamina is visible in anterior view, as it curves convexly to the lateral distal end of the diapophysis. The ventral lateral side of the transverse process is marked by the prcdf.

The only prezygapophysis present is reconstructed. On the right lateral side, a rugose parapophysis is supported by an anterior centroparapophyseal lamina (cprl), which runs

along a ragged lateral rim of bone from the prezygapophyses to the ventral end of the pedicel of the neural arch, which is similar to those in PVL 4170 (13), see Fig. 16A. The actual prezygapophyses are missing or reconstructed, therefore there is no information known about these in this particular dorsal.

Because most zygapophyseal structures are either broken or reconstructed, not much can be said about the shape of these in dorsal view, however, the wide sheet of bone between the prdl and the pcdl is clearly visible in dorsal view (Fig. 16F). The left pedicel of the neural arch is partially visible. It is positioned slightly posterior to the anterior rim.

The postzygapophyses are ventrally convex, and dorsally stand out from the neural spine, making the spols protrude from the spine in an equal fashion. The podl + lspol complex is seen curving sharply convexely from the lateral end of the right postzygapophysis to the distal end of the diapophysis (Fig. 16C).

The neural spine in anterior view is straight and square in the upper one-third of its dorsoventral height, however, the anterior side tapers to a V-shaped point towards its ventral end (Fig. 16D). The 'V' is rugose. On each lateral side, slightly dorsal to this point, the spinoprezygapophyseal laminae widen the lowermost one-third of the neural spine. The summit of the neural spine is rugose and shows a small oval protrusion on its anterior midline (Fig 16F). The lower half of the neural spine shows a clear division between the lateral and medial spols, between which are evenly sized, slit-like fossae. The spof completely perforates the area between the postzygapophyses in an elliptical shape (Fig. 16C). The top of the neural spine is cone-shaped and rugose. There is no trace of a postspinal scar, as in more anterior dorsals. The neural spine in lateral view is excavated by the prsdf, which is triangular and relatively deep (Fig. 16A, B). The lspol is thick in the ventral half of the neural spine, however, at the lateral sides of the dorsal half of the neural spine it is only a thin edge that protrudes posteriorly from the spine. The lateral spols form a bell-shaped sheet around the lower half of the neural spine in posterior view, whereas the upper

half has the base of the lateral spol only visible as a thin lateral ridge (Fig. 16C). As in the previous dorsals, the distal end of the neural spine is massive, and cone-shaped. In this posterior dorsal, however, the lower half of the spine is bending anteriorly, the upper half of the spine is bending posteriorly (Fig. 16A, B). At the base of the upper half, a ridge is seen curving from the anterior lateral side to the posterior lateral side. In dorsal view, the summit of the neural spine is transversely wider posteriorly than anteriorly, giving it a trapezoidal shape (Fig. 16 E). The surface is rugose.

Dorsal PVL 4170 (15): This dorsal vertebra only has its centrum preserved (Fig. 17; 15). In anterior view, the anterior articular surface of the centrum is almost trapezoidal in shape, with lateral protrusions on the midline. The anterior articular surface is equally as high as it is wide. The posterior articular surface in lateral view is broken and not clearly visible. In lateral view, the centrum shows a concave ventral side, and a slightly more convex than flat anterior articular surface. Towards the dorsal middle part of the centrum, in lateral view, a shallow elliptical fossa is visible. The ventral floor of the neural canal is visible, and the lowermost lateral walls, indicating an elongated elliptical shape of the neural canal, as in the other posterior dorsals. In dorsal view, the neural canal is seen to cut deeply into the centrum, and shows a widening transversely towards the posterior opening. In dorsal view, the neurocentral sutures are either broken or unfused; the former is the more likely option, as the sutures are fused in the other dorsals of PVL 4170.

Dorsal PVL 4170 (16): This dorsal, though well-preserved, and only partially reconstructed, is unfortunately stuck behind a low bar on the ceiling of the Instituto Miguel Lillo, in the hallway where the holotype is mounted. As a result, only the right lateral side and some oblique views of the anterior side could be obtained (Fig. 17; 16).

The centrum is partially reconstructed; however, the dorsal end is original and is heart-shaped. In right lateral view, the centrum is almost quadrangular in shape. The dorsoventral height is slightly greater than the anteroposterior length. The posterior dorsal side of the centrum flares slightly laterally and posteriorly, and the neural canal creates a little 'gutter' on the dorsal surface of the centrum. On the lateral side of the centrum, dorsal to the axial midpoint, is an oval fossa, which is axially longer than dorsoventrally high. This fossa is dorsoventrally higher than in the previous dorsals, making it appear more round than elliptical.

The neural arch is supported by lateral pedicels, which rest more on the anterior side of the centrum than on the posterior. The pedicels of the neural arch in anterior view are of irregular shape, and show an almost anastomosing structure. The posterior part of the pedicels rests a few centimeters medial to the dorsal posterior rim of the posterior articular surface. From there, the posterior part of the pedicel inclines towards the medial side in lateral view. The dorsal end of the pedicels is axially constricted. The right lateral pedicel is broken off laterally. The anterior medial area, between the prezygapophyses, is excavated; this is probably due to a thin sheet of bone having been broken away, revealing the internal pneumatic structure.

The diapophysis is not very clearly visible in anterior view. The diapophyses are located slightly posterior to the midline of the neural arch. In lateral view, the articular surface is a thin, semi-lunate dorsoventrally elongated ridge.

The prezygapophyses are supported below by stout colums that project obliquely anteriorly and dorsally; these are also convex anteriorly.

The prezygapophyses have a flat axial articular surface, and are supported from below by stout convex columns.

The postzygapophyses are situated at around the same elevation as the prezygapophyses.

The articular surface of the postzygapophyses is slightly inclined ventrally. The hyposphene

extends further posteriorly than the postzygapophyses, and has a ragged outline in lateral view; this could however be caused by damage to the bone.

The neural spine is slightly inclined towards the posterior side in its lower half, the upper half is more or less erect in the dorsoventral plane. It is slightly wider at its base, however the upper 2/3rd is of an equal axial width. The summit is rod-shaped. The accessory lamina seen in the previous two dorsals is seen around halfway to the summit, running in a semicircular line from anterior dorsal to posterior ventral.

Dorsal PVL 4170 (17): The posteriormost dorsal is only partially preserved, and therefore is partially reconstructed (Fig. 17; 17). It is also not possible to unmount this dorsal, therefore the view is limited to the anterior side and the (partial) lateral side. The centrum shows deep lateral depressions, and is more oval than round, as in the previous dorsals. The neural arch is similar in morphology to the previous posterior dorsals, with stout prpls and a deep depression between each lateral side of the neural arch. The prezygapophyses are inclined medially, rather than being horizontally aligned with the sagittal plane. The neural spine has very sharp outstanding sprls and spols between which the spine has deep depressions on anterior and lateral sides, which are oriented dorsoventrally. The spine summit is a massive block of bone, and has a square shape. Two rudimentary but clearly visible aliform processes are positioned slightly ventral to the dorsal spine summit on each lateral side.

Sacrals PVL 4170 (18): The complete sacrum is well-preserved (see Bonaparte 1986b, Fig. 43 and 44, and this manuscript, Fig. 18, lower row, A-D). Unfortunately, because the holotype specimen is mounted, it is difficult to access. Most recent pictures can only show the neural arches and the spines, as the rest of the view is blocked by the ilium laterally (Fig. 18C), by the dorsal vertebrae anteriorly, and by the caudal vertebrae posteriorly, although the caudal vertebrae can be unmounted. Bonaparte's 1986 *Patagosaurus* description shows a detailed

illustration, however; see Bonaparte (1986b), and Fig. 18D. The sacrum consists of five sacral vertebrae, of which all centra are fused. This is in contrast to *Vulcanodon*, *Barapasaurus,* *Shunosaurus* and *Spinophorosaurus*, who are reported to have had four sacral centra (Remes et al. 2009; Bandyopadhyay et al. 2010; Carballido et al. 2017b). *Ferganasaurus* and *Jobaria tiguidensis* had five sacral centra (Alivanov and Averianov 2003; Carballido et al. 2017b). *Haplocanthosaurus, Camarasaurus* and diplodocids had five (Although some have been reported to have had six, Tschopp et al. 2015; Carballido et al. 2017b). In PVL 4170 (18), the second, and third of the neural spines are fused together by their anterior and posterior sides. This is similar to *Barapasaurus* (Bandyopadhyay et al. 2010), but different from *Ferganasaurus* and neosauropods; e.g. *Ferganasaurus verzilini* Alifanov & Averianov, 2003 and diplodocids fuse the sacral neural spines 2-4, whereas *Camarasaurus* Cope, 1877 and *Haplocanthosaurus* fuse sacral neural spines 1-3 (Alivanov and Averianov 2003; Upchurch 2004). All neural spines are rugosely striated (Fig. 18B). They all possess sprl and spol, which are roughly similar to the morphology of the posteriormost dorsal vertebrae. No spdl is present. The dorsal rim of the ilium terminates at about the diapophyseal height of the sacrum (Fig. 18C). The neural spines extend dorsally beyond the upper rim of the ilium for about 30 cm. In mamenchisaurids, as well as in *Camarasaurus* and basal titanosauriforms, the neural spines of the sacrum are much shorter (not as dorsoventrally high as the neural arch and centrum combined), and more robust (Ouyang and Ye 2002; Taylor 2009). In neosauropods such as *Apatosaurus*, *Diplodocus* and *Haplocanthosaurus*, however, the neural spines do extend further beyond the ilium. In *Haplocanthosaurus*, the neural spine is and are as dorsoventrally high as the neural arch and centrum together, like in *Patagosaurus;* however, some diplodocids have higher sacral neural spines. (Gilmore 1936; Hatcher 1901, 1903). The sacral ribs do not project over the ilium, as they do in neosauropods (Carballido et al. 2017b).

The first sacral PVL 4170 18.1 is, as in most sauropods, relatively similar to the posteriormost dorsal (Upchurch 2004). The centrum is oval, and dorsoventrally elongated (Fig. 18D). The neural canal is oval and also dorsoventrally elongated, as in the posterior dorsals. The sacral rib is unattached to the diapophysis in this sacral vertebra. It is a lateral dorsoventrally elongated extension, as in most sauropods, a C-shaped plate that extends laterally towards the medial side of the ilium (Upchurch et al. 2004). The prezygapophyses are anteriorly elongated, and flat dorsally, and have a deep U-shaped recess between them, as in the posterior dorsals (Fig. 18A). They connect to the neural spine via the spinoprezygapophyseal laminae, which project as sharp ridges off the lateral sides of the anterior side of the neural spine. Lateral and anterior to the postzygapophysis, the podl runs to the transverse process of the first sacral. As in the posterior dorsals, dorsal to the postzygapophyses, a rudimentary aliform process is present. From here, the lateral spol flares out laterally and dorsally before it joins the postzygapophysis. The sprl encases a deep triangular depression, which is visible on the lateral side of the neural spine, which could be the sacral equivalent of the spdf in *Patagosaurus* (see Wilson et al. 2011).

The neural spine inclines slightly anteriorly, as in the posteriormost dorsals. The anterior surface of the neural spine shows rugosities for ligament attachments. On the lateral side of the neural spine, a triangular depression runs over about 2/3rds of the dorsoventral length (Fig. 18A, D), with a sharp dorsal semicircular rim. Dorsal to this rim, the spine becomes solid. The spine summit is rounded laterally and has a crest-like shape in anterior view.

The second and third sacral neural spines PVL 4170 18.2 and 18.3 are fused (Fig. 18A, C, D). Both the second and third sacral vertebrae have large C-shaped sacral ribs that connect to the medial side of the ilium. These sacral ribs project laterally and slightly posteriorly from the neural arch above the centra. Between these sacral ribs, dorsoventrally elongated and axially short intervertebral foramina (ivf; Wilson et al. 2011) are visible as slit-like apertures,

which in this sacrum are fenestrae that connect to large internal pneumatic chambers inside the sacral centra.

The second sacral neural spine is projecting mainly dorsally, and only slightly anteriorly (Fig. 18A, C, D). At the base of the spine, the sprl and spol and the dorsal side of the sacral transverse process border a triangular sdf, as in the first sacral. This fossa is more oval-to-triangular, which is different from the first sacral. This fossa is also present on the third sacral and is more pronounced there; being axially wider and more triangular. Between both neural spines, a thin plate of bone was probably present, as there is a small slit, which does not appear natural. The neural spines are dorsally connected by rugose bone tissue. In lateral view, this connection has a U-shaped concavity between both neural spine summits.

The fourth sacral vertebra PVL 4170 18.4 inclines slightly more posteriorly than the previous sacrals (Fig. 18A, C, D). The sacral rib of this sacral is a C- or heartshaped laterally projecting bony plate. Between this sacral rib and the sacral rib of the third sacral, a large dorsoventrally elongated slitlike opening is seen to connect to the internal pneumatic chamber of the sacrum.

The prezygapophyses are not visible; the postzygapophyses are rhomboid, laterally projecting protrusions. The hyposphene is equally rhomboid.

In anterior view, the neural spine is transversely shorter than the previous sacrals, however, axially it is equally wide, giving the spine summit a rhomboidal shape. At the anterior side of the base of the spine, a triangular protrusion is visible, which appears broken, therefore this sacral might have been connected to the third sacral by a bony protrusion at the bases of the neural spines. On the lateral side of the spine, a deep groove is seen to run concavely from the dorsal anterior lateral side to the ventral posterior lateral side, as in some anterior caudals (see caudals later). The dorsal lateral side of the neural spine shows a weakly developed aliform process. In posterior view, the lateral spinopostzygapophyseal laminae

1573 are seen to protrude dorsally from the neural spine, which is very rugosely dorsoventrally
1574 striated.
1575 The fifth sacral PVL 4170 18.5 is slightly different in morphology from the previous four, in
1576 that it is slightly posteriorly offset from the others (Fig. 18A, B). The posterior articular
1577 surface of the centrum is clearly visible in this last sacrum, and is flat to slightly
1578 amphicoelous. It is oval in shape, and slightly dorsoventrally elongated, and slightly
1579 transversely flattened. The neural canal is a dorsoventrally elongated oval shape. Directly
1580 dorsal to the neural canal, a small triangular and posteriorly projected protrusion is visible,
1581 which resembles the small anteriorly projected protrusions above the neural canal of some
1582 of the dorsal vertebrae. The lamina that projects laterally towards the sacral rib has a
1583 dorsolaterally directed bulge, so that the rib projects laterally in two stages (Fig. 18B). The
1584 main body of the sacral ribs of this last sacral are directed laterally, but also bend anteriorly
1585 towards the other sacrals. The postzygapophyses are diamond-shaped, as is the
1586 hyposphene. The spol in posterior view are slightly offset from the spine, and at about half
1587 of the dorsoventral height of the spine, protrude in a rounded triangular shape. This might
1588 have been a ligament attachment site. The spine itself is rugosely striated and resembles the
1589 fourth sacral in morphology.
1590
1591 *Caudals:* The holotype PVL 4170 has a few anterior, mid, and mid-posterior caudals
1592 preserved. The caudal numbering is rather discontinuous, indicating that the caudal series
1593 was already incomplete when it was found. Two caudals are without collection reference
1594 numbers, but will be described here for completeness, and positioned in the caudal series
1595 relative to their size and morphology. Two caudals are repeated, as one is a cast of the
1596 other.
1597 Anterior- to anterior-mid caudals (PVL 4170 19-20-21) have dorsoventrally high and axially
1598 short centra (Fig. 19), as seen in *Cetiosaurus, Tazoudasaurus* and *Chebsaurus*. They display

rounded triangular-to-heart-shaped anterior vertebral articular surfaces, and slightly more heart-shaped posterior vertebral articular surfaces, the most acute tip being the ventral side. The centrum in lateral view is concavely curved on the ventral side, with the slope on the anterior half less acute than on the posterior half. A faint raised ridge of bone is seen in some caudals on the lateral centrum, ventral to the diapophyses. This is also seen in *Cetiosaurus*, and could be a rudimentary lateral ridge as seen in neosauropods (Tschopp et al. 2015). The posterior dorsal rim of the centrum shows an inlet for the neural canal, as in the cervicals and dorsals, and stretches slightly beyond the posterior end of the base of the neural spine.

In ventral view, two parallel axially positioned struts are visible, between which is a 'gully'; an axially running depression. This feature is seen in other basal eusauropods (*Cetiosaurus oxoniensis* and the Rutland *Cetiosaurus*; (Upchurch and Martin 2002, 2003) as well as an unnamed specimen from Skye, UK (Liston 2004), though is not as prominently developed in *Patagosaurus* as in the latter taxa. This feature is named the 'ventral hollow' in neosauropods, and is also found in derived non-neosauropodan eusauropods (Mocho et al., 2016), as well as in a possible neosauropodan caudal centrum from the Callovian of the UK (Holwerda et al. 2019). Pronounced chevron facets are present, as in all sauropods (e.g. *Cetiosaurus oxoniensis, Lapparentosaurus, 'Bothriospondylus madagascariensis'* Bonaparte, 1986b, *Chebsaurus* and in caudals from unnamed taxa from the Late Jurassic of Portugal (Upchurch & Martin 2003; Läng and Mahammed 2010; Mannion 2010; Mocho *et al.* 2016)) but not as prominent as in *Vulcanodon* (Raath 1972; Cooper 1984) or *Cetiosaurus*.

The transverse processes are short and blunt, and project slightly posteriorly as well as laterally. Below them, rounded shallow depressions are visible, which are a vestigial caudal remnant of the pleurocoels. These depressions are both in anterior and middle caudals bordered by slight rugosities protruding laterally from the centrum, which could be very rudimentary lateral and ventrolateral ridges, but this is unsure, and not recorded in non-

neosauropodan eusauropods (Mocho et al. 2016). The neural arch is both dorsoventrally as well as axially shortened compared to the dorsals and sacrals. Lamination is rudimentarily present; in particular the sprl, spol, stpol and tprl are visible anteriorly and posteriorly. Small, blunt pre- and postzygapophyses are also present. The prezygapophyses rest on short, stout stalks that project anteriorly and dorsally. The postzygapophyses are considerably smaller than the prezygapophyses, and project only posteriorly as small triangular protrusions. These are, however, still prominent in anterior caudals; more so than in *Spinophorosaurus* (Remes *et al.* 2009). Prezygapophyses and postzygapophyses are strongly diminished in the anterior caudals and continue to do so towards the posterior caudals. Prezygapophyses are expressed as small oval protrusions, in anterior caudals still projecting from stalks, in middle and posterior simply projecting from the neural arch. The postzygapophyses are even further diminished, are only seen as small triangular protrusions from the base of the neural spine, and disappear completely in posterior caudals. The hypophsene remains visible, however, as a straight rectangular structure projecting at 90° with the horizontal. The neural spine is dorsoventrally high, and projects dorsally and posteriorly.

The most distinctive features of this set of vertebrae, however, are the elongated neural spines. These taper posteriorly, and dorsally, in a gradual gentle curve, which becomes more straightened towards the dorsal end. Towards the tip of the neural spine, the lateral surface expands axially. The spine summit displays the same characteristic saddle shape as in the posterior dorsals, in that in lateral view both anterior and posterior dorsal ends bulge slightly, with a slight depression on the midline between these bulges. In lateral view, as well as posterior view, the posterior side of the spine shows long coarse rugose dorsoventrally running striations, probably for ligament attachments. In particular, one or two grooves of approximately 1 cm wide are seen aligned in the dorsoventral plane, a few centimeters from the posterior rim in lateral view. These run from the midline of the spine, a few centimeters below the spine summit, to the posterior rim of the spine, just above the hyposphene.

Middle caudals (PVL 4170 22-25) are more elongated axially, with the axial length slightly higher than the height or width of the centrum (Fig. 20). However, the centrum height and width are still similar to the anterior-mid caudals (see Table 2). The centrum in lateral view shows a concave surface between two slightly raised ridges, as seen in *Cetiosaurus*. The ventral side of the centra is concavely and symmetrically curved, as opposed to the more anterior caudals. The base of the spine is axially wider than in the anterior caudals, and together with the base of the prezygapophyses, forming the simplified neural arch, rest more on the anterior half of the centrum, a feature commonly seen in non-neosauropodan eusauropods as well as in neosauropods (Tschopp et al. 2015). The posterior dorsal side of the centrum inclines slightly dorsally. The diapophyses are reduced to small rounded stumps that protrude laterally and slightly dorsally. They are positioned on the ventral and posterior side of the neural spine bases. Below the transverse processes a very shallow depression can be seen, unlike in *Tazoudasaurus* where well-defined round fossae are still present on the middle caudals (To1-288, Allain and Aquesbi 2008). Most prezygapophyses are broken; their bases are visible as broad stout bulges. The base of the neural spine bulges out laterally, and is extended axially to the base of the prezygapophyses, creating a broad stout pillar in lateral view. The spine is inclined posteriorly, and shows a gentle sinusoidal curvature on the posterior rim. The neural arch and spine shift towards the anterior side of the centrum in middle and posterior caudals.

Posterior-mid caudals (PVL 4170 (26) – (30) increase in axial centrum length and decrease in centrum height, giving the centrum a dorsoventrally flattened oval shape. The posterior articular surfaces of the centra have a small inlet on their dorsal rim, rendering them heart-shaped. From PVL 4170 (26) the transverse processes diminish into slight bulges underneath which a small shallow elliptical depression is visible. The postzygapophyses are present as stunted, slightly square ventral protrusions on the neural spine; the prezygapophyses are more developed and protrude as short stout struts anteriorly and dorsally from just above

the base of the neural spine. The neural spine inclines heavily posteriorly, and becomes rectangular; losing the sinusoidal curvature.

The last preserved, posteriormost caudals of the holotype (note that these are not the posterior-most caudals of the skeleton, PVL 4170 (31) – (34) display an elongated centrum, further decreased centrum height and a symmetrically curved concave ventral side. Most neural spines are broken off or damaged; only PVL 4170 (32) has a neural spine that curves posteriorly and aligns with the axial plane. The diapophyses are further reduced as small rugose stumps, and the elliptical depression below these is barely discernible. The prezygapophyses are short stunted protrusions on the anterior end of the spine, nearly equal in height with the spine. The articular surfaces are round rather than heart-shaped.

PVL 4170 (19):

The first caudal that is preserved is an anterior- to mid- caudal. The centrum is dorsoventrally higher than transversely wide, and is axially short, as in the posterior dorsals and sacrals (Fig. 21 A, B).

In anterior view, the anterior articular surface of the centrum is oval, and dorsoventrally higher than transversely wide (Fig. 21D). However, the upper 1/3rd of the anterior articular surface is transversely broader than the transverse width of the midpoint, and towards the lower 1/3rd this width decreases further. The ventral side of the articular surface is slightly V-shaped (Fig. 21E). The dorsal section of the articular surface shows a protruding sharp 'lip-like' rim. 'Lips' on the dorsal rim of the articular surface of the caudals are an autapomorphy in *Cetiosaurus* (Upchurch and Martin 2003). However, *Patagosaurus* has less distinctive 'lips' than *Cetiosaurus,* potentially hinting at a shared feature for Cetiosaurids. The articular surface is concave, with the deepest point slightly dorsal to the midpoint. In posterior view, the articular surface of the centrum is heart-shaped, due to two parallel elevations of the dorsal rim between which a gully for the neural canal exists (Fig. 21C). The articular surface

is less concave than its anterior counterpart, and also less extensive; the outer rim stretches towards the centre of the articular surface, which is flattened, and only the area slightly dorsal to the midpoint is slightly concave. In lateral view, the centrum is ventrally mildly concave, and the rims of both posterior and anterior articular surfaces show thick circular striations, seen in weight-bearing bones of sauropods, e.g. *Cetiosaurus, Giraffatitan, Tornieria* (H. Mallison pers. comm.; see Fig. 21A, B). The centrum is dorsoventrally much higher than it is axially long, however; this length has decreased with respect to the sacrals and the posterior dorsals. The neural canal is triangular to rounded in shape, both in anterior and posterior views.

The diapophyses project laterally and dorsally in anterior view, and in dorsal view, they are also seen to project slightly posteriorly (Fig. 21D, F). Their shape is triangular with a stunted distal tip; the dorsal angle made with the centrum is less acute than the ventral one. Between the diapophyses and the neural arch, a raised ridge of bone is present, similar to that of anterior caudals of *Cetiosaurus* (Upchurch and Martin 2003). Whether this is a rudimentary lateral ridge, seen in neosauropods (Tschopp et al. 2015) is unsure.

The neural arch is formed of a square elevated platform upon which the prezygapophysis and the neural spine rest (Fig. 21A, B, F). The prezygapophysis projects anteriorly and dorsally from the neural arch, at an angle of ±100° with the horizontal. The base of the prezygapophyses is stout, after which it tapers towards the distal end. The medial articular surface of the prezygapophysis is round with an internal rounded depression. In posterior and lateral view, the hyposphene is visible as a squared protrusion at the posterior base of the neural spine. It makes an angle of 90° with respect to the axial and dorsoventral planes. The postzygapophyses are only visible as raised oval facades, dorsal to the hyposphene. The postzygapophyses are formed as triangular lateral protrusions, which project from the base of the neural spine, between which is an oval depression, likely a rudimentary caudal spof.

The neural spine is diverted to the left lateral side in anterior view; this is probably a taphonomic alteration (Fig. 21D). It has roughly the same morphology as in the dorsals; a constricted base and a widened summit, with gently curving lateral sides. The spine is heavily striated on the surface of the upper 2/3rds of the dorsoventral height. The neural spine in lateral view gently curves convexly posteriorly and concavely anteriorly. The summit has a distinct saddle shape in lateral view. The spine summit is elevated in the centre and has two anterior and posterior rims, which are at a lower elevation than the middle part, as is seen in the neural spine summits of the dorsal vertebrae. The neural spine is rugosely striated in the dorsoventral plane in posterior view, and is offset to the right (Figure 21C). Two spol are clearly visible.

PVL 4170 (20): This anterior caudal resembles PVL 4170 (19). In anterior view, the anterior articular surface is asymmetrically oval, with a slightly flattened dorsal rim, and a slightly triangular ventral one (Figure 22D). It is also transversely broadest slightly dorsal to the midline. The dorsal edge shows lateral elevations, between which a slight rounded indentation exists on the midline. In posterior view, the articular surface of the centrum is more heart-shaped than oval (Fig. 22C). It has a thick rim, showing circular striation marks, which is not as concave as the inner part of the articular surface. This concave surface, however, is less concave than the anterior articular surface. The posterior dorsal rim of the centrum does not extend posteriorly, but it faces ventrally in an oblique angle towards the axial plane, as in PVL 4170 (19), however, the posterior dorsal rim of the centrum extends further ventrally in PVL 4170 (20). In lateral view, the centrum is axially short and dorsoventrally elongated as in the posterior dorsals and the sacrals. The ventral side of the centrum, however, is symmetrically concavely curved, with posterior and anterior rims bulging out concavely towards the ventral side.

The neural canal is visible as a semi-circular indentation in the neural arch. It is much broader ventrally than in PVL 4170 (19), see Fig. 22C, D.

In ventral view, the anterior chevron facets are broken off Fig. 22F). The centrum is concave on both lateral sides, and shows a slight depression beneath the diapophysis. Right at the base of the diapophysis however, it shows a slight convexity.

The centrum is anteriorly slightly convex, and posteriorly slightly convex, in dorsal view.

The left diapophysis is preserved, and this projects laterally in anterior view, with an angle of 90° with respect to the dorsoventral plane (Fig.22C, D). The diapophysis in dorsal view projects posteriorly and slightly dorsally. The diapophysis is flat and rectangular in dorsal view, with the anterior edge being convex and the posterior one concave.

The prezygapophyses are visible above the neural canal as short rounded triangular stubs, which project dorsally and slightly laterally (Fig. 22A, B, D). In dorsal view, the prezygapophyses are rounded-triangular protrusions that fork from the base of the neural arch, and which bend slightly medially, towards each other. The postzygapophyses are broken off, although the bases are present, showing a dorsoventrally elongated, dorsally triangular and ventrally oval shape (Fig. 22C).

The neural spine is stout and cone-shaped in anterior view, and displays paired sprl (Fig. 22D). The base of the neural spine is axially constricted; the neural spine broadens axially towards its dorsal end. The spine shows rugose longitudinal striations on its lateral sides (Fig. 22A, B). Though possibly broken and damaged, it shows a similar curve as in PVL 4170 (19), in that the posterior side curves convexly and the anterior concavely, allowing the neural spine to curve gently in a sort of L-shape. The tip of the neural spine is not as saddle-shaped as in PVL 4170 (19), however, there is still a slight curvature of the neural spine summit visible on its posterior side (Fig. 22A, B). The spine summit is similar in shape to those of the posterior dorsals of PVL 4170 (19), in that the sides of the summit are tapering slightly

ventrally from a 'platform' that is the dorsalmost part. The summit is a rhomboid-shaped knob, which is transversely broader anteriorly than posteriorly (Fig. 22E).

PVL 4170 (21): This anterior - mid caudal has a much more heart-shaped anterior articular surface than PVL 4170 (19-20), however, the lower half of the articular surface is reconstructed, therefore it is not certain that the original form persists (Fig. 23D). The deepest concavity is not at the midpoint but slightly above it, about 1/3rd of the dorsoventral length of the articular surface down from its dorsal rim. The dorsal rim has a slight 'lip'; an anteriorly protruding part of the rim that cups the articular surface. The midpart of this lip is bent ventrally with two lateral bulges, giving it a heart-shape, as in PVL 4170 (19-20), see Fig. 23C. In posterior view, the articular surface of the centrum is rounded-to-triangular in shape. The posterior articular surface is less concave than the anterior articular surface. In lateral view the centrum is more elongated than in PVL 4170 (19-20). In ventral view, the posterior edge of the centrum shows slightly developed chevron facets (Fig. 23E). The lateral sides of the centrum are strongly concave, the axial centrum length is increased in this caudal vertebra, compared to PVL 4170 (19-20).

The neural canal is near semi-circular with the horizontal axis on the ventral side. In dorsal view, the posterior dorsal rim of the centrum retreats towards the neural arch in a U-shaped recess, posterior to the neural canal opening (Fig. 23C).

The left diapophysis is preserved; the right is broken off (Fig. 23C, D). The left diapophysis is a stout straight element in anterior view, and is slightly tilted towards the anterior and dorsal side. The extremity is roughly triangular in outline (Fig. 23B). In dorsal view, the diapophysis is seen to bend posteriorly as in PVL 4170 (19-20). The prezygapophyses are flattened in dorsal view, and slightly spatulate. The diapophysis is seen to deflect slightly posteriorly Fig. 23F).

The prezygapophyses are stout dorsoventrally broad struts (Fig. 23A, B, D). They are triangular in shape, with dorsoventrally elongated struts, and are directed dorsally. The neural arch is tilted, probably due to taphonomical alteration. The postzygapophyses are small rounded triangular bosses posterior to a large bulge on the neural spine (Fig. 23A, B, C). This bulge is set right ventral to an axial constriction of the neural spine, after which it constricts slightly again.

The spine summit is similar to PVL 4170 (19) - (20). It constricts transversely at about 1/3rd of the dorsoventral length towards the summit, after which it slightly transversely widens towards the summit; the sprl follow a similar pattern (Fig. 23A, B, F). Dorsal to the postzygapophyses, the spine also bends more posteriorly after this bulge, similar to PVL 4170 (20). The top 1/3rd of the spine shows ligament attachment sites in lateral view. The neural spine expands slightly towards the summit in a rhomboid shape, with dorsoventrally deep striations for ligament attachments. The summit is 'saddle shaped', as in the other anterior caudals PVL 4170 (19-20), see Fig. 23F.

PVL 4170 (22): This anterior middle caudal has a partially broken neural spine and partially broken right prezygapophysis Fig. 24A, B). In anterior view, the articular surface of the centrum is oval, with the dorsal edge similar to PVL 4170 (19) – (21), see Fig. 24D. In posterior view, the articular surface is oval to round, with the long axis on the dorsoventral plane (Fig. 24C). The rim that cups the articular surface is thinner than in PVL 4170 (19) – (21). In lateral view, the ventral side of the centrum is concave, and in ventral view the anterior rim showing chevron facets (Fig. 24A, E). Because the ventral side of the centrum slopes down, the posterior end lies lower than the anterior end (Fig. 24A). In ventral view, the centrum is symmetrically concave transversely. The axial midline is smooth, with no keel or struts, however, anteriorly two large, rugose semi-circular chevron facets are visible, and posteriorly two smaller semi-circular ones (Fig. 24E).

The neural canal is triangular to semi-circular. In posterior view, the neural canal is semi-oval (Fig. 24C, D).

The prezygapophyses are less triangular than in PVL 4170 (21), rather they are blunted triangular to rounded (Fig. 24A, D). The prezygapophyses are stout struts that protrude anteriorly and dorsally from the neural arch. They have a rounded tip at their extremities. In dorsal view, the prezygapophyses show stout beams and stout sprl. Posteriorly, the same U-shaped recess is visible as in PVL 4170 (19) – (21), ventral to the hyposphene and postzygapophyses, which together have the same morphology as the previous caudals PVL 4170 (19) – (21) and the posterior dorsals PVL 4170 (16) - (17), see Fig. 24A, C.

The diapophyses bend towards the posterior side (Fig. 24B). The centrum is broadened transversely around the diapophyses.

The neural spine is inclined posteriorly, directly dorsally from an axial thickening of the neural spine (Fig. 24A). This part however, is broken off.

PVL 4170 (23): In anterior view, this middle caudal has a round articular surface (Fig. 25C). The articular surface is concave, with the deepest point in the center. The same thick rim is present as in PVL 4170 (19) –(22), however it is less rugose in this caudal. In posterior view, the articular surface is round (Fig. 25D). The rim surrounding the articular surface shows rounded striations as in the previous caudals. In ventral view, the centrum is of a similar morphology to in PVL 4170 (22), see Fig. 25E. It has two well-developed chevron facets on the anterior ventral rim of the anterior articular surface. These chevron facets are connected medially by a rugose elevated ridge of bone. On the posterior rim two small semi-circular chevron facets are discernible.

The neural canal is rounded to triangular in shape, with the horizontal plane on the ventral side (Fig. 25C, D).

The prezygapophyses are directed more dorsally than anteriorly (Figure 25A, C). In dorsal view, the prezygapophyses are bent towards their medial side, as in PVL 4170 (22), see Fig. 25B. In lateral view, the neural arch is of similar morphology as in PVL 4170 (22), however, the prezygapophyses are directed more dorsally than ventrally and the diapophyses are shorter in length (Fig. 25A).

The diapophyses are thickened axially compared to previous caudals, and remain closer to the central body, where the centrum is thickened transversely (Fig. 25B). Both the diapophyses and postzygapophyses are reduced in size compared to previous caudals. The postzygapophyses are present as small triangular bosses (Fig. 25A, D).

The neural spine is of equal transverse width, unlike the previous caudals (Figure 25A). The neural spine is still elongated as in previous caudals; however, it is straighter and does not bend dorsally more than 1/3rd of its dorsoventral length onwards. The axial thickening however, is still visible as in the previous caudals. The spine summit is slightly saddle shaped as in the previous anterior caudals (Fig. 25B). The neural spine summit does still show the elevated rhomboid morphology as in the previous anterior caudals and in the posterior dorsals of PVL 4170.

PVL 4170 (24): In anterior view, this caudal has a more oval than round articular surface, with the long axis in the dorsoventral plane (Fig. 26D). This is different to the other caudals; however, it and its surrounding thick rim are also partially damaged on the anterior surface. In posterior view, the articular surface of the centrum is oval, with the long axis in the transverse axis, giving the articular surface a more flattened appearance (Fig. 26C). In lateral view, the centrum shows an elliptical fossa ventral to the diapophyses (Fig. 26A, B). In ventral view, the centrum is smooth, without a keel or rugosities, with only a faint ventral groove, and is transversely concave (Fig. 26F). The anterior chevron facets are similar to those in PVL 4170 (23), however they are less developed (Fig. 26F).

The neural canal is more semi-circular than triangular (Fig. 26C, D). The neural arch supporting the posterior neural canal opening is triangular in shape, and the neural canal itself is oval with an elongation on the dorsoventral plane (Fig. 26C).

The right prezygapophysis is slightly damaged; the left is complete (Fig. 26A, B, E). Its articular surface bends towards the lateral side, unlike in the previous caudals. The prezygapophyses are more elongated, and the postzygapophyses (Fig. 26C) are more pronounced in this caudal, unlike PVL 4170 (23), which might mean that this caudal should be switched with the former caudal, in terms of vertebral order.

The neural spine is straight and rectangular in shape in anterior, posterior and lateral view, showing a more basal morphology than the previous caudals (Fig. 26A, B, E). The spine summit has a faint saddle shape, however not as pronounced as in previous anterior caudals; the summit shows a flatter surface, with only a slight posterior elevation (Fig. A, B, E).

PVL 4170 (25): In anterior view, the dorsal rim of the anterior articular surface is well developed, and shows a slight indentation below the neural canal, giving it a small heartshape as in the more anterior caudals (Fig. 27D). In posterior view, the articular surface of the centrum is round, and shows pronounced round striations on the rim (Fig. 27E). In lateral view, the centrum displays a larger anterior articular surface than posteriorly (Fig.27A, B), as in other middle caudals of eusauropods (Upchurch 2004). The anterior rim is also more rugose than the posterior one. In ventral view, the centrum shows two large chevron facets on the anterior side, and two smaller ones on the posterior side (Fig. 27C). The neural canal is similar in morphology to that of PVL 4170 (23) – (24), see Fig. 27D, E.

The prezygapophyses are connected medially by a ridge of bone, which is different from the previous caudal vertebrae, where a deep U-shaped gap between the prezygapophyses exists

(Fig. 27A, B, D, F). The prezygapophyses themselves are damaged. In dorsal view, the prezygapophyses and spinoprezygapophyseal laminae are clearly visible as stout beams, as in PVL 4170 (22). The posterior dorsal rim of the centrum shows a sharp U-shaped recess towards the postzygapophyses, which are positioned in an angle at almost 90° to the horizontal, Fig. 27A, B, E). The postzygapophyses are visible as lateral triangular protrusions ventral to the neural spine.

The diapophyses in this caudal are reduced to small protrusions on the more dorsal side of the centrum, indicating the transition from the middle caudals to a more posterior caudal morphology (Fig. 27E, F). They are shaped as round bosses on the lateral sides of the centrum, in dorsal view.

The neural spine is straight, and increases in axial width towards the summit (Fig.27A, B, F). It is more inclined posteriorly than dorsally, confirming its middle-posterior caudal position. On the lateral side, rugose dorsoventrally positioned striations are visible. The spine summit is not straight, but shows a faint saddle shape (Fig. 27A, B).

PVL 4170 (26): In anterior view, the articular surface of the centrum is oval and dorsoventrally flattened as in PVL 4170 (25), see Fig. 28B. In posterior view, the articular surface is oval and elongated in the dorsoventral axis (Fig. 28A). It has rough circular striations as in the other caudals. In lateral view, the centrum is axially elongated, suggesting a possibly more posterior position than the numbering might indicate (Fig. 28C, D). In dorsal view, the axial elongation of the centrum is apparent, again indicating this caudal might be more posterior than middle (Fig. 28F). This could also imply that some caudals that originally existed between PVL 4170 (25) and (26) are missing here. The outline of the centrum is symmetrical in dorsal view; the flaring of the extremities and the constriction of the centrum in the middle (Fig. 28F). In ventral view, the centrum is smooth and concave, and the chevron facets are not pronounced (Fig. 28E).

The same indentation as in most caudals, ventral to the neural canal, is visible, however, this part is also partially broken. The anterior neural canal is large and triangular to oval in shape (Fig. 28B). It occupies most of the anterior surface of the neural arch. The posterior neural canal is oval and also dorsoventrally elongated (Fig. 28A).

The prezygapophyses are still protruding anteriorly, however as in PVL 4170 (25), the recess between them is not pronounced (Fig. 28B, C, D). The prezygapophyses are inclined dorsally and medially, and make an angle of about 45 degrees with respect to the centrum, with the triangular articular surface on the medial side. The postzygapophyses are reduced to triangular bosses, ventral to the neural spine (Fig. 28A, C, D).

The diapophyses are reduced to bulges on the lateral side of the centrum, beneath which a slight depression still remains (Figure 28C, D, F).

The neural spine is partially broken off at the base. Dorsal to the postzygapophyses, the neural spine displays rough dorsoventrally elongated striations (Fig. 28C, D). The neural spine is projecting dorsally and posteriorly, being parallel to the centrum. In dorsal view, all extremities are symmetrical, giving the caudal the outline of a cross in dorsal view (Fig. 28F).

PVL 4170 (27): The centrum of this middle-posterior caudal amphicoelus and symmetrically shaped. In anterior view, the articular surface is oval and dorsoventrally flattened as in PVL 4170 (25) – (26), see Fig. 29F. Similarly, the dorsal rim of the articular surface is heart-shaped. In lateral view, the anterior articular surface is slightly longer dorsoventrally than the posterior one (Fig. 29C, D). The anterior also shows the chevron facets clearly as ventral rugose protrusions. The centrum on the ventral side is concave, and on the lateral axial surface the centrum seems to be slightly transversely flattened (Fig. 28B). In posterior view, the articular surface is oval, with the elongation in the dorsoventral plane (Fig. 28E). It is also flattened transversely. In ventral view, no chevron facets are visible, however, the centrum shows a flattening in the axial midline, which is slightly concave (Fig. 29B).

On the lateral sides of the centrum, the diapophyses are visible as rudimentary, rugose rounded bulges (Fig. 29C, D). The prezygapophyses are damaged, however, this renders the neural canal clearly visible as a semi-circular/triangular structure (Fig. 29E, F).

The neural spine is broken; however, it is straight and directed posteriorly and dorsally, it being more flattened towards the centrum than in previous caudals, indicating again a more posterior caudal morphology (Fig. 29C, D). In dorsal view, the spine is clearly flattened towards the centrum (Fig. 29A).

PVL 4170 (30 / 31 /32): The last preserved caudals are middle/posterior caudals. They are dorsoventrally and transversely smaller than previous caudals, and show an even more simplified morphology than middle caudals. The anterior articular surface is oval with the elongation axis on the dorsoventral plane, see Fig. 30A. The posterior articular surface is smaller in size and more rounded than oval (Fig. 30B). These caudals do not have the prezygapophyses, postzygapophyses or neural spines preserved (Fig. 30), except for PVL 4170 (32). In lateral view, PVL 4170 (32) has prezygapophyses present as small rounded protrusions that project anteriorly. The postzygapophyses are no longer visible. PVL 4170 (32) has a short, robust spine. It is inclined posteriorly and ventrally, back towards the centrum, indicating a posterior caudal position.

APPENDICULAR SKELETON

Ilium PVL 4170 (34): According to the Cerro Cóndor Norte quarry map (Fig 1), two ilia were recovered in the original excavations. However, the whereabouts of the second ilium are unknown. Even though the MACN in Buenos Aires hosts several ilia, which can be attributed to *Patagosaurus*, none of these are large enough to match the holotype ilium in the collections of the Instituto Miguel Lillo in Tucuman.

The right ilium is axially longer than dorsoventrally high (Fig. 31C). The dorsal rim is convex as in most sauropods, however, the curvature resembles the high dorsal rim of basal neosauropods/derived eusauropods (e.g. *Apatosaurus, Haplocanthosaurus, Diplodocus, Cetiosaurus*) more than those of more basal forms, which tend to be less convex, as seen in *Tazoudasaurus* (Allain et al. 2004; Allain and Acquesbi 2008). The iliac body is not entirely straight; it is offset from the axial plane to the lateral side at the anterior lobe, whereas the midsection is axially aligned, and the posterior end is slightly offset to the medial side. The ilium of the eusauropod *Lapparentosaurus* also follows this curvature. *Cetiosaurus oxoniensis* shows a more or less straight anterior half of the iliac body, though the posterior half is also slightly offset medially.

The preacetabular process in lateral view is hook-shaped (Fig. 31C); a common feature among sauropods, and found in the eusauropods *Cetiosaurus*, *Barapasaurus*, *Omeisaurus junghsiensis*, and *Shunosaurus lii* (Tang et al. 2001; Upchurch and Martin 2003; Bandyopadhyay et al. 2010), although not in *Tazoudasaurus* (Allain and Aquesbi 2008). The anteriormost part of the process has a thickened rugose dorsal side, which is much thicker than the dorsal edge of the more posterior part of the ilium, and is slightly constricted dorsoventrally. However, the posteriormost dorsal rim of the iliac blade shows another thickened ridge. Ventrally the preacetabular process slopes down gently, not in a sharp curve, towards the pubic peduncle of the ilium.

The preacetabular process in anterior view (Fig. 31A) is dorsally rugose and pitted for muscle and cartilage attachment. It is slightly bent towards the lateral side, thus not entirely aligned in the axial plane. The pubic peduncle in anterior view is a stout element, which flares out distally and is less wide at its proximal base. The articular surface of the distal end of the pubic peduncle is not symmetrical, but slightly triangular in shape. The dorsal part of the preacetabular lobe is similar to *Haplocanthosaurus* in that it has a similar thickening rugosity of the anteriormost hook-shaped process, but differs from *Haplocanthosaurus* in that it

2011 constricts slightly behind this process, whereas in *Haplocanthosaurus* the dorsal rugosity
2012 behind the anterior process continues smoothly (Hatcher 1903; Upchurch et al. 2004). The
2013 constriction does seem to be natural and not due to damage.
2014 The pubic peduncle is a slender rod-shaped element, which widens towards the distal end,
2015 both anteriorly and posteriorly, in lateral view (Fig. 31C). The anterior distal side of this
2016 peduncle bulges slightly convexly. The posterior side of the pubic peduncle (or the anterior
2017 edge of the acetabulum) is concave. The extremity of the peduncle is convex anteriorly and
2018 flat posteriorly, and the surface is rugose.
2019 The acetabulum is relatively wide as in *Barapasaurus*, *Haplocanthosaurus*, and diplodocids
2020 (Hatcher 1903; Upchurch et al. 2004; Bandyopadhyay 2010), but differs in width from
2021 *Cetiosaurus*, *Tazoudasaurus* and titanosauriforms (Upchurch and Martin 2003; Allain and
2022 Aquesbi 2008; Díez Díaz et al. 2013; Poropat et al. 2015), see Figure 31C. Its dorsal rim is
2023 transversely acute towards the medial side. The rim itself is concave.
2024 The ischial lobe is clearly visible as the ventral half of the heart-shaped posterior end of the
2025 illiac blade (Fig. 31B, C). In lateral view it is a semi-round structure. The surface of the ischial
2026 peduncle bulges out laterally, giving it a slight offset from the iliac blade to the lateral and
2027 ventral side. It is also offset ventrally and posteriorly from the acetabulum (Fig. 31B). The
2028 articular surface for the ischium is oval in shape and rugosely pitted and striated. The ischial
2029 peduncle of the ilium in lateral view is a semi-round, non-prominent lobe.
2030
2031 *Pubis PVL 4170 (35):* The right pubis is almost complete. In lateral view, the pubic shaft
2032 shows a slightly convex dorsal side and a slightly concave ventral side of the shaft, providing
2033 the shaft with a slight curvature in lateral view (Fig. 32A). The shaft is gracile, taking up
2034 approximately 2/3rds of the entire pubic length. The shaft is more compressed
2035 lateromedially than that of *Cetiosaurus oxoniensis* (Upchurch and Martin, 2003)
2036 *Mamenchisaurus youngi* (Pi et al. 1996), or *Bothriospondylus madagascariensis* (Mannion

2010). Moreover, the length of the pubis is more or less similar to that of the ischium. In this way it more resembles that of *Haplocanthosaurus* than other sauropods (Hatcher 1903). The shaft and proximal part are aligned (Fig. 32A); in that there is no torsion of the pubis as in more derived sauropods (Upchurch and Martin 2003; Upchurch et al. 2004). Interestingly, the African and Malagasi basal eusauropods *Spinophorosaurus* and '*Bothriospondylus'* have a much more 'robust' pubis than *Patagosaurus* (Remes et al. 2009; Läng 2010). The pubis of *Tazoudasaurus* appears to be of the more robust type as well, however this is not entirely clear, as it belongs to a juvenile (Allain et al. 2008). The elongated and slender shaft is also seen in *Vulcanodon* (Cooper 1984), however in this taxon the pubic apron is smaller. Also, in *Vulcanodon*, the pubis is much shorter than the ischium, as in most sauropods (Cooper 1984; Upchurch et al. 2004).

The distal expansion of the pubis in lateral view flares more dorsally than ventrally, and tapers acutely to a point (Fig. 32B, D). This distal shape is similar to that of *Barapasaurus* (Bandhyopadhyay 2010) is more flared than *Haplocanthosaurus* (Hatcher 1903). The distal end of the pubis in distal view is suboval in shape (Fig. 32B, D).

The pubic apron is slightly convex ventrally in lateral view, with the ischial peduncle tapering obliquely (Fig. 32A). The pubic peduncle of the pubis projects medially and slightly ventrally. Even though the mirroring pubis is not present, the pubic basin can be estimated to be wider than that of *Barapasaurus,* in which the pubic basin is narrow.

The pubic foramen is 'pear-shaped' in lateral view; a dorsoventrally elongated oval that is constricted slightly dorsal to the middle (Fig. 32A).

The pubic rim of the acetabulum is a steeply sloping surface from the iliac peduncle to the ischial peduncle in lateral view. This rim tapers ventrally and posteriorly towards the acetabulum.

The ischial peduncle has a roughly triradiate, transversely narrow and dorsoventrally elongated articulation surface, with the narrowest point on the ventral side. The length of

2063 the ischial peduncle of the pubis is less than 33% of the length of the entire pubis; further
2064 reinforcing the elongation of this pubis. In *Haplocanthosaurus* the length of the ischial
2065 peduncle is also less than 33%, in *Cetiosaurus* as well (Hatcher 1903; Upchurch and Martin
2066 2003). The iliac peduncle is dorsally elevated from the pubic apron and the shaft, as in
2067 *Cetiosaurus*. The iliac articulation surface is rugose, and curves slightly medially and
2068 posteriorly. There is no 'hook'-shaped ambiens process present as in *Lapparentosaurus*,
2069 *Bothriospondylus* or derived sauropods (Mannion 2010). The pubic symphysis projects
2070 medially and ventrally, as in most sauropods (Upchurch et al. 2004)
2071
2072 *Ischia PVL 4170 (36):* The fused distal parts of both ischia are preserved, with fusion
2073 occurring at around 2/3 of the shaft length (Fig. 33). The proximal parts are recreated in
2074 plaster; therefore, these will not be described. However, part of the shaft of the right
2075 ischium is preserved (Fig. 33C). In lateral view, the ventral side is concave, and the shaft
2076 expands both dorsally and ventrally towards the limit of the distal end (as far as it is
2077 preserved).
2078 There is a peculiar oval depression on the lateral side of the right ischium, approximately at
2079 the height of the fusion with the left ischium (Fig. 33A). This could be a pathology, however,
2080 seeing as the femur originally was overlaying the ischium in situ during excavations (see Fig.
2081 1), this depression is most probably taphonomic in nature. The extremities of the fused
2082 ischia flare out distally towards the sagittal plane. In posterior view, the distal ends are
2083 directed laterodorsally and medioventrally (Fig. 33B). The fusion forms a wide V-shape with
2084 an angle of 110° with the horizontal; an intermediate stage between the coplanar
2085 *Camarasaurus* ischial fusion state and that of diplodocoids, *Cetiosaurus, 'Bothriospondylus*
2086 *madagascariensis'* and *Vulcanodon* (Janensch 1961; Cooper 1984; Upchurch and Martin
2087 2003; Mannion 2010; Tschopp et al. 2015). In dorsal view, the shaft of the right ischium
2088 bends and bulges slightly towards the lateral side at 2/3rd of shaft length, but this is probably

due to the taphonomic/pathological damage, as the left ischial shaft is concave laterally in dorsal view. The surfaces of the ischial extremities are convex and rugose (Fig. 33B).

Femur PVL 4170 (37): The right femur is well-preserved (Figure 34). It is a stout element, transversely nearly three times wider than axially long. This makes it anteroposteriorly shorter than transversely, as in most sauropods other than Titanosauriformes. The stoutness already distinguishes it from *Lapparentosaurus* (MNHN-MAA 67), has a more slender femur, albeit this taxon is only known from juveniles. The shaft has an elliptical cross-section. There is no lateral bulge present as in Titanosauriformes (Upchurch et al. 2004). The fourth trochanter is positioned slightly medial to the dorsoventral midpoint of the shaft; therefore, it is not entirely medially positioned. This is also seen in *Tazoudasaurus, Cetiosaurus, Volkheimeria*, and neosauropods like *Tornieria* (Bonaparte 1986a; Upchurch and Martin 2003; Allain and Aquesbi 2008; Remes 2009).

In anterior view, on the proximal side of the femur, a distinct groove is present, which runs along the midline from the proximal end to about 3/5th of the femoral length (Fig. 34). This groove ends in a square-shaped depression, which has a rugose surface on its lateral side. The lateral side of the femur is slightly convex, and the medial side slightly concave, giving the femur a curved appearance. It is not entirely certain whether this is due to taphonomy, or if it is the actual natural curvature. In the latter case, this could have implications for the stance and gait of *Patagosaurus*, (Wilson and Carrano 1999), as the pubic basin might be wide compared to other sauropods. This cannot be proven, however, without the other pubis present, which was never recovered from the Cerro Cóndor Norte locality.

The distal end of the anterior side of the femur shows a slight sub-quadrangular depression between the lateral and medial condyles, which forms a triangular shape more dorsally, as is common in basal sauropods. The lateral condyle is slightly offset, but this could be due to the taphonomic deformation slightly dorsal to it.

In posterior view, the curvature of the femur is still visible (Fig. 34). A deep longitudinal muscle attachment scar is visible at around the midpart of the shaft. The greater trochanter is clearly visible in posterior view, as a small rounded protrusion, projecting dorsally from the proximolateral end of the femur. Directly medial to this, the proximal end of the femur shows a slight depression, before the medial onset of the femoral head. Distally, in posterior view, the tibial condyle is slightly damaged. It expands strongly medially, and medioposteriorly; this is also seen in *Cetiosaurus* (Upchurch and Martin 2003). Between the tibial and fibular condyles, the distal end of the posterior part of the femur shows a deep depression, also seen in *Cetiosaurus*, and possibly *Lapparentosaurus* (MNHN-MAA 64). The fibular condyle is offset to the lateral side, and clearly protrudes posteriorly as a teardrop-shaped solid structure. The distal lateral condyle flares to the lateral side.

In dorsal view, the proximal end of the femur is strongly rugose and pitted, for cartilage and muscle attachments. Medial to the greater trochanter, the proximal end is axially constricted, after which the femoral head widens again. Unfortunately, the femoral head is not very clearly visible due to the mounting of the specimen, however, it is rounded, standing out medially at about 20 cm. The medial end of the femoral head is not completely rounded, but a little pointed, though not as abruptly as in *Cetiosaurus*.

DISCUSSION

COMPARATIVE MORPHOLOGICAL CHARACTERS OF *PATAGOSAURUS FARIASI*

Cervicals: the number of cervicals of *Patagosaurus* is possibly closer to that of *Cetiosaurus* and *Spinophorosaurus*, and possibly slightly lower than that of the Rutland *Cetiosaurus*. It is most likely also lower than in neosauropods, placing it within known derived non-neosauropodan eusauropods (Mannion et al. 2019).

One feature that differentiates *Patagosaurus* from other sauropods is the wide angle between the postzygodiapophyseal laminae and the posterior centrodiapophyseal lamina. This angle is as wide as 55° to the horizontal (contra McPhee et al. (2016) who measured 41°) and is not found in any basal non-neosauropodan eusauropod (all have an angle between the podl and pcdl of between 30 and 40°). In basal sauropods and sauropodomorphs, this angle is much lower, and even in many and even in many eusauropods the angle is less wide (McPhee et al 2015). Thus, this elevation seems to mark the transition from sauropodomorphs to sauropods. *Shunosaurus* and *Kotasaurus* (Tang et al. 2001; Yadagiri 2001), have a high projection of the podl, but not a lower projection of the pcdl, therefore still not equating the high angle of *Patagosaurus.* Potentially in *Jobaria* (Wilson 2012), and certainly in neosauropods, such as *Haplocanthosaurus* and *Diplodocus* (Hatcher 1901; 1903), higher angles are reached with higher projections of the podl (Upchurch et al 2004). In general, high posterior cervical neural arches are achieved by mamenchisaurs and titanosauriforms (Mannion et al. 2019).

The cervicals of *Patagosaurus* are different from most other Early and Middle Jurassic non-neosauropodan eusauropods in that they are rather stout and short but high dorsoventrally. The aEI is on average lower than most other eusauropods (*Cetiosaurus*, *Spinophorosaurus*, *Lapparentosaurus*, *Amygdalodon,* see Table 1). However, as the cervical series is not complete, some cervicals that are missing might have had a higher aEI. The aEI is possibly similar to that of *Tazoudasaurus*, however, the morphology of the cervicals between these two taxa is different, and also *Tazoudasaurus* does also not have a complete cervical series (Allain and Aquesbi 2008).

The anterior condyle of the cervicals is most comparable to those of *Cetiosaurus*, especially as there is a rugose rim that cups the condyle, and as there is a protrusion on the condyle. The condylar rim of *Cetiosaurus,* however, is more rugose than in *Patagosaurus* (Upchurch and Martin, 2002; 2003). The cervicals of *Cetiosaurus* used in this study belong to the

Rutland *Cetiosaurus*, which itself might be a slightly more derived, separate taxon than the holotype of *Cetiosaurus oxoniensis* (Läng 2008; P. Upchurch & M. Evans pers.comm.).

The other cervical features, such as a pronounced ventral keel and posteriorly extending ventral end of the posterior cotyle, are more plesiomorphic features shared with *Lapparentosaurus, Amygdalodon, Tazoudasaurus*, and *Spinophorosaurus*. *Cetiosaurus oxoniensis* (Upchurch and Martin 2003; 2002) does not seem to have a ventral keel on its anterior cervicals. *Lapparentosaurus* shows a posterior V-shaped forking of the keel, which is not seen in *Patagosaurus.* Moreover, some more derived sauropods possess ventral keels, such as the titanosaurs *Opisthocoelicaudia* and *Diamantinasaurus* (Poropat et al. 2015).

The next outstanding cervical feature is the non-juncture of the intrapostzygapophyseal laminae. This is a feature that distinguishes *Patagosaurus* from *Cetiosaurus*, and unites it with *Tazoudasaurus*, therefore a connection between this non-juncture and the elevation of the neural spine can be ruled out. Whether or not this is a feature shared between Gondwanan sauropods is uncertain. The single intraprezygapophyseal lamina is a feature shared with *Cetiosaurus* and *Tazoudasaurus*. The centrodiapophyseal fossa, as seen in *Patagosaurus*, is not shared with *Tazoudasaurus*, rather, it is shared with *Mamenchisaurus*. The centroprezygapophyseal fossa is shared with *Tazoudasaurus* (To1-354, contra Wilson 2011).

Dorsals:

The slightly rectangular shape of anterior and middle dorsal centra is shared with non-neosauropodan sauropods, and differs from neosauropods (Mannion et al. 2019). The slightly more mediolaterally wide posterior dorsal centra are not as wide as in titanosauriforms (Mannion et al. 2019). The inconspicuous small round depressions on the posterior side of some of the more well preserved posterior dorsals is a feature thus far not seen in any other sauropod, and could be an autapomorphy. However, as it is a small

feature, it might have been missed in osteological descriptions of contemporaneous sauropods to *Patagosaurus*. Most (eu)sauropods do have a rectangular fossa or depression at the posterior side of the transverse process of (posterior) dorsals, bordered by the pcdl, and the podl, which is named the pocdf, or postzygocentrodiapophyseal fossa (Wilson 2011). Whether this has compartmentalized in *Patagosaurus* is not clear, as the pocdf is rather prominently present, however, in *Patagosaurus* this fossa is more expressed towards the neural arch than towards the distal end of the diapophysis, as is the case in *Spinophorosaurus* and *Cetiosaurus* (Rutland *Cetiosaurus* as well as *C. oxoniensis;* Upchurch and Martin 2002, 2003; Remes et al. 2009). One observation is that these latter taxa have more dorsally projecting diapophyses, at an angle of about 45° to the horizontal, compared to a more horizontal and lateral projection in *Patagosaurus*. Whether or not the extra fossa in *Patagosaurus* is correlated to the projection of the diapophyses (e.g. as extra ligament attachement site for additional support) remains an unanswered question. In *Barapasaurus*, no such fossa is seen, whilst the diapophyses of that taxon also project laterally as in *Patagosaurus*.

The rudimentary aliform process in the neural spines of dorsal vertebrae is seen in high ontogenetic stages of development in *Europasaurus holgeri* Sander et al., 2006, where it projects as a triangular protrusion dorsal to the spinal onset of the sprl in anterior view, and dorsal to the lateral spdl + spol complex in posterior view (Carballido and Sander 2014). In *Patagosaurus*, this feature is seen dorsal to the lspol+podl complex. This feature could be a convergence of a laterally projecting triangular process for ligament attachement, found in basal eusauropods in the configuration as in *Patagosaurus*, and in neosauropods in the configuration of *Europasaurus*. Note also that this feature develops more in mature specimens of *Europasaurus* and that the holotype of *Patagosaurus* PVL 4170 is a (sub)adult and still growing (as evidenced by fused but visible neurocentral sutures), and in *Patagosaurus* the feature is only seen in posteriormost dorsals as a very rudimentary form.

Posterior dorsal neural arches with rudimentary aliform processes are now known for *Patagosaurus*, and are also seen in more distinct form in basal macronarians such as *Europasaurus*, and also in *Bellusaurus sui* Mo, 2913 and *Haplocanthosaurus* (Hatcher 1903; Upchurch 1998; Mo 2013; Carballido and Sander 2014; Foster and Wedel 2014).

The absence of a spinodiapophyseal lamina on dorsal vertebrae is another characteristic dorsal feature in *Patagosaurus*. This lamina is seen in dorsals of basal sauropods such as *Tazoudasaurus* and *Barapasaurus*, then disappears in *Patagosaurus*, *C. oxoniensis* and the Rutland *Cetiosaurus*, then reappears in neosauropods such as *Apatosaurus, Diplodocus, Haplocanthosaurus, Camarasaurus, Dicraeosaurus* and *Amargasaurus* (Wilson 1999). It's absence is therefore interpreted as an apomorphic character uniting the cetiosaurids (Holwerda and Pol 2018). In *Patagosaurus*, the diapophyses are supported solely by the acdl, pcdl from the ventral and lateral sides, and prdl and podl from the lateral and dorsal sides. In posterior dorsals, the diapophysis is additionally supported by the lspol+podl complex, which is sometimes mistaken for the spdl (Allain et al. 2008). This podl+lspol complex is also seen in the Rutland *Cetiosaurus*. This complex could possibly be the 'replacement' of the spdl found in basal sauropods and neosauropods. In any case, the absence of the spdl in *Patagosaurus* and *Cetiosaurus* cannot be connected with either neural spine elongation, as neosauropods (and especially diplodocids) display similar spine elongation. Neither can the spdl be correlated with neural spine bifurcation, as the spdl is found in basal non-neosauropodan sauropods.

Whereas anterior dorsals and middle dorsals of *Patagosaurus* resemble other non-neosauropodan eusauropods, particularly *Cetiosaurus*, *Tazoudasaurus* and *Lapparentosaurus*, the posterior dorsals display non-neosauropodan eusauropod features such as unbifurcated neural spines, simple hyposphene/hypantrum complexes (hyposphene

rhomboid and small, hypanthrum a rugose scar) and unexcavated parapophyses. The neural spine summit, however, resembles more those of the non-neosauropodan eusauropod *Lapparentosaurus* and also of the basal neosauropod *Haplocanthosaurus*. The phylogenetic position of *Lapparentosaurus* is not completely resolved, as the type specimen is a juvenile, and has been retrieved as either a brachiosaurid by Bonaparte (1986a), as a titanosauriform (Upchurch 1998), and as non-neosauropodan eusauropod (Läng 2008; Mannion et al. 2013), therefore it is not possible to draw any conclusions from this.

The lamination of the anterior dorsals is largely similar to that of *Cetiosaurus* and *Tazoudasaurus*, in that the spol flare out laterally and ventrally, broadening the neural spine. However, the transition from anterior to middle to posterior dorsal vertebrae brings some changes in lamination. The centroprezygapophyseal laminae extend dorsoventrally as the neural arch, pedicels and neural canal extend in dorsoventral height. This is seen in several other sauropods, although not in the same degree as in *Patagosaurus*. The configuration of the intrapostzygapophyseal laminae shifts from a non-juncture to a juncture, and then these laminae disappear. Instead, a single intrapostzygapophyseal lamina appears. This seems to be unique for a select group of eusauropods (see Allain and Aquesbi 2008; Carballido and Sander 2014). The posterior dorsals also display a split in the spol, into a medial and a lateral running lamina. This is described for *Europasaurus* (Carballido 2012), a basal macronarian. However, this pattern is also observed in the Rutland *Cetiosaurus*. It is therefore possibly a more widespread configuration than for solely (basal) macronarians, and also existed in non-neosauropodan eusauropods. Throughout the dorsal vertebral column, the cpol becomes a rather secondary lamina to the tpols and stpol. In *Europasaurus*, this feature coincides with a division of the cpol into a lateral and medial one, however, in *Patagosaurus*, only one cpol exists, which matches the description of the medial cpol of *Europasaurus*.

Posterior dorsals show the dorsoventrally elongated neural spine seen in *Cetiosaurus*, and also in *Haplocanthosaurus* and flagellicaudatans (Hatcher 1901; 1903). The posterior

inclination of the neural spines of posterior dorsals is also seen in *Klamelisaurus sui* Zhao, 1993*, Mamenchisaurus* and *Omeisaurus* (Xijing 1993; Tang et al. 2001; Ouyang and Ye 2002; Moore et al. 2017). The deep excavations of the fossae on the posterior dorsal neural spines, especially on the lateral sides, noted by Bonaparte (1986a), is also seen in *Cetiosaurus*, mamenchisaurids and neosauropods, suggesting a widespread character (Upchurch and Martin 2002, 2003; Upchurch et al. 2004).

The presence of a single intraprezygapophyseal and single intrapostzygapophyseal lamina is a relatively newly named feature for sauropods, as this was named a median strut or single lamina below the hypantrum/hyposphene (Upchurch et al. 2004; Wilson 1999) before Carballido and Sander (2014) named it the stprl. These laminae are noted only for *Camarasaurus* and the titanosauriform *Tehuelchesaurus benetezii* Rich et al., 1999 (Carballido et al. 2011; Carballido and Sander 2014); however, they appear to also be present in *Patagosaurus*. The presence of a small stprl accompanied by a large oval cprf on either lateral side, is shared with many other eusauropods, showing this to be a plesiomorphic character common in the cetiosaurids, and reappearing in Macronaria and basal titanosauriforms.

Sacrum: One possible source of bias in the comparison of the sacrum of *Patagosaurus* with other sauropods is that not many sacra of basal sauropods or non-neosauropodan eusauropods are preserved. Sacral elements are known from *Lapparentosaurus* and *Tazoudasaurus*, but mostly from juvenile individuals. Neither show the neural spine elongation of PVL 4170 (18). The sacral count of Patagosaurus shows one more sacral vertebra than the basal eusauropods *Barapasaurus*, *Spinophorosaurus* and *Shunosaurus*, and resembles that of derived non/neosauropodan eusauropods such as *Ferganasaurus* and *Jobaria*, as well as basal neosauropods such as *Haplocanthosaurus* (Lang and Mahammed 2010, Tschopp et al. 2015, Carballido et al. 2017b). The fusion of sacral neural spines

number 2-3, however, shows a more basal non-neosauropodan state. The morphology of the neural spines resembles that of *Haplocanthosaurus* in particular (Hatcher 1903). The neural spine elongation of PVL 4170 (18) is at an intermediate stage between *Shunosaurus*, *Camarasaurus*, *Haplocanthosaurus* and diplodocids, but without the sacral ribs extending beyond the ilium, the sacral neural spines of *Patagosaurus* do not resemble those of neosauropods.

Caudals: The anterior caudal vertebrae of *Patagosaurus* strongly resemble those of *Spinophorosaurus* and *Cetiosauriscus* (P. Upchurch pers. comm*.,* Charig 1993; Heathcote and Upchurch 2003, Noè et al. 2010). *Cetiosauriscu*s is currently under revision, and its phylogenetic position is debated. According to Heathcote and Upchurch (2003); Rauhut et al. (2005); and Tschopp et al. (2015), it is a non-neosauropodan eusauropod, although in the last analysis, it is also recovered as a basal diplodocoid as well. Holwerda et al. (2019) recover it as a diplodocimorph in some analyses. A formal redescription is ongoing (P.Upchurch pers. comm.). The middle and posterior caudals of *Patagosaurus* are more resembling those of the holotype of *Cetiosaurus.*

The elongated neural spines of PVL 4170, which are not straight but curve convexly posteriorly at 2/3rd of the height of the spine, are possibly a diagnostic feature that is not seen in other sauropods, even though anterior neural spine elongation is seen in *Cetiosauriscus*, and diplodocids (Charig 1980; Upchurch et al. 2004; Noè et al. 2010).

Appendicular elements: The round dorsal rim and hook-shaped anterior lobe of the ilium, together with the elongated pubic peduncle are diagnostic features for the ilium of *Patagosaurus.* Whereas *Cetiosaurus oxoniensis* displays a more flattened dorsal rim (Upchurch and Martin 2002), and *Chebsaurus* possibly as well (Läng and Mahammed 2010), *Barapasaurus* does share a rounded ilium (Bandyopadyay 2010), but not as highly dorsally

projecting as in *Patagosaurus*. The morphology of PVL 4170 is more similar to *Haplocanthosaurus,* and with diplodocids (Hatcher 1903, Wedel and Taylor 2013; Tschopp et al. 2015).

Together with the sacrum, which is similar to (basal) neosauropods (*Haplocanthosaurus, Diplodocus* and *Apatosaurus*), the sacricostal complex of *Patagosaurus* is more of a neosauropod build, supporting a phylogenetic position as a derived eusauropod (Holwerda and Pol 2018). Similarly, the 110° angle with the horizontal of the fused distal ischia, shows an intermediate stage between neosauropods and basal eusauropods. Finally, the intermediate morphology of the pubis, showing a torsion similar to that seen in neosauropods like *Tornieria* (Remes 2009), but showing a kidney-shaped pubic foramen as *in Cetiosaurus oxoniensis*, adds to the pelvic complex of *Patagosaurus* resembling a derived non-neosauropodan eusauropod, or basal neosauropod.

The femur of the holotype of *Patagosaurus* is a stout element, which does not resemble the elongated femora of neosauropods, but rather that of *Cetiosaurus, Tazoudasaurus* and *Barapasaurus*. The slightly convex femur towards the lateral side shows a possible gait modification that is diagnostic for *Patagosaurus* and that has not been found in the other aforementioned Jurassic sauropods. While the femoral morphology of *Cetiosaurus* is similar to that of *Patagosaurus*, the femur of the former is straighter. A wide-gauge, which might be inferred from the femoral morphology of *Patagosaurus*, is more common in titanosaurs (Henderson 2006) and Titanosauriformes (Wilson and Carrano 1999). There are, however, earlier ichnological indications of a possible wide-gauge: a footprint site from the early Middle Jurassic from the UK shows the presence of both a narrow-, as well as wide-gait sauropod track (Day et al. 2004), and also footprints from the Late Jurassic of Morocco show a wide-gauge (Marty et al. 2010). The trackmaker from these sites unfortunately cannot be identified.

PNEUMATICITY IN BASAL EUSAUROPODS

The cervicals of *Patagosaurus* show anteriorly deep pleurocoels with a gradual shallowing towards the posterior end, and with clearly defined anterior, dorsal and ventral rims, but no clearly defined posterior rim. The anteriorly deep part of the pleurocoel is visible as a circular concavity. Damage in some cervicals show that only a thin plate of bone divided mirroring pleurocoels (e.g PVL 4170 6). Bonaparte (1979, 1986a, 1999) already noted the presence of a pleurocoel. Note that the pleurocoel is present, but is shallower in the dorsals, as is also noted by Bonaparte (1986a). The pleurocoel is defined for sauropods either as a pneumatopore or as a pneumatic structure (Wilson 2002; Wedel 2003, 2005, 2013; Upchurch et al. 2004), however, Carballido and Sander (2014) defined the structure using *Patagosaurus* as an example, as a lateral excavation on the centrum, with clear anterior, dorsal and ventral margins, and a posterior margin that could be either well-defined or more gradually merging with the lateral body of the centrum (Carballido & Sander 2014). As already remarked on by Bonaparte (1986a, 1999) and Carballido and Sander (2014), *Patagosaurus* does not show the internal pneumatic structure that neosauropods display. This type of pleurocoel outline is seen in other Jurassic non-neosauropodan eusauropods, such as the Rutland *Cetiosaurus, Barapasaurus*, *Tazoudasaurus, Spinophorosaurus, Lapparentosaurus* (Bonaparte 1986c; Upchurch and Martin 2003; Allain and Aquesbi 2008; Remes et al 2009). The lack of a clear posterior margin of the pleurocoel is also common, except in the Rutland *Cetiosaurus* (Upchurch and Martin 2003). The anterior depth of the pleurocoel in *Patagosaurus*, however, is probably unique to this taxon. In S*pinophorosaurus* (Remes et al., 2009), as well as *Lapparentosaurus* (MNHN-MAA 13), the pleurocoel is shallow at its anterior margin, and even shows a shallowing at its anterior ventral margin. In *Barapasaurus* (Bandyopadhyay 2010), the entire pleurocoel is shallow. In *Shunosaurus*, the pleurocoel is anteriorly deep, but the concavity is more elongated and elliptic in shape, while in *Patagosaurus* this is circular and restricted to the anterior-most part of the pleurocoel. In

Klamelisaurus (Zhao 1993) the pleurocoel is entirely shallow, and in the mamenchisaurids *Mamenchisaurus youngi* (Ouyang and Ye 2002), *Zigongosaurus* (Hou et al. 1976), *Tonganosaurus* Liu et al., 2010, and *Qijianglong* Xing et al., 2015 the pleurocoel is compartmentalized by one or more accessory laminae into small deep pockets over the length of the centrum. Only in the Rutland *Cetiosaurus* (Upchurch and Martin 2003), the pleurocoel is anteriorly deep as well. In some cervicals, an oblique accessory lamina, which divides the pleurocoel into a deeper anterior section and a shallower posterior section, is faintly present. This feature is also seen in the Rutland *Cetiosaurus*, in mamenchisaurids, and in neosauropods like *Apatosaurus* (Upchurch and Martin 2003; Xing et al. 2015; Taylor and Wedel 2017). The poor development of this oblique accessory lamina, however, and the irregularity of its presence are probably not enough to make it a character. Note that in the roughly contemporaneous Rutland *Cetiosaurus* (Upchurch and Martin 2003) this lamina is more consistently present.

Dorsals: The pneumatic structure on dorsal neural arches, appearing first in the middle dorsal neural arches and expanding in the posterior dorsal neural arches, is the key feature that Bonaparte mentioned for *Patagosaurus*, also using it to distinguish it from *Volkheimeria*, the other sauropod described from Cerro Cóndor (Bonaparte 1979, 1986b, 1999). This feature is still the main autapomorphy for *Patagosaurus,* and marks new pneumatic features for basal eusauropods that were previously unknown. Pneumaticity in sauropods is well-known for neosauropods (Wedel 2003; Wedel et al. 2005; Schwarz and Fritsch 2006; Schwarz et al. 2007; Fanti et al. 2013; Taylor and Wedel 2013). It is not well understood for basal non-neosauropod eusauropods, and *Patagosaurus* is the first taxon to give conclusive evidence for this structure. However, other basal sauropods may have this structure (e.g. *Cetiosaurus, Barapasaurus, Tazoudasaurus,* see Figure 35B). The centrodiapophyseal fenestrae, which extend ventrally in a pneumatic chamber separated

from the neual canal, is a feature possibly shared with *Cetiosaurus* and *Barapasaurus* (Bandyopadhyay et al. (2010); this feature often pairing these taxa with *Patagosaurus* as sister-taxa in phylogenetic analyses, e.g. Remes et al. (2009a)); however, it is not clearly shown whether these latter taxa possess the same ventral pneumatic chamber as in *Patagosaurus*. This feature has however been shown to be present in the basal neosauropod *Haplocanthosaurus* (Foster and Wedel 2014).

A preliminary phylogenetic analysis using the holotype PVL 4170 by Holwerda & Pol (2018) and implementing the dorsal neural spine pneumaticity shows a close affinity of *Patagosaurus* with the Rutland *Cetiosaurus*, and *Patagosaurus* being nested within specimens referred to *Cetiosaurus*. It is furthermore more derived than *Barapasaurus*, and more basal to mamenchisaurids, and neosauropods (see Figure 35A).

CONCLUSIONS

To summarize and conclude, the holotype of the Middle Jurassic sauropod *Patagosaurus fariasi* shows a set of morphological features that are typically broadly non-neosauropodan eusauropod and are shared with other non-neosauropodan eusauropods. This includes features in the cervical vertebrae, such as unbifurcated neural spines, presence of a ventral keel, unexcavated parapophyses and the absence of neosauropodan laminae. In the dorsal vertebrae, these features include amphicoelus middle and posterior dorsal centra, the absence of the spdl and unbifurcated neural spines. In caudal vertebrae, this includes simple lamination, and small transverse processes. In the pelvis and femur, these include V-shaped fusion of distal ischia, and a stout femur. However, some elements seem to be slightly more derived, and are found in derived eusauropods and/or (non)-neosauropods. These include deep excavations in cervical and dorsal vertebrae, elongated neural spines in dorsal, sacral and anterior caudal vertebrae, and convex femur. The dorsal vertebral pneumaticity

patterns found in *Patagosaurus* may unite it with other derived non-neosauropodan eusauropods such as *Cetiosaurus*. Finally, the main diagnostic characters for *Patagosaurus fariasi* are low (a)EI for cervical vertebrae, high neural spines in dorsal, sacral and anterior caudal vertebrae, cervical and dorsal vertebral pneumaticity, and convex femur.

ACKNOWLEDGEMENTS

The authors would like to dedicate this manuscript to the memory of Jaime Powell, curator of vertebrate palaeontology at the Instituto Miguel Lillo (PVL), Tucuman, Argentina, and also to the memory of José Bonaparte, director of vertebrate palaeontology both at PVL and the Museo Argentino de Ciencias Naturales Bernardino Rivadavia (MACN).

Furthermore, the authors are endebted to editor Emmanuel Côtez, and to the critical and thorough reviews of Phil Mannion and Verónica Díez Díaz, whose comments improved this paper. This research was funded by DFG grant RA 1012/13-1 to OR.

REFERENCES

ALIFANOV V.R. & AVERIANOV A.O. 2003. — Ferganasaurus verzilini, gen. et sp. nov., a new neosauropod (Dinosauria, Saurischia, Sauropoda) from the Middle Jurassic of Fergana Valley, Kirghizia. *Journal of Vertebrate Paleontology* 23 (2): 358–372

ALLAIN R. & AQUESBI N. 2008. — Anatomy and phylogenetic relationships of *Tazoudasaurus naimi* (Dinosauria, Sauropoda) from the late Early Jurassic of Morocco. *Geodiversitas* 30 (2): 345–424

ALLAIN R., AQUESBI N., DEJAX J., MEYER C., MONBARON M., MONTENAT C., RICHIR P., ROCHDY M., RUSSELL D. & TAQUET P. 2004. — A basal sauropod dinosaur from the Early Jurassic of Morocco. *Comptes Rendus Palevol* 3 (3): 199–208

BANDYOPADHYAY S., GILLETTE D.D., RAY S. & SENGUPTA D.P. 2010. — Osteology of *Barapasaurus tagorei* (Dinosauria: Sauropoda) from the Early Jurassic of India. *Palaeontology* 53 (3): 533–569

BARRETT P.M. & UPCHURCH P. 2007. — The evolution of herbivory in sauropodomorph dinosaurs. *Special Papers in Palaeontology* 77: 91–112

BARRETT P.M. 2006. — A sauropod dinosaur tooth from the Middle Jurassic of Skye, Scotland. *Earth and Environmental Science Transactions of the Royal Society of Edinburgh* 97 (01): 25–29. https://doi.org/10.1017/S0263593300001383

BARRETT P.M. & UPCHURCH P. 2005. — Sauropodomorph diversity through time, *The Sauropods: evolution and paleobiology*. p. 125–156.

BECERRA M.G., GOMEZ K.L. & POL D. 2017. — A sauropodomorph tooth increases the diversity of dental morphotypes in the Cañadón Asfalto Formation (Early–Middle Jurassic) of Patagonia. *Comptes Rendus Palevol* 16 (8): 832–840

BONAPARTE J.F. 1999. — Evolución de las vértebras presacras en Sauropodomorpha. *Ameghiniana* 36 (2): 115–187

BONAPARTE J.F. 1996. — *Dinosaurios de America del Sur*. Museo Argentino de Ciencias Naturales. 174 pp.

BONAPARTE J.F. 1986. — The dinosaurs (Carnosaurs, Allosaurids, Sauropods, Cetiosaurids) of the Middle Jurassic of Cerro Cóndor (Chubut, Argentina) ., Masson, Paris. *Annales de Paléontologie (Vert.-Invert.)* 72 (3): 325–386.

BONAPARTE J.F. 1986. — Les dinosaures (Carnosaures, Allosauridés, Sauropodes, Cétosauridés) du Jurassique Moyen de Cerro Cóndor (Chubut, Argentina)., Masson, Paris. *Annales de Paléontologie (Vert.-Invert.)* 72 (3): 247–289

BONAPARTE J.F. 1986. — The early radiation and phylogenetic relationships of the Jurassic sauropod dinosaurs, based on vertebral anatomy, *in* PADIAN K. (ed.), *The Beginning of the Age of Dinosaurs*. Cambridge, Cambridge University Press. p. 247–258.

BONAPARTE J.F. 1979. — Dinosaurs: A Jurassic Assemblage from Patagonia. *Science* 205 (4413): 1377–1379. https://doi.org/10.1126/science.205.4413.1377

BRUSATTE S.L., CHALLANDS T.J., ROSS D.A. & WILKINSON M. 2015. — Sauropod dinosaur trackways in a Middle Jurassic lagoon on the Isle of Skye, Scotland. *Scottish Journal of Geology* 5:1-9

BUFFETAUT E., SUTEETHORN V., LE LOEUFF J., CUNY G., TONG H. & KHANSUBHA S. 2002. — The first giant dinosaurs: a large sauropod from the Late Triassic of Thailand. *Comptes Rendus Palevol* 1 (2): 103–109

CABALERI N., VOLKHEIMER W., SILVA NIETO D., ARMELLA C., CAGNONI M., HAUSER N., MATTEINI M. & PIMENTEL M.M. 2010. — U-Pb ages in zircons from las Chacritas and Puesto Almada members of the Jurassic Cañadón Asfalto Formation, Chubut province, Argentina*In:* p. 190–193.

CABALERI N., ARMELLA C., 2005. — Influence of a biohermal belt on the lacustrine sedimentation of the Cañadón Asfálto Formation (Upper Jurassic, Chubut province, Southern Argentina). *Geologica Acta* 3:205-214.

CABALERI N., ARMELLA C., NIETO, D.G.S., 2005. — Saline paleolake of the Cañadón Asfálto Formation (Middle-Upper Jurassic), Cerro Cóndor, Chubut province (Patagonia), Argentina. *Facies* 51: 350–364.

CABRERA, A., 1947. — Un saurópodo nuevo del Jurásico de Patagonia. *Notas del Museo de La Plata, Paleontologia* 95:1–17.

CARBALLIDO J.L., POL D., CERDA I. & SALGADO L. 2011. — The osteology of Chubutisaurus insignis del Corro, 1975 (Dinosauria: Neosauropoda) from the 'middle'Cretaceous of central Patagonia, Argentina. *Journal of Vertebrate Paleontology* 31 (1): 93–110

CARBALLIDO J.L., HOLWERDA F.M., POL D. & RAUHUT O.W. 2017. — An Early Jurassic sauropod tooth from Patagonia (Cañadón Asfalto Formation): implications for sauropod diversity. *Publicación Electrónica de la Asociación Paleontológica Argentina* 17 (2): 50–57

CARBALLIDO J.L., POL D., OTERO A., CERDA I.A., SALGADO L., GARRIDO A.C., RAMEZANI J., CÚNEO N.R. & KRAUSE J.M. 2017. — A new giant titanosaur sheds light on body mass evolution among sauropod dinosaurs. *Proceedings of the Royal Society B* 284 (1860): 20171219. https://doi.org/10.1098/rspb.2017.1219

CARBALLIDO J.L. & SANDER P.M. 2014. — Postcranial axial skeleton of *Europasaurus holgeri* (Dinosauria, Sauropoda) from the Upper Jurassic of Germany: implications for sauropod ontogeny and phylogenetic relationships of basal Macronaria. *Journal of Systematic Palaeontology* 12 (3): 335–387. https://doi.org/10.1080/14772019.2013.764935

CARBALLIDO J.L., SALGADO L., POL D., CANUDO J.I. & GARRIDO A. 2012. — A new basal rebbachisaurid (Sauropoda, Diplodocoidea) from the Early Cretaceous of the Neuquén Basin; evolution and biogeography of the group. *Historical Biology* 24 (6): 631–654. https://doi.org/10.1080/08912963.2012.672416

CASAMIQUELA R.M. 1963. — CONSIDERACIONES ACERCA DE AMYGDALODON CABRERA (SAUHOPODA, CETIOSAURIDAE) DEL JURASICO MEDIO DE LA PATAGONIA. *Ameghiniana* 3 (3): 79–95

CHARIG A.J. 1993. — Case 1876. *Cetiosauriscus* von Huene, 1927 (Reptilia, Sauropodomorpha): proposed designation of *C. stewarti* Charig, 1980 as the type species. *Bulletin of Zoological Nomenclature* 50: 282–283

CHARIG A.J. 1980. — A diplodocid sauropod from the Lower Cretaceous of England, *in* JACOBS L.L. (ed.), *Aspects of Vertebrate History. Essays in Honor of Edwin Harris Colbert.* Flagstaff, Museum of Northern Arizona Press. p. 231–244.

CHATTERJEE S. & ZHENG Z. 2002. — Cranial anatomy of Shunosaurus, a basal sauropod dinosaur from the Middle Jurassic of China. *Zoological Journal of the Linnean Society* 136 (1): 145–169

CHURE D., BRITT B., WHITLOCK J. & WILSON J. 2010. — First complete sauropod dinosaur skull from the Cretaceous of the Americas and the evolution of sauropod dentition. *Naturwissenschaften* 97 (4): 379–391. https://doi.org/10.1007/s00114-010-0650-6

COOPER M.R. 1984. — A reassessment of *Vulcanodon karibaensis* Raath (Dinosauria: Saurischia) and the origin of the Sauropoda. *Palaeontologia africana* 25: 203–231

COPE E.D. 1877. — On a gigantic saurian from the Dakota epoch of Colorado. *Paleontological Bulletin* 25: 5–10

CÚNEO R., RAMEZANI J., SCASSO R., POL D., ESCAPA I., ZAVATTIERI A.M. & BOWRING S.A. 2013. — High-precision U–Pb geochronology and a new chronostratigraphy for the Cañadón Asfalto Basin, Chubut, central Patagonia: Implications for terrestrial faunal and floral

evolution in Jurassic. *Gondwana Research* 24 (3): 1267–1275. https://doi.org/10.1016/j.gr.2013.01.010

DAY J.J., NORMAN D.B., GALE A.S., UPCHURCH P. & POWELL H.P. 2004. — A Middle Jurassic dinosaur trackway site from Oxfordshire, UK. *Palaeontology* 47 (2): 319–348

DÍEZ DÍAZ V., TORTOSA T. & LE LOEUFF J. 2013. — Sauropod diversity in the Late Cretaceous of southwestern Europe: The lessons of odontology. *Annales de Paléontologie* 99 (2): 119–129. https://doi.org/10.1016/j.annpal.2012.12.002

DONG Z. & TANG Z. 1984. — Note on a new mid-Jurassic sauropod (*Datousaurus bashanensis* gen. et sp. nov.) from Sichuan Basin, China. *Vertebrata PalAsiatica* 22 (1): 69–75

DONG Z., ZHOU S.W. & ZHANG Y. 1983. — Dinosaurs from the Jurassic of Sichuan. *Palaeontologica Sinica, New Series C* 162 (23): 1–136

FIGARI E.G., SCASSO R.A., CÚNEO R.N. & ESCAPA I. 2015. — Estratigrafía y evolución geológica de la Cuenca de Cañadón Asfalto, provincia del Chubut, Argentina. *Latin American journal of sedimentology and basin analysis* 22 (2): 135–169

FOSTER J. 2014. — Haplocanthosaurus (Saurischia: Sauropoda) from the lower Morrison Formation (Upper Jurassic) near Snowmass, Colorado. *Volumina Jurassica* (Vol. 12, 2): 197--210. https://doi.org/10.5604/17313708 .1130144

FRENGUELLI J. 1949. — Los estratos con “Estheria” en el Chubut (Patagonia). *Revista de la Asociación Geológica Argentina* 4 (1): 1–4

GALTON P.M. 2005. — Bones of large dinosaurs (Prosauropoda and Stegosauria) from the Thaetic Bone Bed (Upper Triassic of Aust Cliff, southwest England. *Revue de Paléobiologie* 24 (1): 51

HARRIS J.D. 2006. — The axial skeleton of the dinosaur *Suuwassea emilieae* (Sauropoda: Flagellicaudata) from the Upper Jurassic Morrison Formation of Montana, USA. *Palaeontology* 49 (5): 1091–1121

HATCHER J.B. 1903. — Osteology of *Haplocanthosaurus*, with description of a new species and remarks on the probable habits of the Sauropoda and the age and origin of the *Atlantosaurus* beds: Additional remarks on *Diplodocus*. *Memoirs of the Carnegie Museum* 2: 1–72

HATCHER J.B. 1901. — *Diplodocus* (Marsh): its osteology, taxonomy, and probable habits, with a restoration of the skeleton. *Memoirs of the Carnegie Museum* 1: 1–63

HAUSER N., CABALERI N.G., GALLEGO O.F., MONFERRAN M.D., NIETO D.S., ARMELLA C., MATTEINI M., GONZÁLEZ P.A., PIMENTEL M.M., VOLKHEIMER W. & OTHERS 2017. — U-Pb and Lu-Hf zircon geochronology of the Cañadón Asfalto Basin, Chubut, Argentina: Implications for the magmatic evolution in central Patagonia. *Journal of South American Earth Sciences* 78: 190–212

HE X., LI K. & CAI K. 1988. — *The Middle Jurassic dinosaur fauna from Dashanpu, Zigong, Sichuan. Vol. IV. Sauropod Dinosaurs (2)* Omeisaurus tianfuensis. Chengdu, China, Sichuan Publishing House of Science and Technology. 143 p.

HE X., LI K., CAI K. & GAO Y. 1984. — *Omeisaurus tianfuensis*—a new species of *Omeisaurus* from Dashanpu, Zigong, Sichuan. *Journal of Chengdu College Geology, Supplement* 2: 13–32

HEATHCOTE J. & UPCHURCH P. 2003. — The relationships of *Cetiosauriscus stewarti* (Dinosauria; Sauropoda): implications for sauropod phylogeny. *Journal of Vertebrate Paleontology* 23 (Suppl. 3): 60A

HENDERSON D.M. 2006. — Burly gaits: centers of mass, stability, and the trackways of sauropod dinosaurs. *Journal of Vertebrate Paleontology* 26 (4): 907–921

HOLWERDA F.M., EVANS M. & LISTON J.J. 2019. — Additional sauropod dinosaur material from the Callovian Oxford Clay Formation, Peterborough, UK: evidence for higher sauropod diversity. *PeerJ* 7: e6404

HOLWERDA F.M. & POL D. 2018. — Phylogenetic analysis of Gondwanan basal eusauropods from the Early-Middle Jurassic of Patagonia, Argentina. *Spanish Journal of Palaeontology* 33(2):298-298

HOLWERDA F.M., POL D. & RAUHUT O.W.M. 2015. — Using dental enamel wrinkling to define sauropod tooth morphotypes from the Cañadón Asfalto Formation, Patagonia, Argentina. *PLOS ONE* 10 (2): e0118100. https://doi.org/10.1371/journal.pone.0118100

HOU L., ZHOU S. & CAO Y. 1976. — New discovery of sauropod dinosaurs from Sichuan. *Vertebrata PalAsiatica* 14 (3): 160–165

VON HUENE. 1927. —Sichtung der Grundlagen der jetzigen Kenntnis der Sauropoden. *Eclogae Geologica Helvetiae* 20:444–470.

IRMIS R.B. 2010. — Evaluating hypotheses for the early diversification of dinosaurs. *Earth and Environmental Science Transactions of the Royal Society of Edinburgh* 101 (3–4): 397–426

JAIN S.L., KUTTY T.S., ROY-CHOWDHURY T. & CHATTERJEE S. 1975. — The sauropod dinosaur from the Lower Jurassic Kota formation of India. *Proceedings of the Royal Society of London B: Biological Sciences* 188 (1091): 221–228

JANENSCH W. 1961. — Die Gliedmassen und Gliedmassengürtel der Sauropoden der Tendaguru-Schichten. *Palaeontographica-Supplementbände* 4: 177–235

LÄNG É. 2008. — Les cétiosaures (Dinosauria, Sauropoda) et les sauropodes du Jurassique moyen: révision systématique, nouvelles découvertes et implications phylogénétiques Ph. D. dissertation. Paris, France, *Centre de recherche sur la paléobiodiversité et les paléoenvironnements*. 639 p.

LÄNG E. & MAHAMMED F. 2010. — New anatomical data and phylogenetic relationships of Chebsaurus algeriensis (Dinosauria, Sauropoda) from the Middle Jurassic of Algeria. *Historical Biology* 22 (1–3): 142–164. https://doi.org/10.1080/08912960903515570

LAOJUMPON C., SUTEETHORN V., CHANTHASIT P., LAUPRASERT K. & SUTEETHORN S. 2017. — New evidence of sauropod dinosaurs from the Early Jurassic period of Thailand. *Acta Geologica Sinica-English Edition* 91 (4): 1169–1178

LISTON J.J. 2004. — A re-examination of a Middle Jurassic sauropod limb bone from the Bathonian of the Isle of Skye. *Scottish Journal of Geology* 40 (2): 119–122

LIU L.K.Y.C.-Y. & ZHENG-XIN J.W. 2010. — A NEW SAUROPOD FROM THE LOWER JURASSIC OF HUILI, SICHUAN, CHINA. *Vertebrata Palasiatica* 3:185-202.

LONGMAN H.A. 1927. — *The giant dinosaur: Rhoetosaurus brownei*. Queensland Museum 8 (3): 183-194

MAHAMMED F., LÄNG É., MAMI L., MEKAHLI L., BENHAMOU M., BOUTERFA B., KACEMI A., CHÉRIEF S.-A., CHAOUATI H. & TAQUET P. 2005. — The 'Giant of Ksour', a Middle Jurassic sauropod dinosaur from Algeria. *Comptes Rendus Palevol* 4 (8): 707–714

MANNION P.D. 2010. — A revision of the sauropod dinosaur genus '*Bothriospondylus*' with a redescription of the type material of the Middle Jurassic form '*B. madagascariensis*'. *Palaeontology* 53 (2): 277–296. https://doi.org/10.1111/j.1475-4983.2009.00919.x

MANNION P.D. & UPCHURCH P. 2010. — Completeness metrics and the quality of the sauropodomorph fossil record through geological and historical time. *Paleobiology* 36 (2): 283–302

MANNION P.D., UPCHURCH P., BARNES R.N. & MATEUS O. 2013. — Osteology of the Late Jurassic Portuguese sauropod dinosaur *Lusotitan atalaiensis* (Macronaria) and the evolutionary history of basal titanosauriforms. *Zoological Journal of the Linnean Society* 168 (1): 98–206. https://doi.org/10.1111/zoj.12029

MANNION P.D., UPCHURCH P., SCHWARZ D. & WINGS O. 2019. — Taxonomic affinities of the putative titanosaurs from the Late Jurassic Tendaguru Formation of Tanzania: phylogenetic and biogeographic implications for eusauropod dinosaur evolution.

Zoological Journal of the Linnean Society 185 (3): 784–909. https://doi.org/10.1093/zoolinnean/zly068

MARSH O.C. 1890. — Description of new dinosaurian reptiles. *American Journal of Science (series 3)* 39: 81–86

MARSH O.C. 1878. — Principal characters of American Jurassic dinosaurs, Part I. *American Journal of Science (series 3)* 16 (95): 411–416. https://doi.org/10.2475/ajs.s3-16.95.411

MARSH O.C. 1877. — Notice of some new dinosaurian reptiles from the Jurassic Formation. *American Journal of Science (series 3)* 14: 514–516

MARTY D., BELVEDERE M., MEYER C.A., MIETTO P., PARATTE G., LOVIS C., & THüring B. 2010. — Comparative analysis of Late Jurassic sauropod trackways from the Jura Mountains (NW Switzerland) and the central High Atlas Mountains (Morocco): implications for sauropod ichnotaxonomy. *Historical Biology: An International Journal of Paleobiology* 22:1-3, 109-133

MATTINSON J.M. 2005. — Zircon U–Pb chemical abrasion ("CA-TIMS") method: combined annealing and multi-step partial dissolution analysis for improved precision and accuracy of zircon ages. *Chemical Geology* 220 (1): 47–66

MCPHEE B.W., BONNAN M.F., YATES A.M., NEVELING J. & CHOINIERE J.N. 2015. — A new basal sauropod from the pre-Toarcian Jurassic of South Africa: evidence of niche-partitioning at the sauropodomorph–sauropod boundary? *Scientific Reports* 5: 13224. https://doi.org/10.1038/srep13224

MCPHEE B.W., UPCHURCH P., MANNION P.D., SULLIVAN C., BUTLER R.J. & BARRETT P.M. 2016. — A revision of Sanpasaurus yaoi Young, 1944 from the Early Jurassic of China, and its relevance to the early evolution of Sauropoda (Dinosauria). *PeerJ* 4: e2578

MCPHEE B.W., YATES A.M., CHOINIERE J.N. & ABDALA F. 2014. — The complete anatomy and phylogenetic relationships of *Antetonitrus ingenipes* (Sauropodiformes, Dinosauria): implications for the origins of Sauropoda. *Zoological Journal of the Linnean Society* 171 (1): 151–205. https://doi.org/10.1111/zoj.12127

MO J. 2013. — *Topics in Chinese Dinosaur Paleontology-Bellusaurus sui*, *in* XU X. (ed.). Zhengzhou, China, Henan Science and Technology Press. 231 p.

MOORE A., XU X. & CLARK J. 2017. — Anatomy and systematics of *Klamelisaurus gobiensis*, a mamenchisaurid sauropod from the Middle-Late Jurassic Shishugou Formation of China*In:* 77th annual meeting of the SVP, Calgary, Canada. Taylor & Francis. p. 165A.

NAIR J.P. & SALISBURY S.W. 2012. — New anatomical information on *Rhoetosaurus brownei* Longman, 1926, a gravisaurian sauropodomorph dinosaur from the Middle Jurassic of Queensland, Australia. *Journal of Vertebrate Paleontology* 32 (2): 369–394. https://doi.org/10.1080/02724634.2012.622324

NICHOLL C.S., MANNION P.D. & BARRETT P.M. 2018. — Sauropod dinosaur remains from a new Early Jurassic locality in the Central High Atlas of Morocco. *Acta Palaeontologica Polonica* 63 (1): 147–157.

NOÈ L.F., LISTON J.J. & CHAPMAN S.D. 2010. — 'Old bones, dry subject': the dinosaurs and pterosaur collected by Alfred Nicholson Leeds of Peterborough, England. *Geological Society, London, Special Publications* 343 (1): 49–77

NULLO F.E. 1983. — *Descripción geológica de la Hoja 45 c, Pampa de Agnia, provincia del Chubut: carta geológico-económica de la República Argentina, escala 1: 200.000*. *Servicio Geológico Nacional* 199:1-94.

OLIVERA D.E., ZAVATTIERI A.M. & QUATTROCCHIO M.E. 2015. — The palynology of the Cañadón Asfalto Formation (Jurassic), Cerro Cóndor depocentre, Cañadón Asfalto Basin, Patagonia, Argentina: palaeoecology and palaeoclimate based on ecogroup analysis. *Palynology* 39 (3): 362–386

OUYANG H. & YE Y. 2002. — *The first mamenchisaurian skeleton with complete skull, Mamenchisaurus youngi*. Chengdu, China, Sichuan Publishing House of Science and Technology. 138 p.
PENG Z., YE Y., GAO Y., SHU C.K. & JIANG S. 2005. — *Jurassic Dinosaur Faunas in Zigong*. Chengdu, China, Sichuan Peoples Publishing House. 69–98 p.
PHILLIPS J. 1871. — *Geology of Oxford and the Valley of the Thames*. Clarendon Press. Oxford, 390p.
PI L., OU Y. & YE Y. 1996. — A new species of sauropod from Zigong, Sichuan, *Mamenchisaurus youngi. In:* Papers on Geosciences Contributed to the 30th International Geological Congress. 87–91p.
PIATNITZKY C. 1936. — Informe preliminar sobre el estudio geológico de la región situada al norte de los lagos Colhué Huapi y Musters. *Boletín Informaciones Petroleras, Yacimientos Petrolíferos Fiscales* 137: 2–15
POL D., RAUHUT O.W.M. & CARBALLIDO J.L. 2009. — Skull anatomy of a new basal eusauropod from the Cañadon Asfalto Formation (Middle Jurassic) of Central Patagonia. *Journal of Vertebrate Paleontology* 29 (Suppl. to 3): 100A.
POROPAT S.F., UPCHURCH P., MANNION P.D., HOCKNULL S.A., KEAR B.P., SLOAN T., SINAPIUS G.H.K. & ELLIOTT D.A. 2015. — Revision of the sauropod dinosaur *Diamantinasaurus matildae* Hocknull et al. 2009 from the mid-Cretaceous of Australia: Implications for Gondwanan titanosauriform dispersal. *Gondwana Research* 27 (3): 995–1033. https://doi.org/10.1016/j.gr.2014.03.014
RAATH M.A. 1972. — Fossil vertebrate studies in Rhodesia: a new dinosaur (Reptilia: Saurischia) from near the Trias-Jurassic boundary. *Arnoldia (Rhodesia)* 7: 1–7
RAUHUT O.W.M. 2002. — Dinosaur evolution in the Jurassic: a South American perspective*In:* 62nd Society of Vertebrate Paleontology annual meeting, Norman, Oklahoma, USA. 22.
RAUHUT O.W.M. 2003. — A dentary of *Patagosaurus* (Sauropoda) from the Middle Jurassic of Patagonia. *Ameghiniana* 40 (3): 425–432
RAUHUT O.W.M. 2003. — Revision of *Amygdalodon patagonicus* Cabrera, 1947 (Dinosauria, Sauropoda). *Fossil Record* 6 (1): 173–181
RAUHUT O.W. 2004. — Braincase structure of the Middle Jurassic theropod dinosaur *Piatnitzkysaurus. Canadian Journal of Earth Sciences* 41 (9): 1109–1122. https://doi.org/10.1139/e04-053
RAUHUT O.W.M., REMES K., FECHNER R., CLADERA G. & PUERTA P. 2005. — Discovery of a short-necked sauropod dinosaur from the Late Jurassic period of Patagonia. *Nature* 435 (7042): 670–672
REMES K. 2009. — Taxonomy of Late Jurassic diplodocid sauropods from Tendaguru (Tanzania). *Fossil Record* 12 (1): 23–46
REMES K., ORTEGA F., FIERRO I., JOGER U., KOSMA R., FERRER J.M.M., IDE O.A. & MAGA A. 2009. — A new basal sauropod dinosaur from the Middle Jurassic of Niger and the early evolution of Sauropoda. *PLoS One* 4 (9): e6924. https://doi.org/10.1371/journal.pone.0006924
RICH T.H., VICKERSRICH P., GIMENEZ O., CUNEO R., PUERTA P. & VACCA R. 1999. — A new sauropod dinosaur from Chubut Province, Argentina. *National Science Museum Monographs* 15: 61–84
RUSSELL D.A. & ZHENG Z. 1993. — A large mamenchisaurid from the Junggar Basin, Xinjiang, People's Republic of China. *Canadian Journal of Earth Sciences* 30 (10): 2082–2095
SANDER P.M., MATEUS O., LAVEN T. & KNÖTSCHKE N. 2006. — Bone histology indicates insular dwarfism in a new Late Jurassic sauropod dinosaur. *Nature* 441 (7094): 739–741. https://doi.org/10.1038/nature04633

SERENO P.C., BECK A.L., DUTHEIL D.B., LARSSON H.C.E., LYON G.H., MOUSSA B., SADLEIR R.W., SIDOR C.A., VARRICCHIO D.J. & WILSON G.P. 1999. — Cretaceous sauropods from the Sahara and the uneven rate of skeletal evolution among dinosaurs. *Science* 286 (5443): 1342–1347

SILVA NIETO D.G., CABALERI N.G., SALANI F.M. & COLUCCIA A. 2002. — Cañadón Asfalto, una cuenca tipo "pull apart" en el área de cerro Cóndor, provincia del Chubut*In:* p. 238–244.

STIPANICIC P.N., RODRIGO F., BAULIES O.L. & MARTÍNEZ C.G. 1968. — Las formaciones presenonianas en el denominado Macizo Nordpatagónico y regiones adyacentes. *Revista de la Asociación Geológica Argentina* 23 (2): 67–98

STUMPF S., ANSORGE J. & KREMPIEN W. 2015. — Gravisaurian sauropod remains from the marine late Early Jurassic (Lower Toarcian) of North-Eastern Germany. *Geobios* 48 (3): 271–279

TANG F., JING X., KANG X. & ZHANG G. 2001. — *[*Omeisaurus maoianus*: a complete sauropod from Jingyuan, Sichuan]*. Beijing, China, China Ocean Press. 112 p.

TASCH P. & VOLKHEIMER W. 1970. — Jurassic conchostracans from Patagonia. *The University of Kansas Paleontological Contributions* 50:1-23.

TAYLOR M.P. 2009. — A re-evaluation of *Brachiosaurus altithorax* Riggs 1903 (Dinosauria, Sauropoda) and its generic separation from *Giraffatitan brancai* (Janensch 1914). *Journal of Vertebrate Paleontology* 29 (3): 787–806

TODD C.N., ROBERTS E.M., KNUTSEN E.M., ROZEFELDS A.C., HUANG H.-Q. & SPANDLER C. 2019. — Refined age and geological context of two of Australia's most important Jurassic vertebrate taxa (*Rhoetosaurus brownei* and *Siderops kehli*), Queensland. *Gondwana Research* 76: 19–25

TSCHOPP E., MATEUS O. & BENSON R.B.J. 2015. — A specimen-level phylogenetic analysis and taxonomic revision of Diplodocidae (Dinosauria, Sauropoda). *PeerJ* 3: e857. https://doi.org/10.7717/peerj.857

UPCHURCH P., BARRETT P.M. & DODSON P. 2004. — Sauropoda, *in* WEISHAMPEL D.B., DODSON P. & OSMÓLSKA H. (eds.), *The Dinosauria. Second edition*. Berkeley, CA, University of California Press. p. 259–322.

UPCHURCH P. & MARTIN J. 2002. — The Rutland *Cetiosaurus*: the anatomy and relationships of a Middle Jurassic British sauropod dinosaur. *Palaeontology* 45 (6): 1049–1074

UPCHURCH P. & MARTIN J. 2003. — The anatomy and taxonomy of *Cetiosaurus* (Saurischia, Sauropoda) from the Middle Jurassic of England. *Journal of Vertebrate Paleontology* 23 (1): 208–231

VOLKHEIMER W., QUATTROCCHIO M.E., CABALERI N.G., GARCÍA V. 2001. — Palynology and paleoenvironment of the Jurassic lacustrine Cañadón Asfalto Formation, at Cañadón Lahuincó locality, Chubut Province, Central Patagonia, Argentina. *Revista Española de Microplaeontología* 40:77-96.

VOLKHEIMER W., QUATTROCCHIO M.E., CABALERI N.G., NARVAEZ P.L. & ROSENFELD U. 2015. — ENVIRONMENTAL AND CLIMATIC PROXIES FOR THE CAÑADÓN ASFALTO AND NEUQUÉN BASINS (PATAGONIA, ARGENTINA): REVIEW OF MIDDLE TO UPPER JURASSIC CONTINENTAL AND NEAR COASTAL SEQUENCES. *REVISTA BRASILEIRA DE PALEONTOLOGIA* 18 (1): 71–82

VOLKHEIMER W., RAUHUT O.W., QUATTROCCHIO M.E. & MARTINEZ M.A. 2008. — Jurassic paleoclimates in Argentina, a review. *Revista de la Asociación Geológica Argentina* 63 (4): 549–556

WANG J., YE Y., PEI R., TIAN Y., FENG C., ZHENG D. & CHANG S.-C. 2018. — Age of Jurassic basal sauropods in Sichuan, China: A reappraisal of basal sauropod evolution. *Geological Society of America Bulletin* 130 (9/10): 1493–1500

WEDEL M.J. 2003. — Vertebral pneumaticity, air sacs, and the physiology of sauropod dinosaurs. *Paleobiology* 29 (2): 243

WEDEL M.J. 2005. — Postcranial skeletal pneumaticity in sauropods and its implications for mass estimates, *in* CURRY ROGERS K. A. & WILSON J.A. (eds.), *The sauropods: evolution and paleobiology*. Berkeley, USA, University of California Press. p. 201–228.

WEDEL M.J. & TAYLOR M.P. 2013. — Caudal pneumaticity and pneumatic hiatuses in the sauropod dinosaurs *Giraffatitan* and *Apatosaurus*. *PLoS ONE* 8 (10): e78213. https://doi.org/10.1371/journal.pone.0078213

WILSON J.A. 2002. — Sauropod dinosaur phylogeny: critique and cladistic analysis. *Zoological Journal of the Linnean Society* 136 (2): 215–275

WILSON J.A. 1999. — A nomenclature for vertebral laminae in sauropods and other saurischian dinosaurs. *Journal of Vertebrate Paleontology* 19 (4): 639–653

WILSON J.A., D'EMIC M.D., IKEJIRI T., MOACDIEH E.M. & WHITLOCK J.A. 2011. — A nomenclature for vertebral fossae in sauropods and other saurischian dinosaurs. *PLoS ONE* 6 (2): e17114

WILSON J.A. 2011. — Anatomical terminology for the sacrum of sauropod dinosaurs. *Contributions from the museum of Paleontology, University of Michigan* 32:59-69.

WILSON J.A. & UPCHURCH P. 2009. — Redescription and reassessment of the phylogenetic affinities of *Euhelopus zdanskyi* (Dinosauria: Sauropoda) from the Early Cretaceous of China. *Journal of Systematic Palaeontology* 7 (02): 199–239. https://doi.org/10.1017/S1477201908002691

WILSON J.A. & CARRANO M.T. 1999. — Titanosaurs and the origin of "wide-gauge" trackways: a biomechanical and systematic perspective on sauropod locomotion. *Paleobiology* 25 (2): 252–267

WILSON J.A. 2011. — Anatomical terminology for the sacrum of sauropod dinosaurs

WOODWARD A.S. 1905. — On parts of the skeleton of *Cetiosaurus leedsi*, a sauropodous dinosaur from the Oxford Clay of Peterborough. *Proceedings of the Zoological Society of London* 1: 232–243

XING L., MIYASHITA T., CURRIE P.J., YOU H., ZHANG J. & DONG Z. 2013. — A new basal eusauropod from the Middle Jurassic of Yunnan, China, and faunal compositions and transitions of Asian sauropodomorph dinosaurs. *Acta Palaeontologica Polonica* 60 (1): 145–154

XING L., MIYASHITA T., ZHANG J., LI D., YE Y., SEKIYA T., WANG F. & CURRIE P.J. 2015. — A new sauropod dinosaur from the Late Jurassic of China and the diversity, distribution, and relationships of mamenchisaurids. *Journal of Vertebrate Paleontology* 35 (1): e889701

XU X., UPCHURCH P., MANNION P.D., BARRETT P.M., REGALADO-FERNANDEZ O.R., MO J., MA J. & LIU H. 2018. — A new Middle Jurassic diplodocoid suggests an earlier dispersal and diversification of sauropod dinosaurs. *Nature communications* 9 (1): 2700

YADAGIRI P. 2001. — The osteology of *Kotasaurus yamanpalliensis*, a sauropod dinosaur from the Early Jurassic Kota Formation of India. *Journal of Vertebrate Paleontology* 21 (2): 242–252

YADAGIRI P. 1988. — A new sauropod *Kotasaurus yamanpalliensis* from Lower Jurassic Kota Formation of India. *Records of the Geological Survey of India* 11: 102–127

YATES A.M. & KITCHING J.W. 2003. — The earliest known sauropod dinosaur and the first steps towards sauropod locomotion. *Proceedings of the Royal Society of London. Series B: Biological Sciences* 270 (1525): 1753–1758. https://doi.org/10.1098/rspb.2003.2417

YATES A.M., BONNAN M.F., NEVELING J., CHINSAMY A. & BLACKBEARD M.G. 2010. — A new transitional sauropodomorph dinosaur from the Early Jurassic of South Africa and the evolution of sauropod feeding and quadrupedalism. *Proceedings of the Royal Society of London B: Biological Sciences* 277 (1682): 787–794. https://doi.org/10.1098/rspb.2009.1440

YOUNG C.-C. 1939. — On a new sauropoda, with notes on other fragmentary reptiles from Szechuan. *Bulletin of the Geological Society of China* 19 (3): 279–315. https://doi.org/10.1111/j.1755-6724.1939.mp19003005.x

YOUNG C.-C. & ZHAO X. 1972. — Description of the type material of *Mamenchisaurus hochuanensis*. *Institute of Vertebrate Paleontology and Paleoanthropology Monograph Series I* 8: 1–30

ZAVATTIERI A.M., ESCAPA I.H., SCASSO R.A. & OLIVERA D. 2010. — Contribución al conocimiento palinoestratigráfico de la Formación Cañadón Calcáreo en su localidad tipo, provincia del Chubut, Argentina*In:*

ZHANG Y. 1988. — *The Middle Jurassic dinosaur fauna from Dashanpu, Zigong, Sichuan, vol. 1: sauropod dinosaur (I): Shunosaurus.* Chengdu, China, Sichuan Publishing House of Science and Technology. 114 p.

ZHANG Y., LI K., ZENG Q. & DOWNS T.B.W. 1998. — A new species of sauropod from the Late Jurassic of the Sichuan Basin (Mamenchisaurus jingyanensis sp. nov.). *Journal of the Chengdu University of Technology* 25 (1)

ZHAO X.J. 1993. — A NEW MID-JURASSIC SAUROPOD (KLAMELISAURUS GOBIENSIS GEN. ET SP. NOV.) FROM XINJIANG, CHINA. *Vertebrata PalAsiatica* 2: 007

ZHAO X.J. 1993. — A new mid-Jurassic sauropod (*Klamelisaurus gobiensis* gen. et sp. nov.) from Xinjiang, China. *Vertebrata PalAsiatica* 2: 243-265.

FIGURE AND TABLE CAPTIONS

Figures

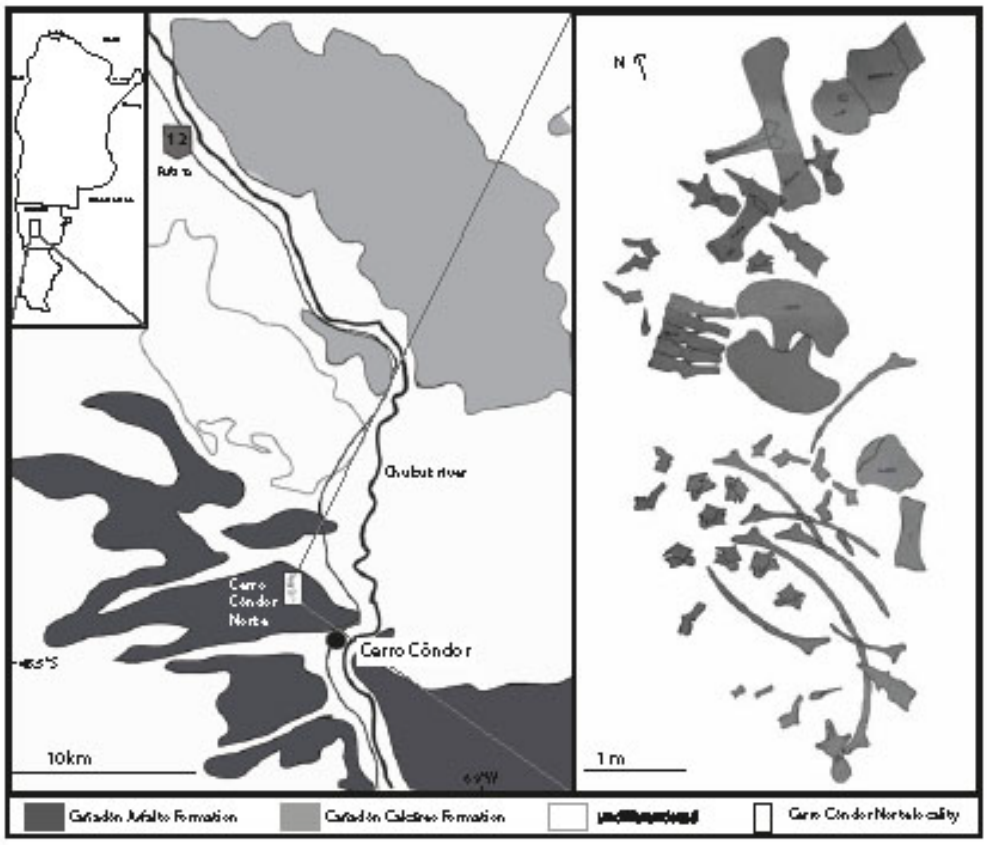

Figure 1: Geological setting of the locality Cerro Cóndor Norte, and bonebed with holotype highlighted

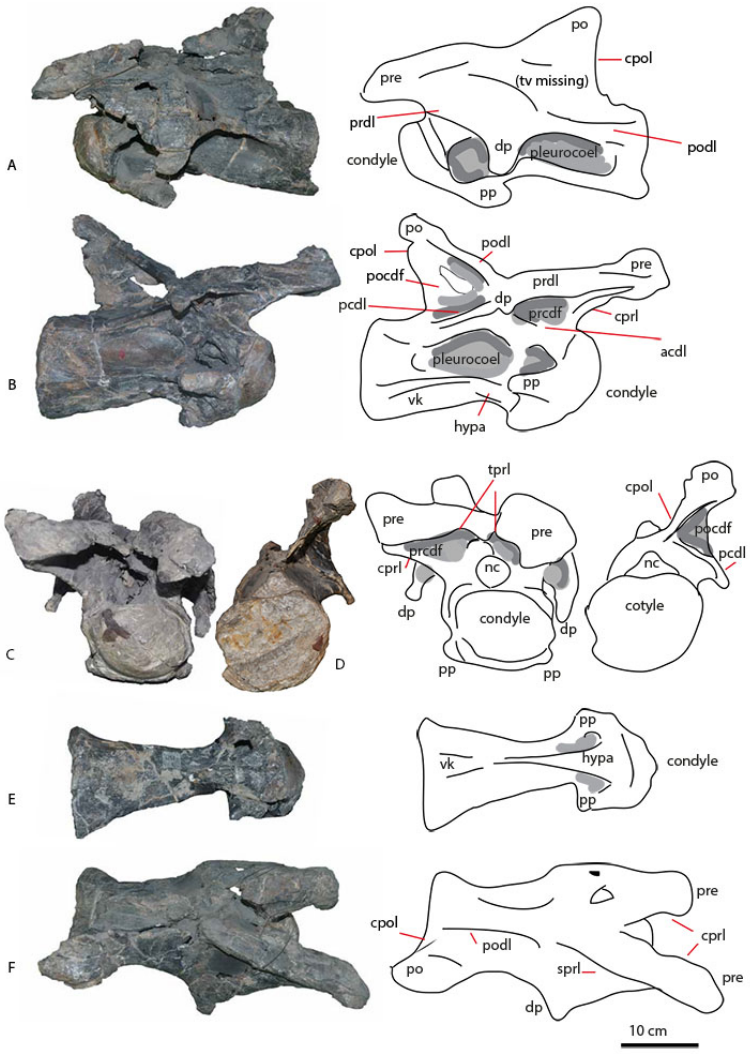

2872
2873 Figure 2: Cervical PVL 4170 (1) in lateral (A,B), anterior (C), posterior (D), ventral (E) and
2874 dorsal (F) views. Abbreviations: acdl = anterior centrodiapophyseal lamina, cprl =
2875 centroprezygapophyseal lamina, cpol = centropostzygapophyseal lamina, dp = diapophysis,
2876 hypa = hypapophysis, nc = neural canal, ns = neural spine, pcdl = posterior
2877 centrodiapophyseal lamina, pp = parapophysis, po = postzygapophysis, prcdf =
2878 prezygapophyseal centrodiapophyseal fossa, pocdf = postzygapophyseal centrodiapophyseal
2879 fossa, prdl = prezygapophyseal diapophyseal lamina, pre = prezygapophysis, spof =
2880 spinopostzygapophyseal fossa, spol = spinopostzygapophyseal lamina, sprf =
2881 spinoprezygapophyseal fossa, sprl = spinoprezygapophyseal lamina, vk = ventral keel.

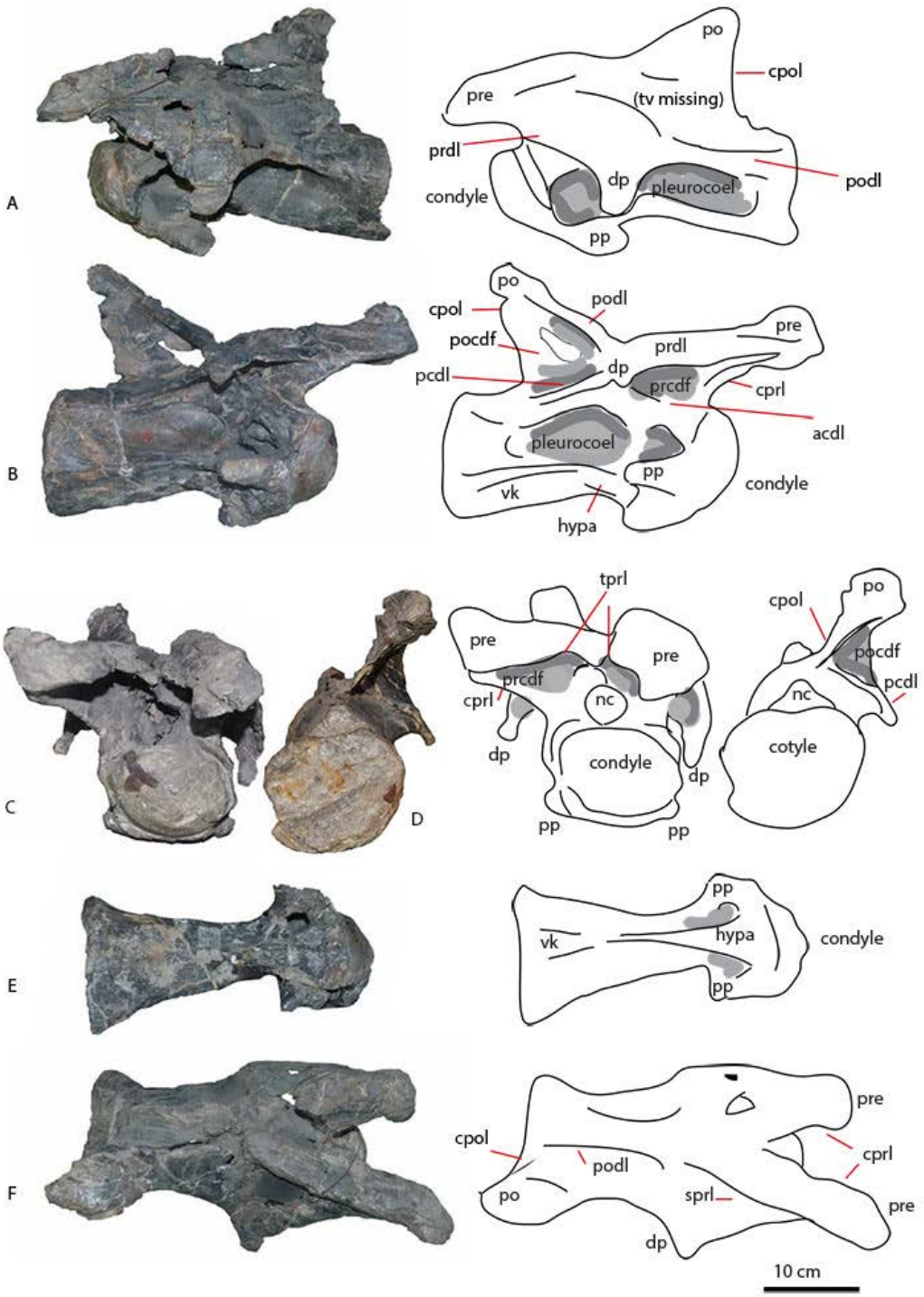

Figure 3: Cervical PVL 4170 (2) in lateral (A,B), anterior (C), posterior (D), ventral (E) and dorsal (F) views. Abbreviations: acdl = anterior centrodiapophyseal lamina, cprl = centroprezygapophyseal lamina, cpol = centropostzygapophyseal lamina, dp = diapophysis, hypa = hypapophysis, nc = neural canal, ns = neural spine, pcdl = posterior centrodiapophyseal lamina, pp = parapophysis, po = postzygapophysis, prcdf = prezygapophyseal centrodiapophyseal fossa, pocdf = postzygapophyseal centrodiapophyseal fossa, prdl = prezygapophyseal diapophyseal lamina, pre = prezygapophysis, spof = spinopostzygapophyseal fossa, spol = spinopostzygapophyseal lamina, sprf = spinoprezygapophyseal fossa, sprl = spinoprezygapophyseal lamina, tprl = intraprezygapophyseal lamina, vk = ventral keel.

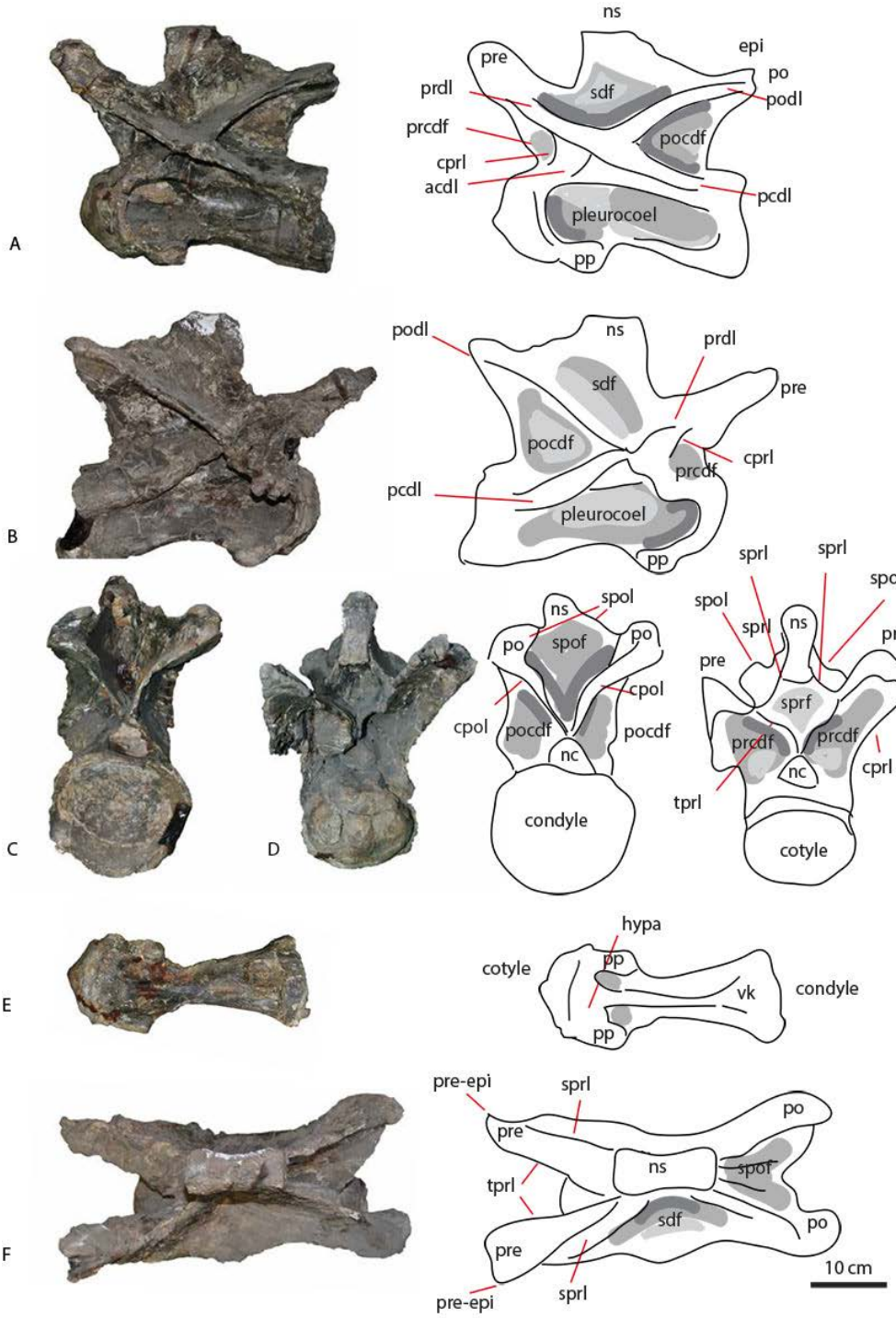

Figure 4: Cervical PVL 4170 (3) in lateral (A,B), posterior, (C) anterior, (D), ventral (E) and dorsal (F) views. Abbreviations: acdl = anterior centrodiapophyseal lamina, cprl = centroprezygapophyseal lamina, cpol = centropostzygapophyseal lamina, dp = diapophysis, hypa = hypapophysis, nc = neural canal, ns = neural spine, pcdl = posterior centrodiapophyseal lamina, pp = parapophysis, po = postzygapophysis, prcdf = prezygapophyseal centrodiapophyseal fossa, pocdf = postzygapophyseal centrodiapophyseal fossa, prdl = prezygapophyseal diapophyseal lamina, pre = prezygapophysis, sdf = spinodiapophysal fossa, spof = spinopostzygapophyseal fossa, spol = spinopostzygapophyseal lamina, sprf = spinoprezygapophyseal fossa, sprl = spinoprezygapophyseal lamina, tprl = intraprezygapophyseal lamina, vk = ventral keel.

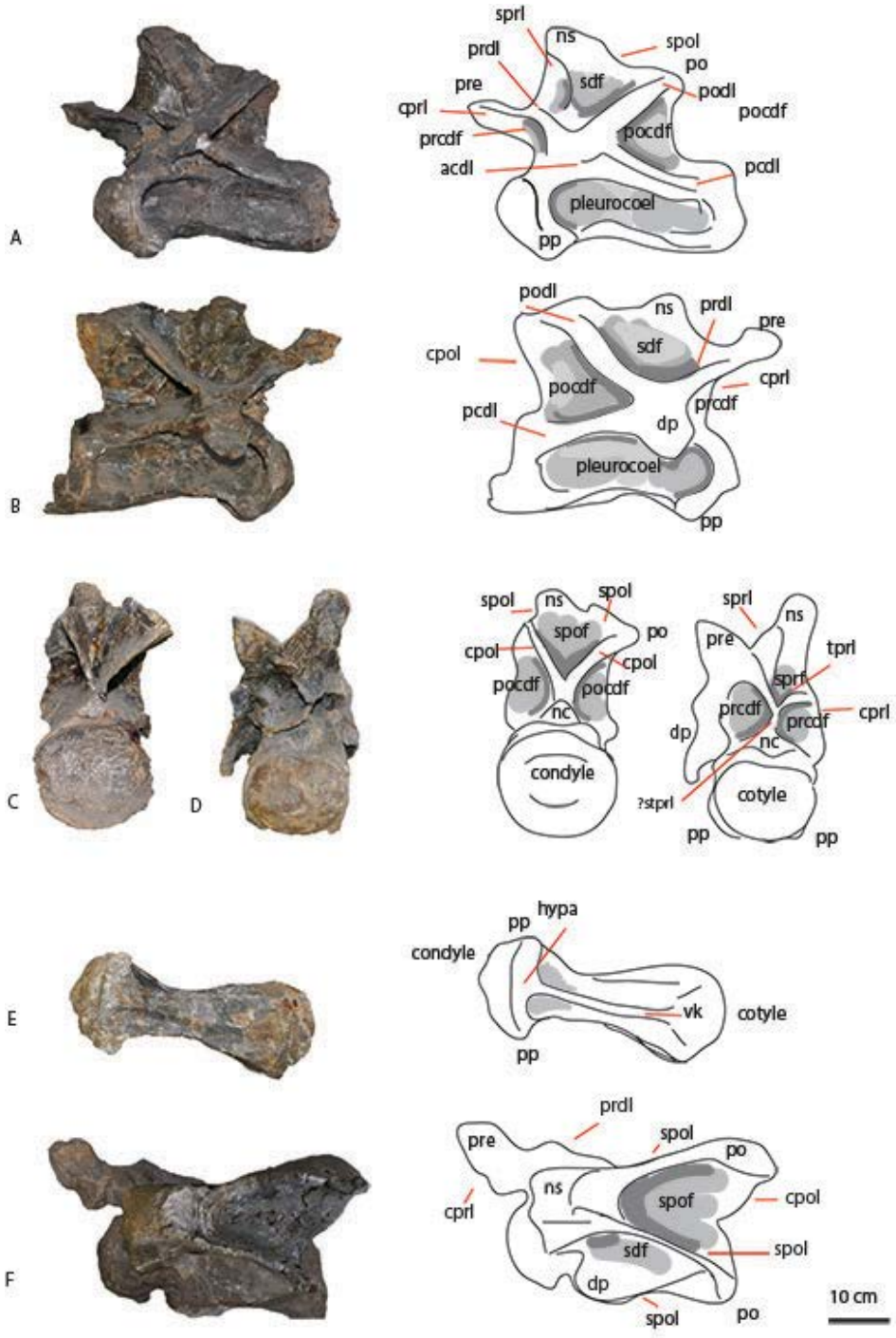

Figure 5: Cervical PVL 4170 (4) in lateral (A,B), posterior (C), anterior (D), ventral (E) and dorsal (F) views. Abbreviations: acdl = anterior centrodiapophyseal lamina, cprl = centroprezygapophyseal lamina, cpol = centropostzygapophyseal lamina, dp = diapophysis, hypa = hypapophysis, nc = neural canal, ns = neural spine, pcdl = posterior centrodiapophyseal lamina, pp = parapophysis, po = postzygapophysis, prcdf = prezygapophyseal centrodiapophyseal fossa, pocdf = postzygapophyseal centrodiapophyseal fossa, prdl = prezygapophyseal diapophyseal lamina, pre = prezygapophysis, sdf = spinodiapophysal fossa, spof = spinopostzygapophyseal fossa, spol = spinopostzygapophyseal lamina, sprf = spinoprezygapophyseal fossa, sprl = spinoprezygapophyseal lamina, tprl = intraprezygapophyseal lamina, vk = ventral keel.

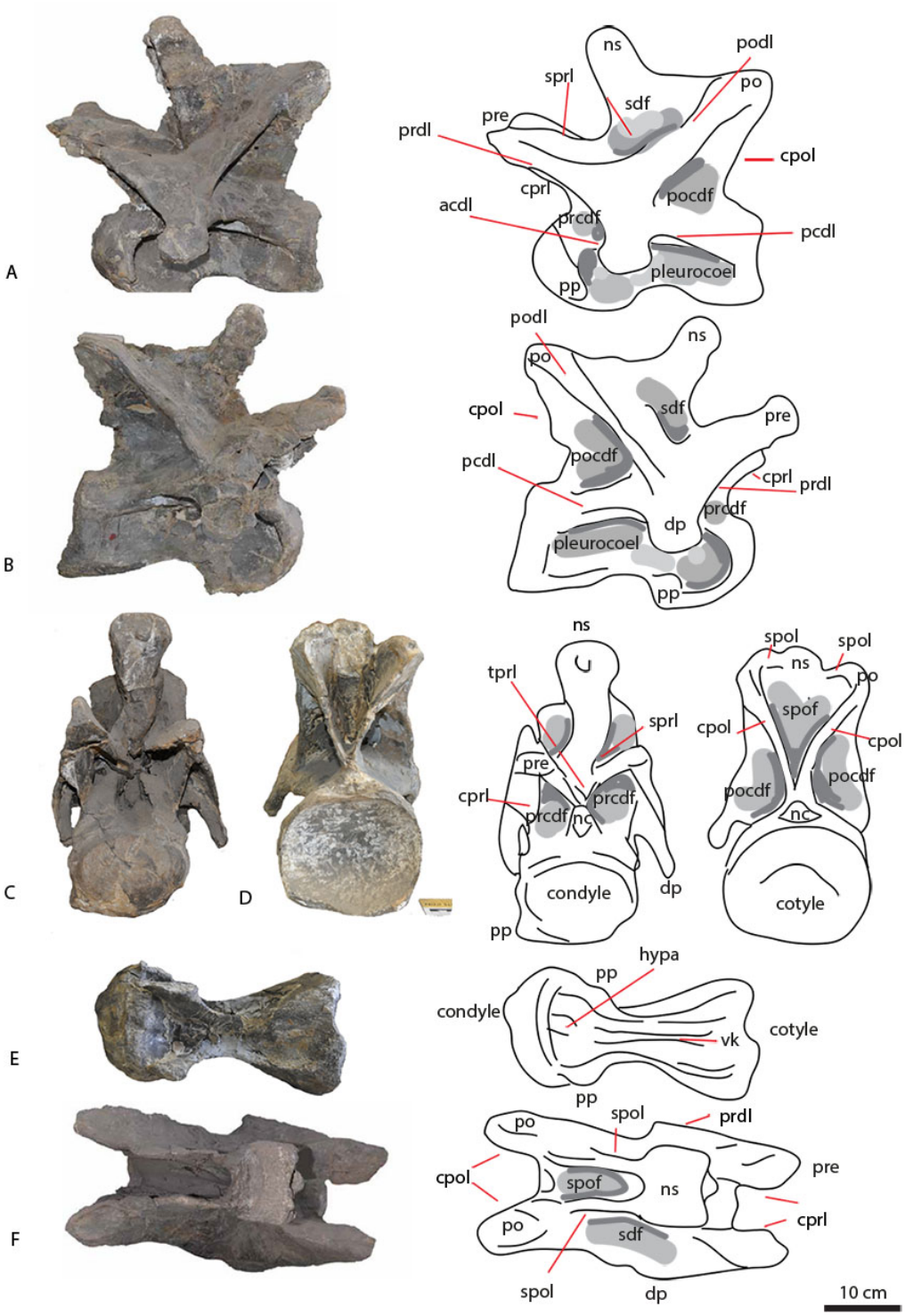

Figure 6: Cervical PVL 4170 in lateral (A,B), anterior (C), posterior (D), ventral (E) and dorsal (F) views. Abbreviations: acdl = anterior centrodiapophyseal lamina, cprl = centroprezygapophyseal lamina, cpol = centropostzygapophyseal lamina, dp = diapophysis, hypa = hypapophysis, nc = neural canal, ns = neural spine, pcdl = posterior centrodiapophyseal lamina, pp = parapophysis, po = postzygapophysis, prcdf = prezygapophyseal centrodiapophyseal fossa, pocdf = postzygapophyseal centrodiapophyseal fossa, prdl = prezygapophyseal diapophyseal lamina, pre = prezygapophysis, sdf = spinodiapophysal fossa, spof = spinopostzygapophyseal fossa, spol = spinopostzygapophyseal lamina, sprf = spinoprezygapophyseal fossa, sprl = spinoprezygapophyseal lamina, tprl = intraprezygapophyseal lamina, vk = ventral keel.

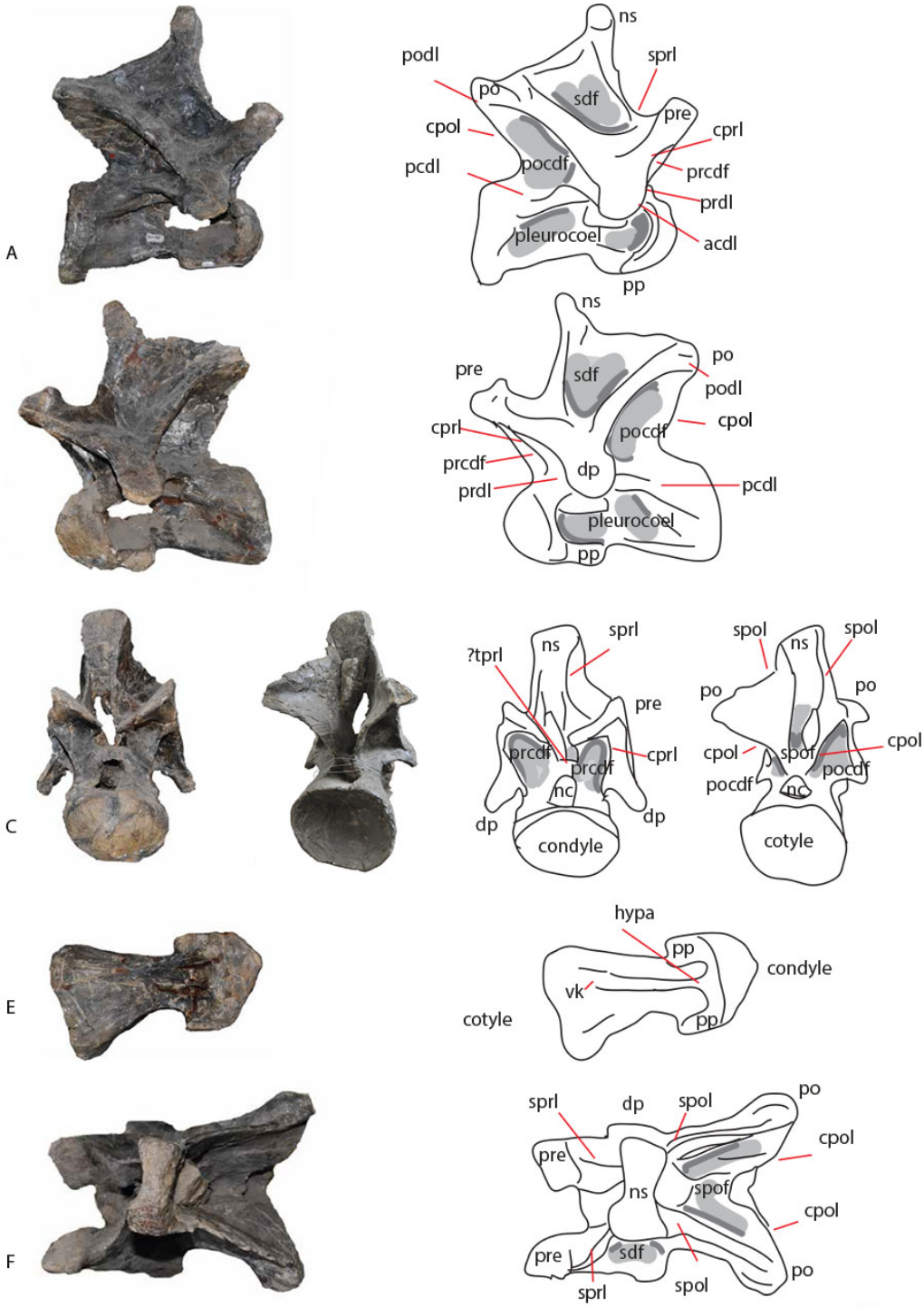

Figure 7: Cervical PVL 4170 (6) in lateral (A,B), anterior (C), posterior (D), ventral (E) and dorsal (F) view. Abbreviations: acdl = anterior centrodiapophyseal lamina, cprl = centroprezygapophyseal lamina, cpol = centropostzygapophyseal lamina, dp = diapophysis, hypa = hypapophysis, nc = neural canal, ns = neural spine, pcdl = posterior centrodiapophyseal lamina, pp = parapophysis, po = postzygapophysis, prcdf = prezygapophyseal centrodiapophyseal fossa, pocdf = postzygapophyseal centrodiapophyseal fossa, prdl = prezygapophyseal diapophyseal lamina, pre = prezygapophysis, sdf = spinodiapophysal fossa, spof = spinopostzygapophyseal fossa, spol = spinopostzygapophyseal lamina, sprf = spinoprezygapophyseal fossa, sprl = spinoprezygapophyseal lamina, tprl = intraprezygapophyseal lamina, vk = ventral keel.

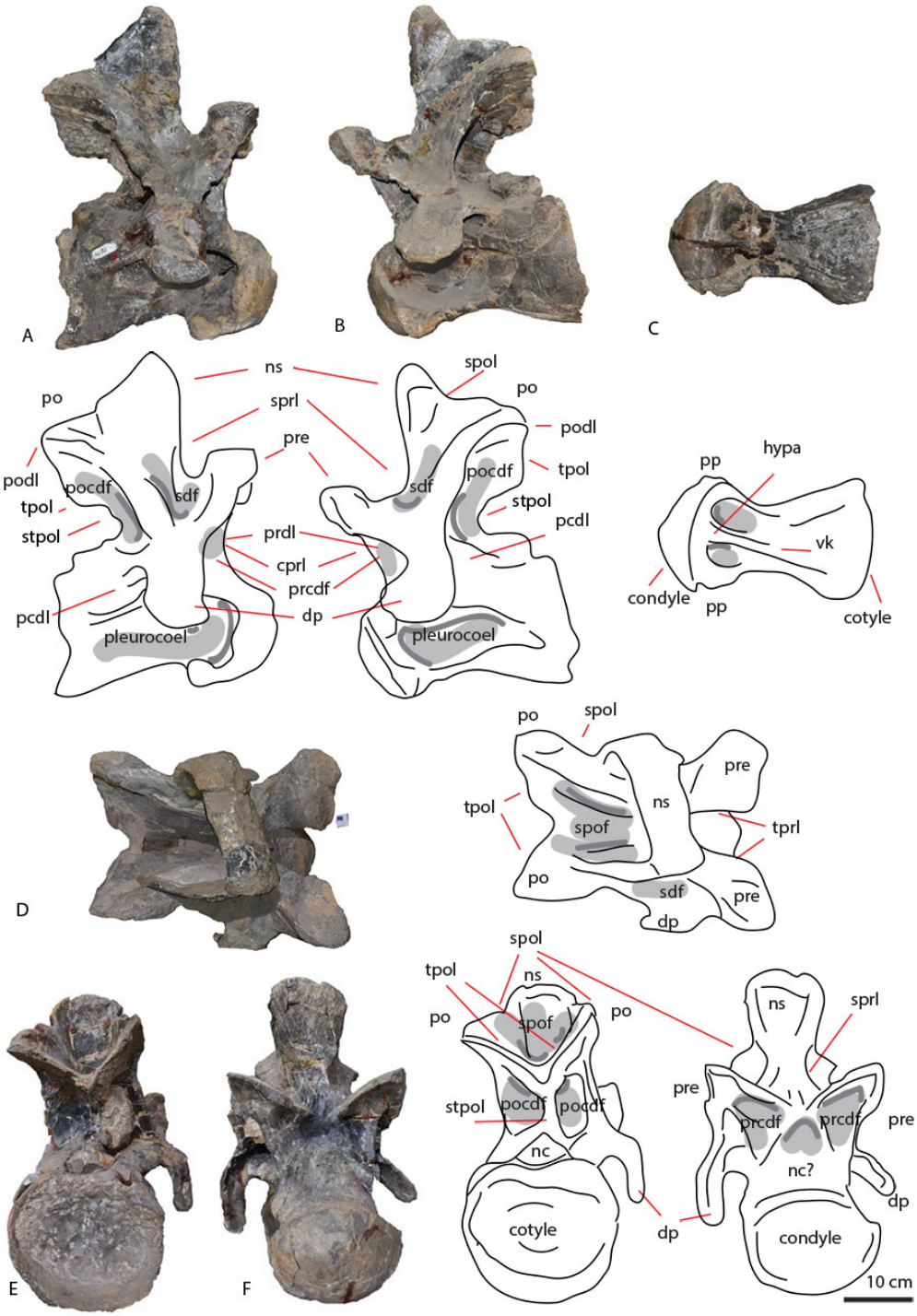

Figure 8: Cervical PVL 4170 (7) in lateral (A,B), ventral (C), dorsal (D), anterior (E) and posterior (F) views. Abbreviations: acdl = anterior centrodiapophyseal lamina, cprl = centroprezygapophyseal lamina, cpol = centropostzygapophyseal lamina, dp = diapophysis, hypa = hypapophysis, nc = neural canal, ns = neural spine, pp = parapophysis, po = postzygapophysis, prcdf = prezygapophyseal centrodiapophyseal fossa, pocdf = postzygapophyseal centrodiapophyseal fossa, prdl = prezygapophyseal diapophyseal lamina, pre = prezygapophysis, sdf = spinodiapophysal fossa, spof = spinopostzygapophyseal fossa, spol = spinopostzygapophyseal lamina, sprf = spinoprezygapophyseal fossa, sprl = spinoprezygapophyseal lamina, tprl = intraprezygapophyseal lamina, tpol = intrapostzygapophyseal lamina, stpol = single intrapostzygapophyseal lamina, vk = ventral keel.

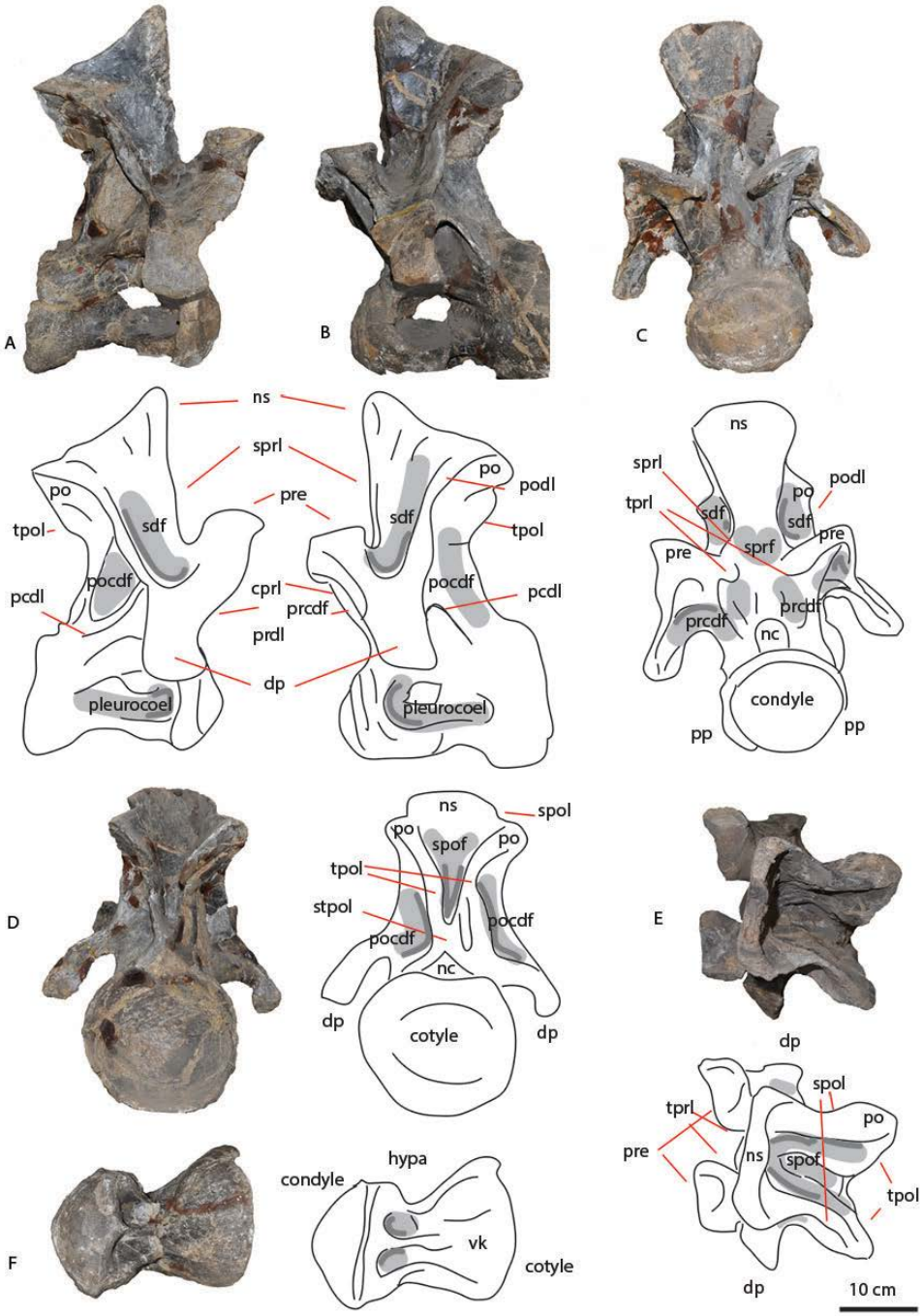

Figure 9: Cervicodorsal PVL 4170 (8) in lateral (A,B), anterior (C), posterior (D), dorsal (E) and ventral(F) views. Abbreviations: acdl = anterior centrodiapophyseal lamina, cprl = centroprezygapophyseal lamina, cpol = centropostzygapophyseal lamina, dp = diapophysis, hypa = hypapophysis, nc = neural canal, ns = neural spine, pp = parapophysis, po = postzygapophysis, prcdf = prezygapophyseal centrodiapophyseal fossa, pocdf = postzygapophyseal centrodiapophyseal fossa, prdl = prezygapophyseal diapophyseal lamina, pre = prezygapophysis, sdf = spinodiapophysal fossa, spof = spinopostzygapophyseal fossa, spol = spinopostzygapophyseal lamina, sprf = spinoprezygapophyseal fossa, sprl = spinoprezygapophyseal lamina, tprl = intraprezygapophyseal lamina, tpol = intrapostzygapophyseal lamina, stpol = single intrapostzygapophyseal lamina, vk = ventral keel.

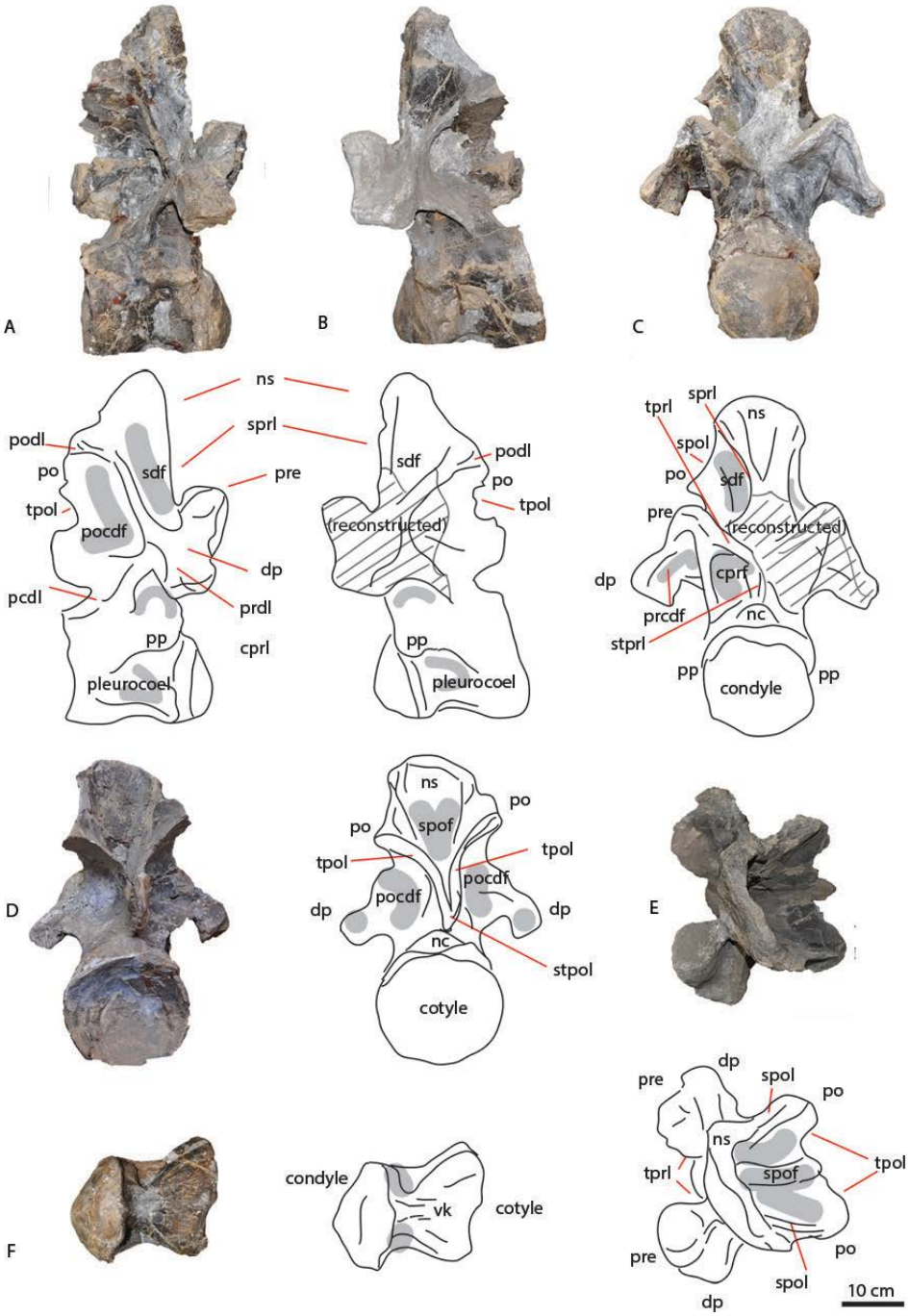

Figure 10: Dorsal PVL 4170 (9) in lateral (A,B), anterior (C), posterior (D), dorsal (E) and ventral (F) views. Note part of this vertebra is reconstructed. Abbreviations: acdl = anterior centrodiapophyseal lamina, cprl = centroprezygapophyseal lamina, cpol = centropostzygapophyseal lamina, dp = diapophysis, hypa = hypapophysis, nc = neural canal, ns = neural spine, pcdl = posterior centrodiapophysesal lamina, pp = parapophysis, po = postzygapophysis, prcdf = prezygapophyseal centrodiapophyseal fossa, pocdf = postzygapophyseal centrodiapophyseal fossa, prdl = prezygapophyseal diapophyseal lamina, pre = prezygapophysis, sdf = spinodiapophysal fossa, spof = spinopostzygapophyseal fossa, spol = spinopostzygapophyseal lamina, sprf = spinoprezygapophyseal fossa, sprl = spinoprezygapophyseal lamina, tprl = intraprezygapophyseal lamina, tpol = intrapostzygapophyseal lamina, stpol = single intrapostzygapophyseal lamina, stprl = single intrapostzygapophyseal lamina, vk = ventral keel.

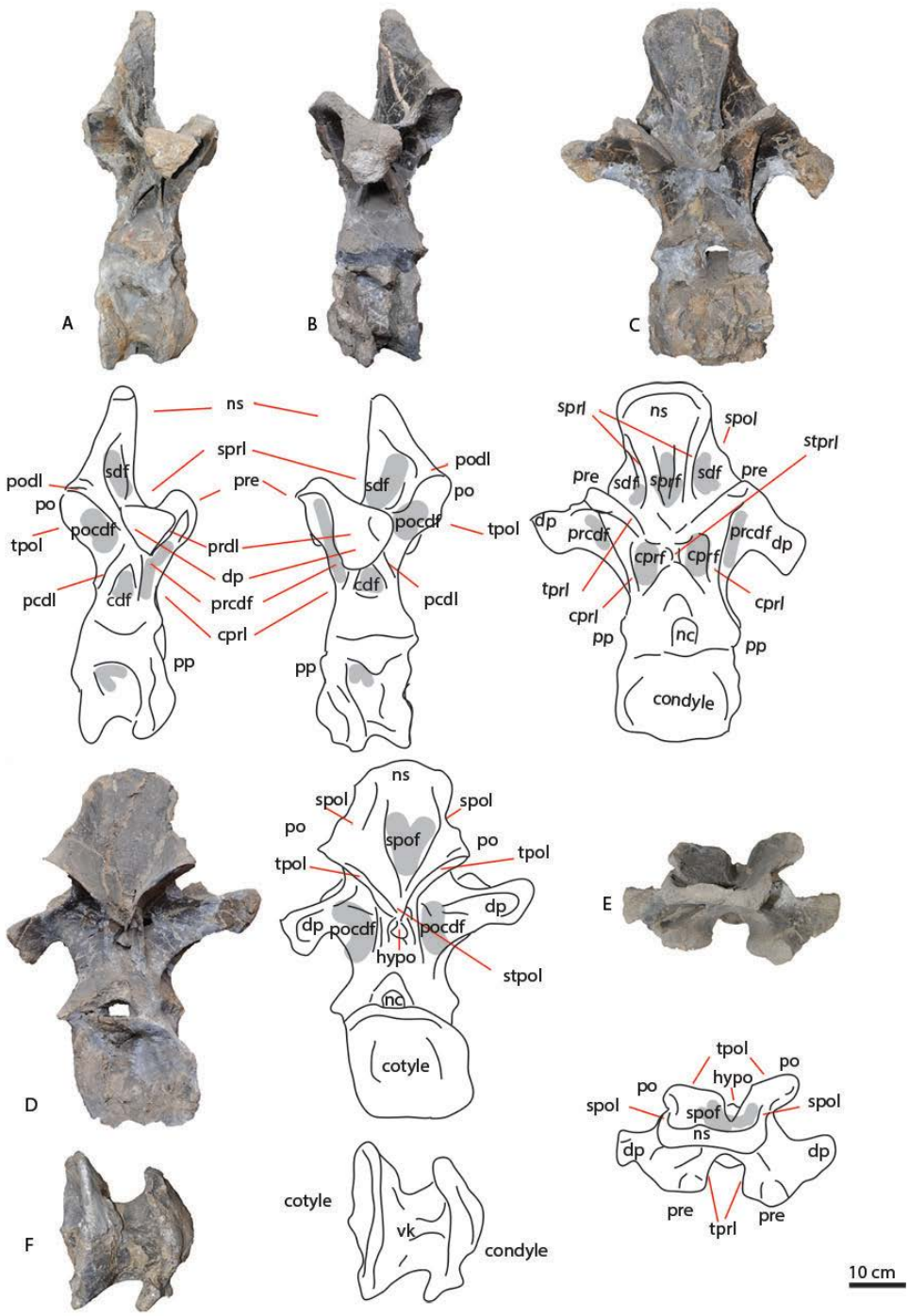

Figure 11: MACN-CH 4170 (10) dorsal vertebra in lateral (A,B) anterior (C), posterior (D), dorsal (E) and ventral (F) views. Abbreviations: acdl = anterior centrodiapophyseal lamina, cdf = centrodiapophyseal fossa, cprl = centroprezygapophyseal lamina, dp = diapophysis, hypa = hypapophysis, nc = neural canal, ns = neural spine, pcdl = posterior centrodiapophyseal fossa, pp = parapophysis, po = postzygapophysis, prcdf = prezygapophyseal centrodiapophyseal fossa, pocdf = postzygapophyseal centrodiapophyseal fossa, prdl = prezygapophyseal diapophyseal lamina, pre = prezygapophysis, sdf = spinodiapophysal fossa, spof = spinopostzygapophyseal fossa, spol = spinopostzygapophyseal lamina, sprf = spinoprezygapophyseal fossa, sprl = spinoprezygapophyseal lamina, tprl = intraprezygapophyseal lamina, tpol = intrapostzygapophyseal lamina, stpol = single intrapostzygapophyseal lamina, stprl = single intrapostzygapophyseal lamina, vk = ventral keel.

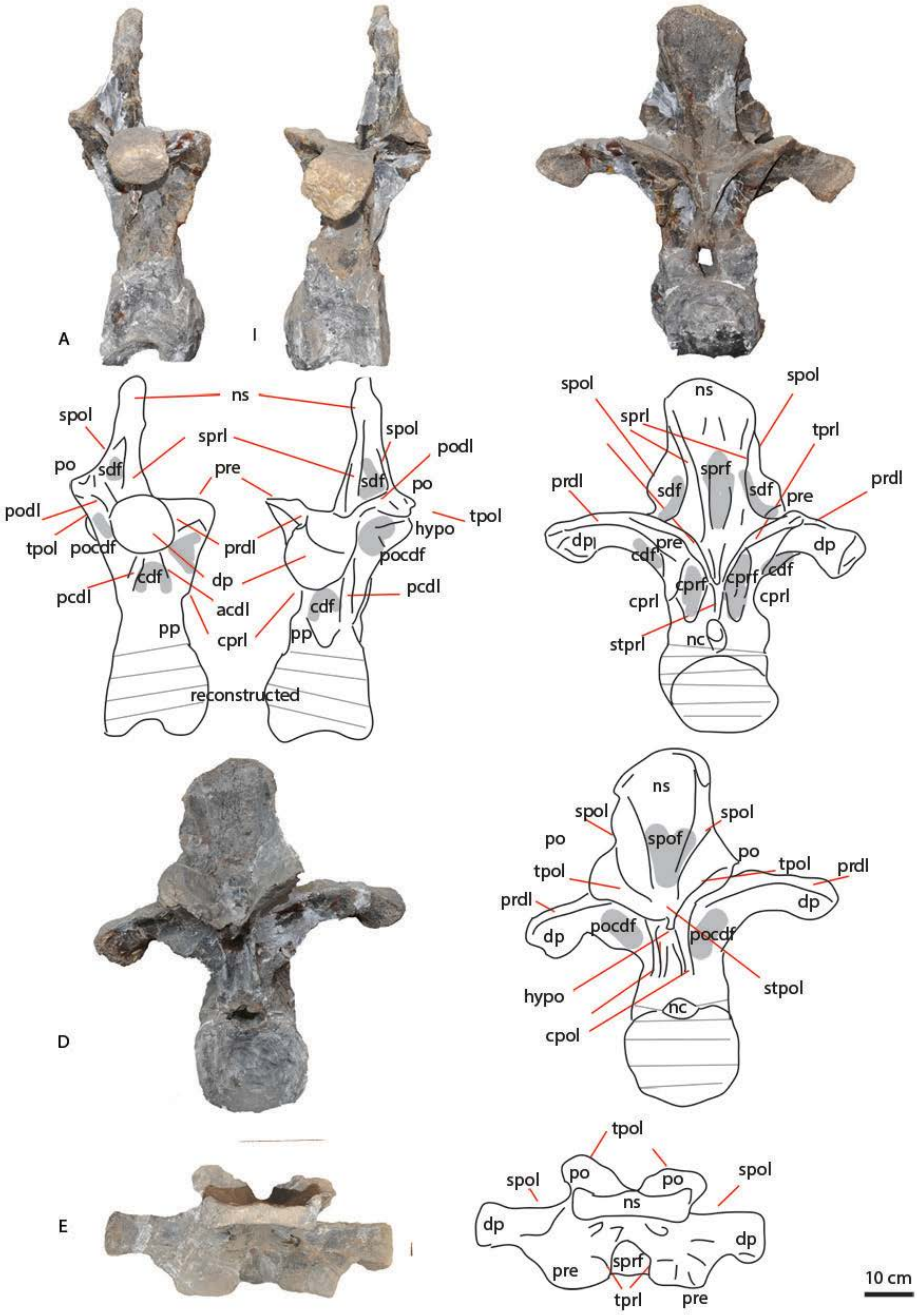

Figure 12: Dorsal MACN-CH 4170 (11) in lateral (A,B) anterior (C), posterior (D), and dorsal (E) views. Note that the centrum is reconstructed, and a ventral view is therefore not given. Abbreviations: acdl = anterior centrodiapophyseal lamina, cdf = centodiapophyseal fossa, cpol = centropostzygapophyseal lamina, cprl = centroprezygapophyseal lamina, dp = diapophysis, hypa = hypapophysis, nc = neural canal, ns = neural spine, pcdl = posterior centrodiapophyseal lamina, pp = parapophysis, po = postzygapophysis, prcdf = prezygapophyseal centrodiapophyseal fossa, pocdf = postzygapophyseal centrodiapophyseal fossa, prdl = prezygapophyseal diapophyseal lamina, pre = prezygapophysis, sdf = spinodiapophysal fossa, spof = spinopostzygapophyseal fossa, spol = spinopostzygapophyseal lamina, sprf = spinoprezygapophyseal fossa, sprl = spinoprezygapophyseal lamina, tprl = intraprezygapophyseal lamina, tpol = intrapostzygapophyseal lamina, stpol = single intrapostzygapophyseal lamina, stprl = single intrapostzygapophyseal lamina, vk = ventral keel.

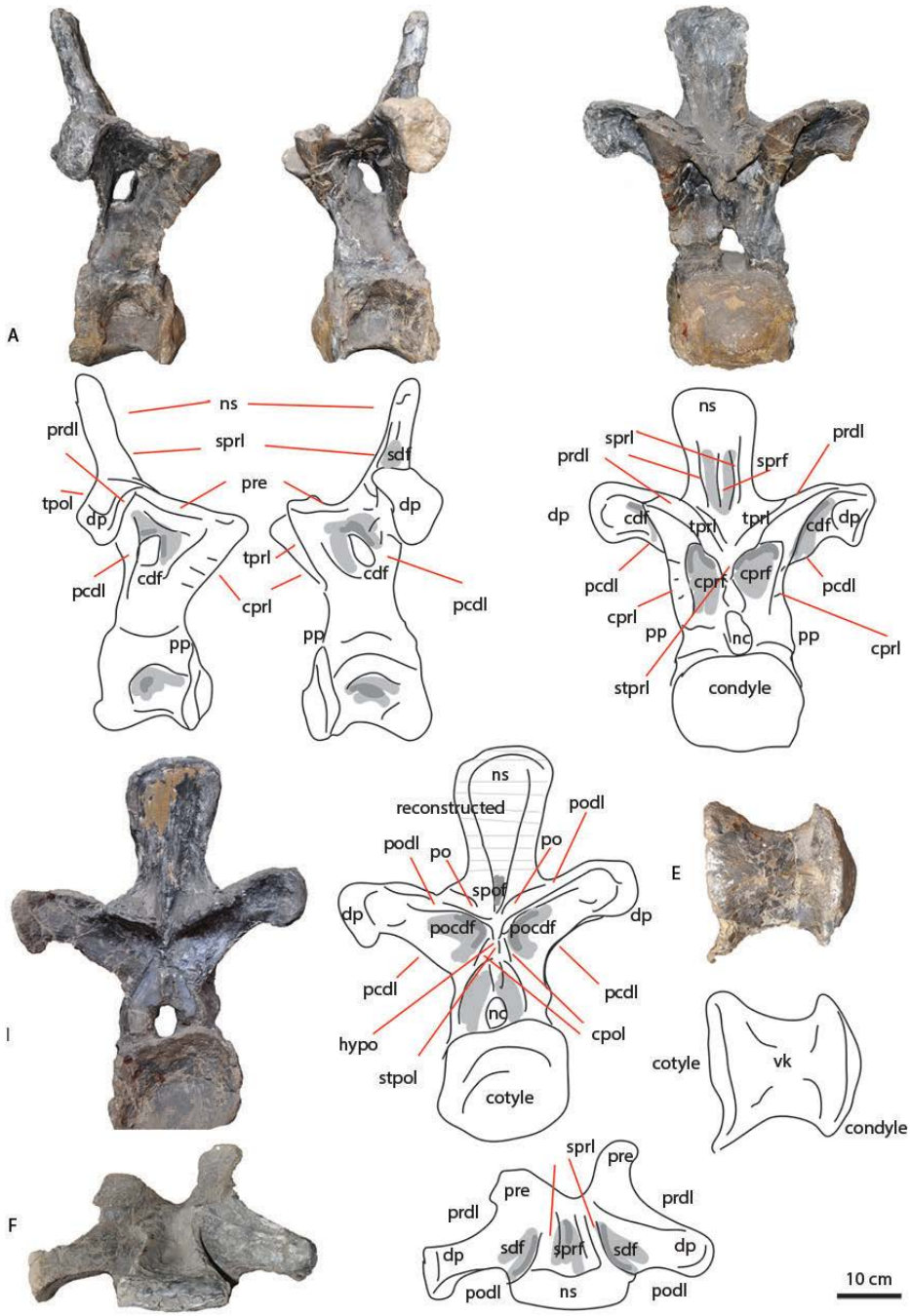

Figure 13: Dorsal MACN-CH 4170 (12) in lateral (A,B) anterior (C), posterior (D), ventral (E) and dorsal (F) views. Note that a large part of the posterior neural arch and spine is reconstructed. Abbreviations: acdl = anterior centrodiapophyseal lamina, cprl = centroprezygapophyseal lamina, dp = diapophysis, hypa = hypapophysis, nc = neural canal, ns = neural spine, pcdl = posterior centrodiapophyseal lamina, pp = parapophysis, po = postzygapophysis, prcdf = prezygapophyseal centrodiapophyseal fossa, pocdf = postzygapophyseal centrodiapophyseal fossa, prdl = prezygapophyseal diapophyseal lamina, pre = prezygapophysis, sdf = spinodiapophysal fossa, spof = spinopostzygapophyseal fossa, spol = spinopostzygapophyseal lamina, sprf = spinoprezygapophyseal fossa, sprl = spinoprezygapophyseal lamina, tprl = intraprezygapophyseal lamina, tpol = intrapostzygapophyseal lamina, stpol = single intrapostzygapophyseal lamina, stprl = single intrapostzygapophyseal lamina, vk = ventral keel.

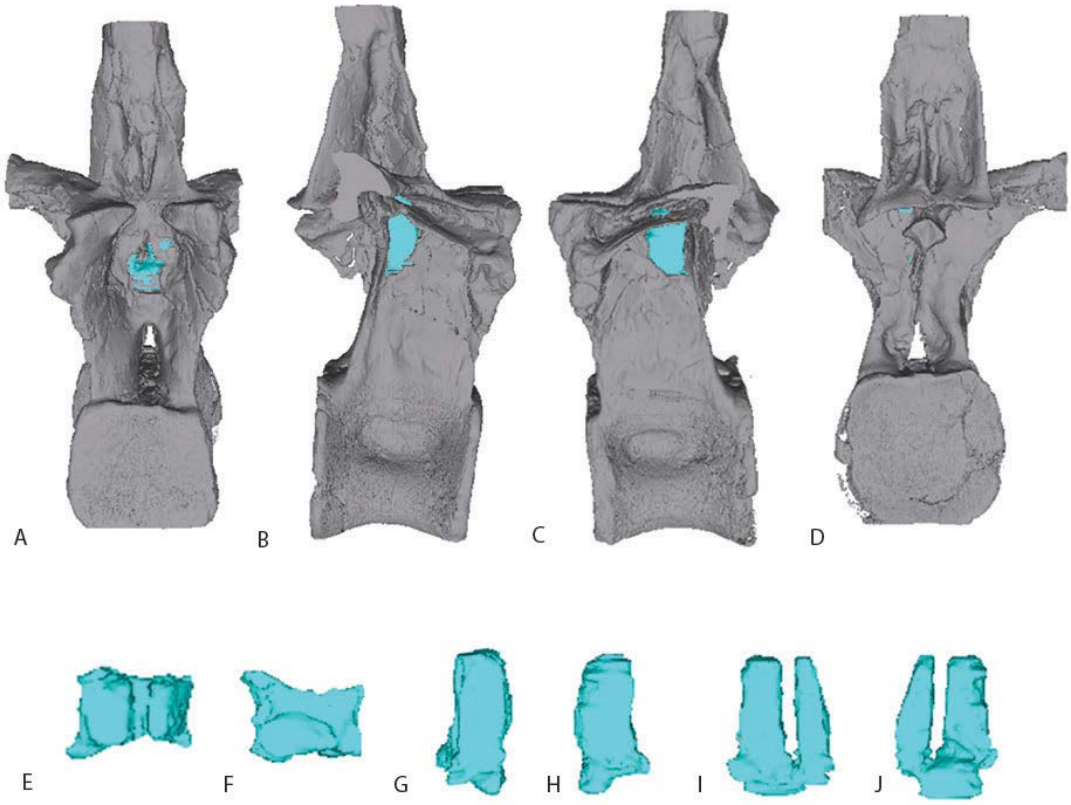

Figure 14: CT scan of PVL 4170 (13) in anterior (A), lateral (B,C) and posterior (D) views, with the shape of the internal pneumatic feature highlighted in light blue, in dorsal (E), ventral (F) lateral (G,H), anterior (I) and posterior (J) views.

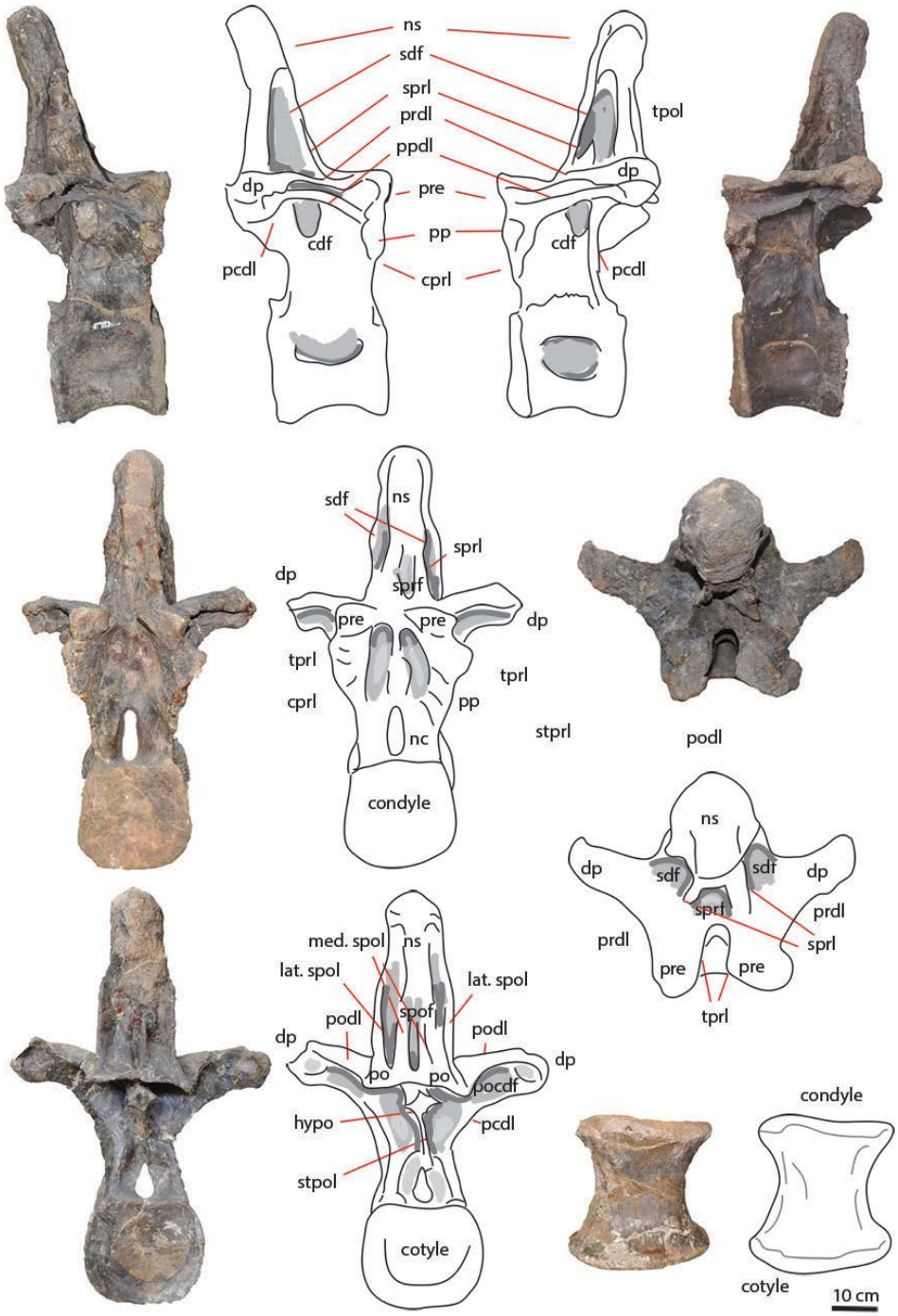

Figure 15 (previous page): Dorsal MACN-CH 4170 (13) in lateral (A,B), anterior (C), dorsal (D), posterior (E) and ventral (F) views. Abbreviations: acdl = anterior centrodiapophyseal lamina, cprl = centroprezygapophyseal lamina, dp = diapophysis, hypa = hypapophysis, nc = neural canal, ns = neural spine, pcdl = posterior centrodiapophyseal lamina, pp = parapophysis, po = postzygapophysis, prcdf = prezygapophyseal centrodiapophyseal fossa, pocdf = postzygapophyseal centrodiapophyseal fossa, prdl = prezygapophyseal diapophyseal lamina, pre = prezygapophysis, sdf = spinodiapophysal fossa, spof = spinopostzygapophyseal fossa, spol = spinopostzygapophyseal lamina, sprf = spinoprezygapophyseal fossa, lat.spol/med.spol = lateral/medial spinopostzygapophyseal lamina, sprl = spinoprezygapophyseal lamina, tprl = intraprezygapophyseal lamina, tpol = intrapostzygapophyseal lamina, stpol = single intrapostzygapophyseal lamina, stprl = single intrapostzygapophyseal lamina, vk = ventral keel.

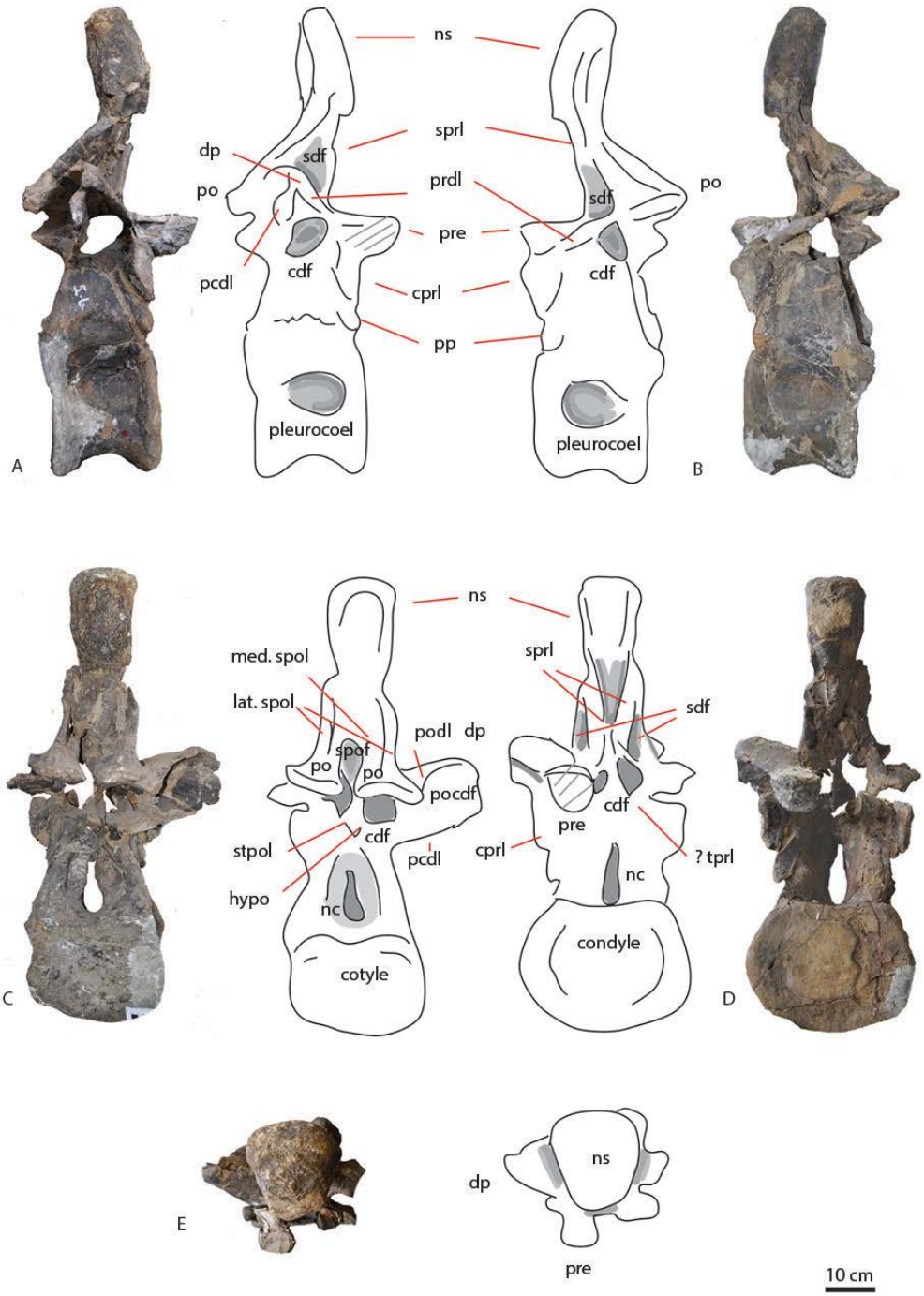

Figure 16: Dorsal MACN-CH 4170 (14) in lateral (A,B), posterior (C) , anterior (D), and dorsal (E) views.Abbreviations: acdl = anterior centrodiapophyseal lamina, cprl = centroprezygapophyseal lamina, dp = diapophysis, hypa = hypapophysis, nc = neural canal, ns = neural spine, pp = parapophysis, po = postzygapophysis, prcdf = prezygapophyseal centrodiapophyseal fossa, pocdf = postzygapophyseal centrodiapophyseal fossa, prdl = prezygapophyseal diapophyseal lamina, pre = prezygapophysis, sdf = spinodiapophysal fossa, spof = spinopostzygapophyseal fossa, spol = spinopostzygapophyseal lamina, sprf = spinoprezygapophyseal fossa, sprl = spinoprezygapophyseal lamina, tprl = intraprezygapophyseal lamina, tpol = intrapostzygapophyseal lamina, lat.spol/med.spol = lateral/medial spinopostzygapophyseal lamina, stpol = single intrapostzygapophyseal lamina, stprl = single intrapostzygapophyseal lamina, vk = ventral keel.

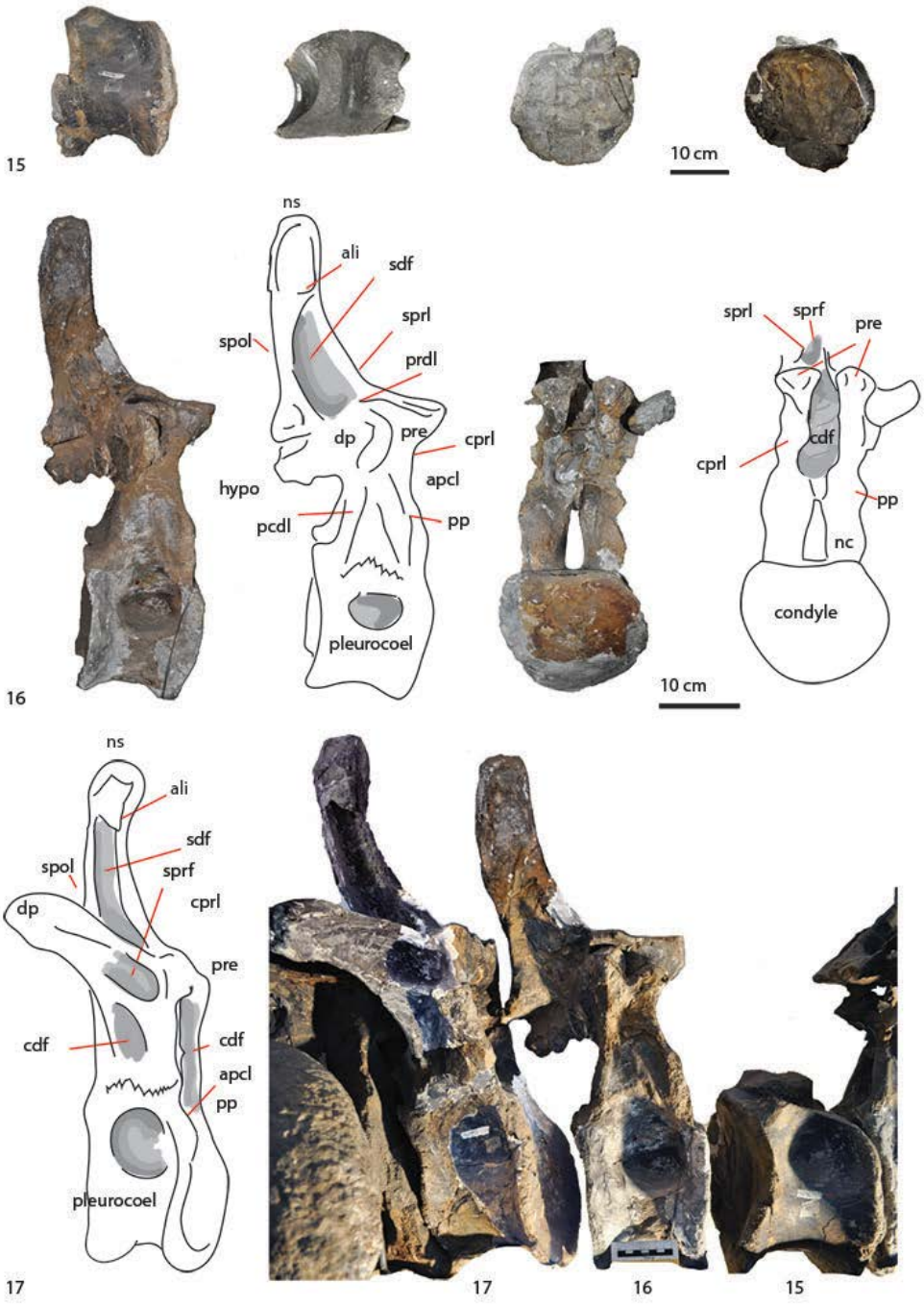

Figure 17: Dorsals PVL 4170 (15,16,17). PVL 4170 (15) in lateral, dorsal, anterior, posterior (oblique) view. PVL 4170 (16) in lateral and anterior view. PVL 4170 (17) in lateral view. Abbreviations: acdl = anterior centrodiapophyseal lamina, ali = aliform process, cprl = centroprezygapophyseal lamina, cpol = centropostzygapophyseal lamina, dp = diapophysis, hypa = hypapophysis, nc = neural canal, ns = neural spine, pp = parapophysis, po = postzygapophysis, prcdf = prezygapophyseal centrodiapophyseal fossa, pocdf = postzygapophyseal centrodiapophyseal fossa, prdl = prezygapophyseal diapophyseal lamina, pre = prezygapophysis, sdf = spinodiapophysal fossa, spof = spinopostzygapophyseal fossa, spol = spinopostzygapophyseal lamina, sprf = spinoprezygapophyseal fossa, sprl = spinoprezygapophyseal lamina, tprl = intraprezygapophyseal lamina, tpol = intrapostzygapophyseal lamina, stpol = single intrapostzygapophyseal lamina, stprl = single intrapostzygapophyseal lamina, vk = ventral keel.

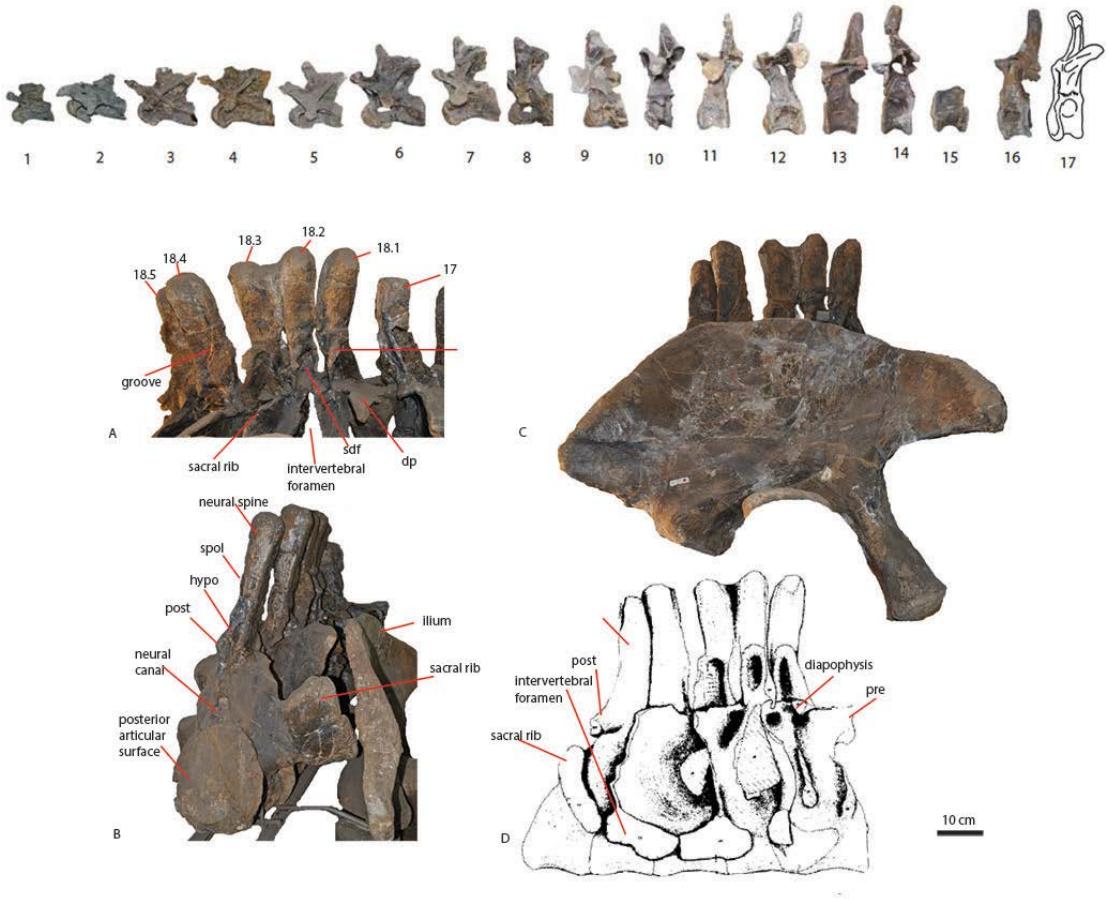

Figure 18: Upper row: All presacral vertebrae of MACN-CH 4170 (1-17) in left lateral view (not to scale). Lower row: all sacral vertebrae of PVL 4170 (18) sacrum. A: PVL 4170 (18.1-5) sacral neural arches and spines in right lateral view with dorsal PVL 4170 (17) on the right. B: PVL 4170 (18) in posterior view. C: PVL 4170 (18) associated with ilium PVL 4170 (34). D: Original drawing of PVL 4170 (Bonaparte, 1986b). Abbreviations: hypo = hyposphene, pre = prezygapophysis, post = postzygapophysis, spol = spinopostzygapophyseal lamina.

Figure 19: Anterior Caudals PVL 4170 (19-20-21) in lateral view.

Figure 20: Middle Caudals PVL 4170 (22-23-24) in lateral view.

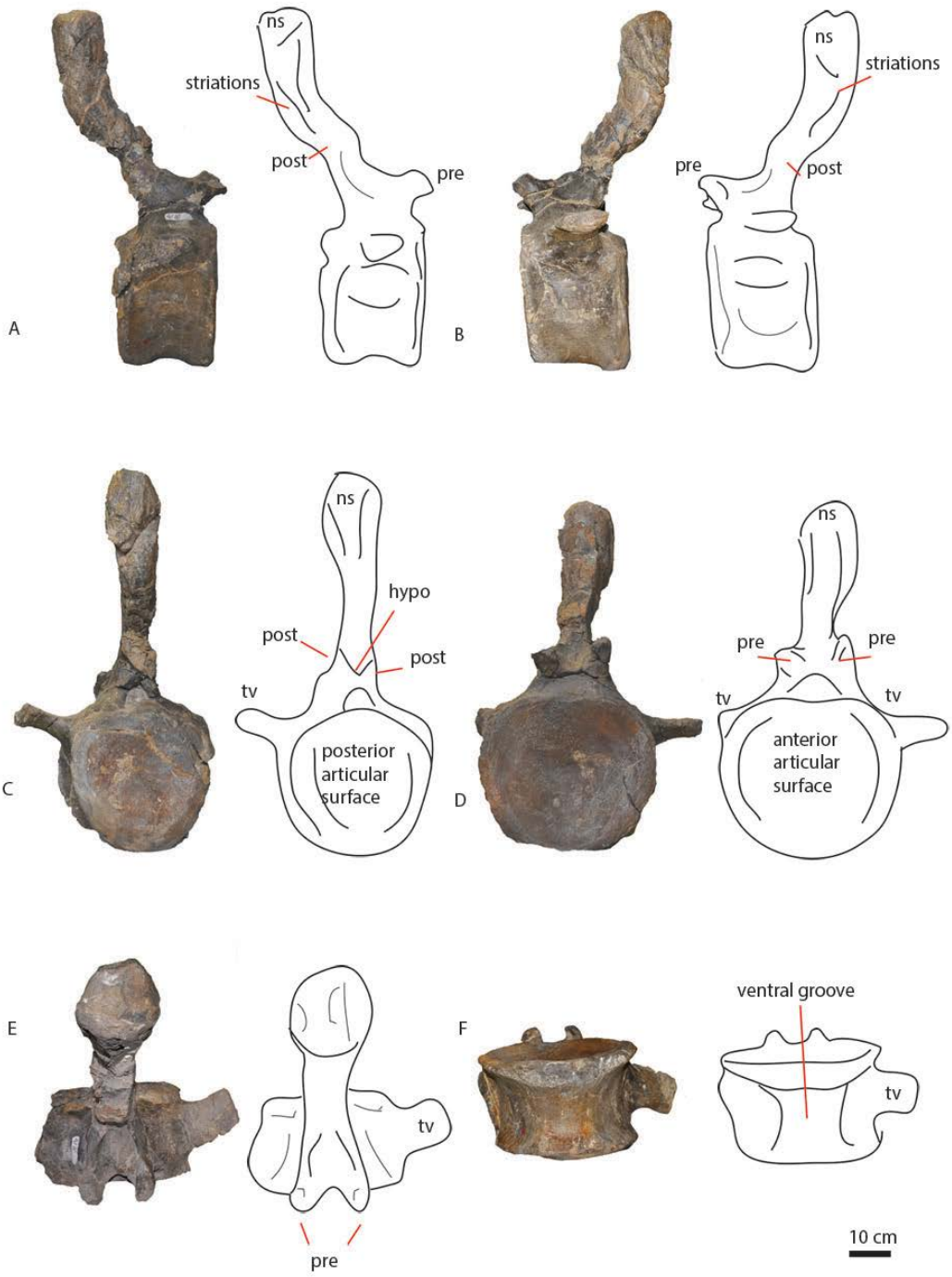

Figure 21: Caudal PVL 4170 (19) in lateral (A,B), posterior (C), anterior (D) and ventral (E) and dorsal (F) views. Abbreviations: hypo = hyposphene, ns = neural spine, post = postzygapophysis, pre = prezygapophysis, tv = transverse process.

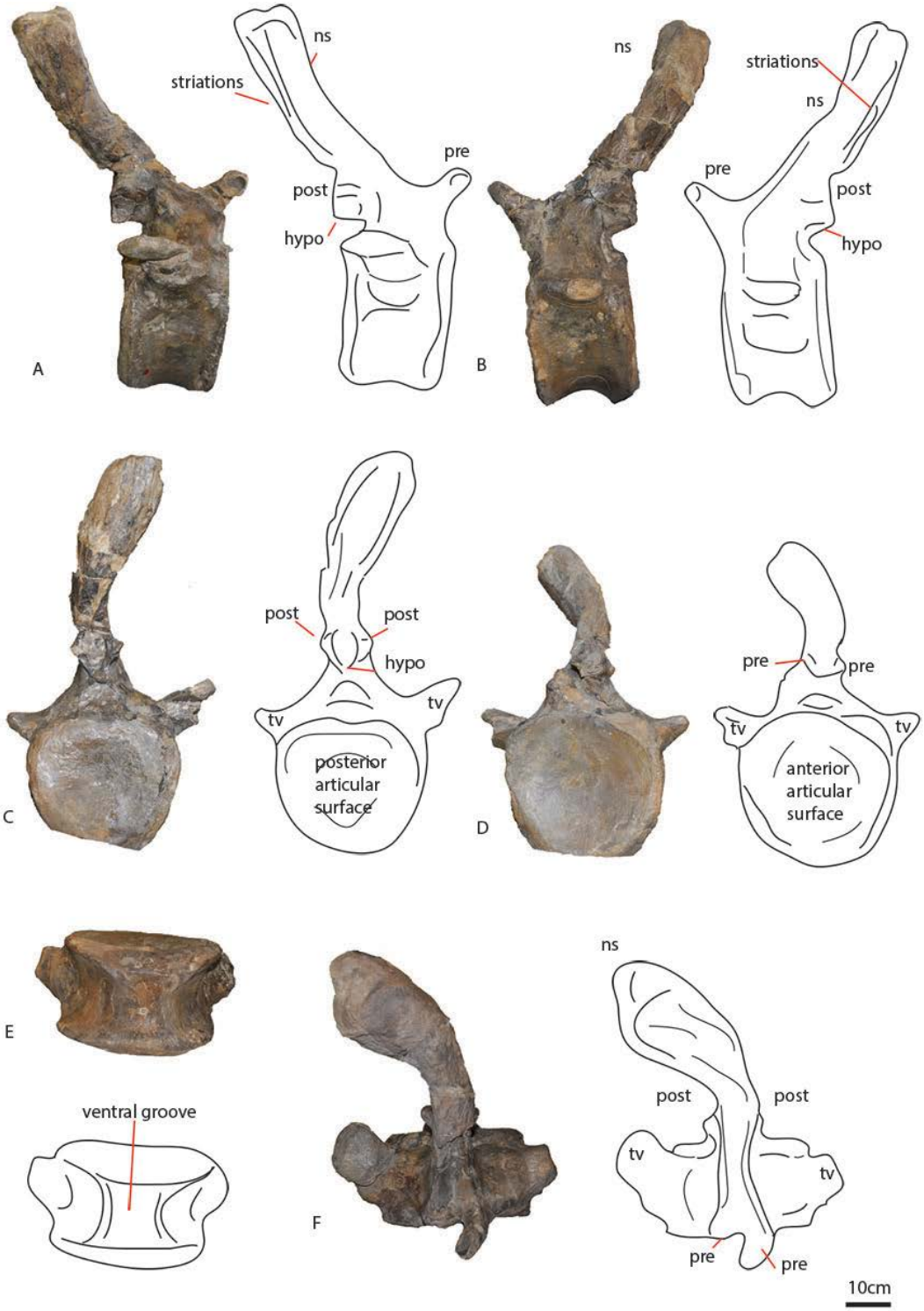

Figure 22: Caudal PVL 4170 (20) in lateral (A,B), posterior (C), anterior (D), dorsal (E) and ventral (F) views. Abbreviations: hypo = hyposphene, ns = neural spine, post = postzygapophysis, pre = prezygapophysis, tv = transverse process.

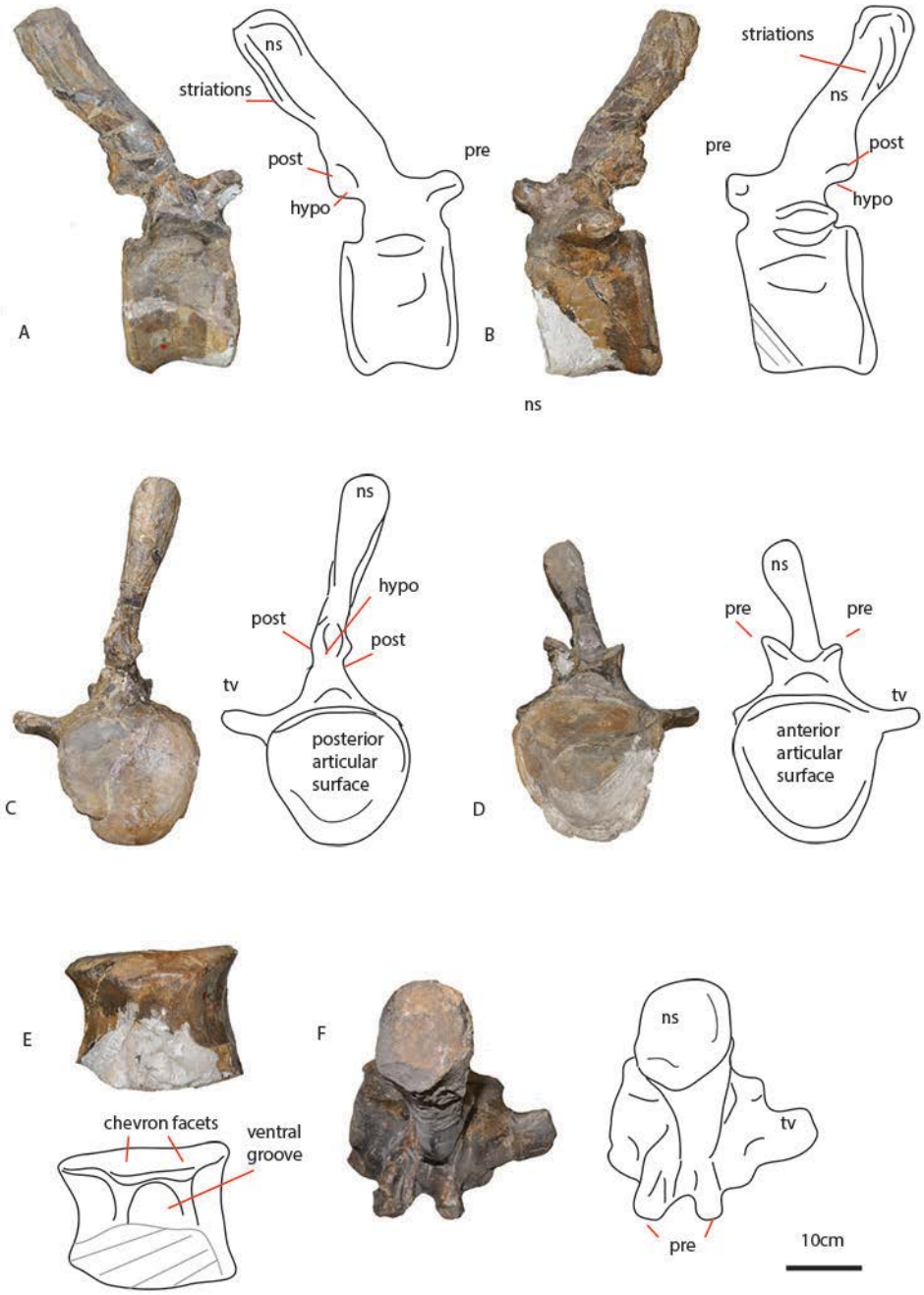

Figure 23: Caudal PVL 4170 (21) in lateral (A,B), posterior (C), anterior (D), ventral (E) and dorsal (F) views. Abbreviations: hypo = hyposphene, ns = neural spine, post = postzygapophysis, pre = prezygapophysis, tv = transverse process.

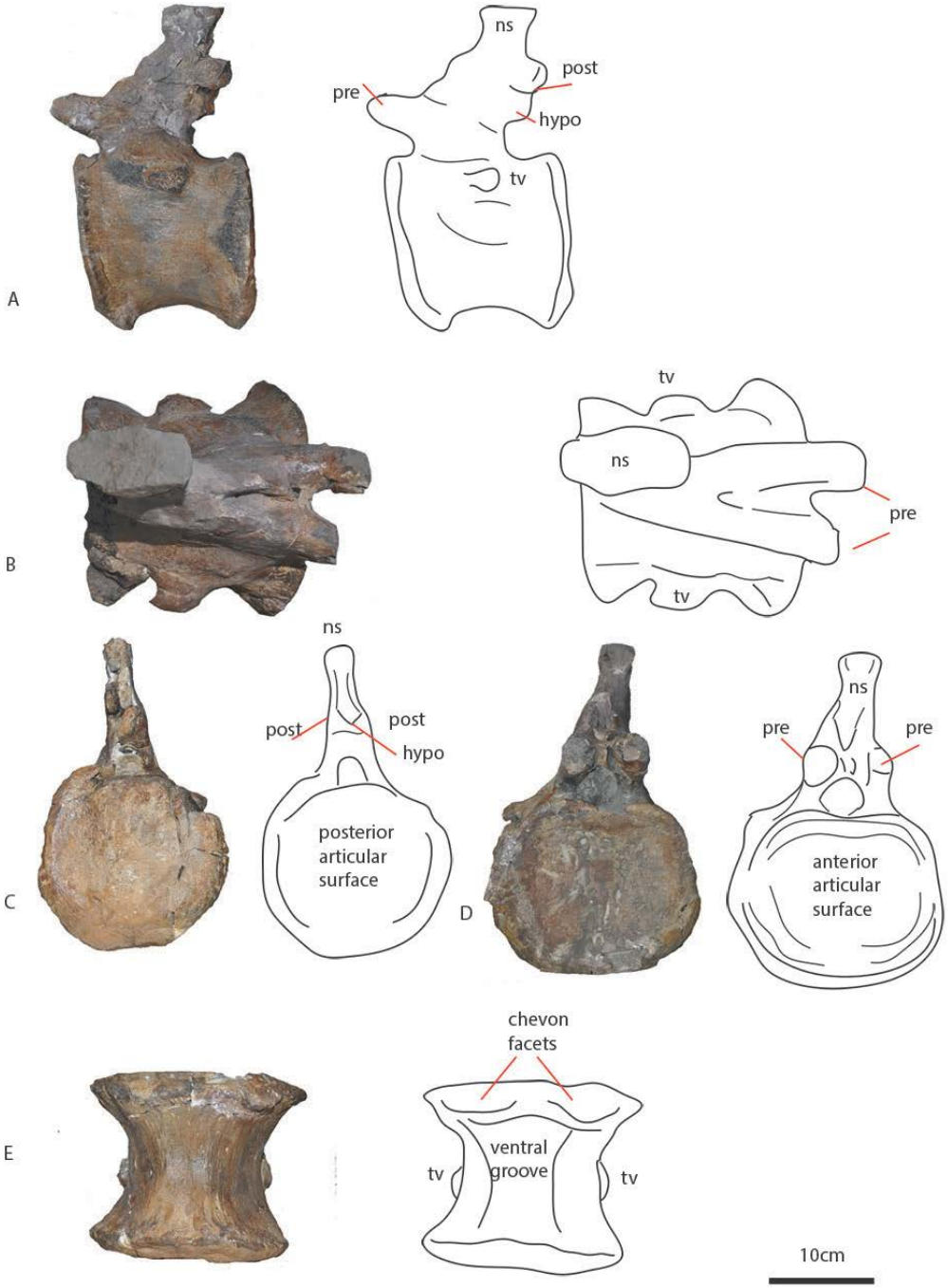

Figure 24: Caudal PVL 4170 (22) in lateral (A), dorsal (B), posterior (C), anterior (D) and ventral (E) views. Abbreviations: hypo = hyposphene, ns = neural spine, post = postzygapophysis, pre = prezygapophysis, tv = transverse process.

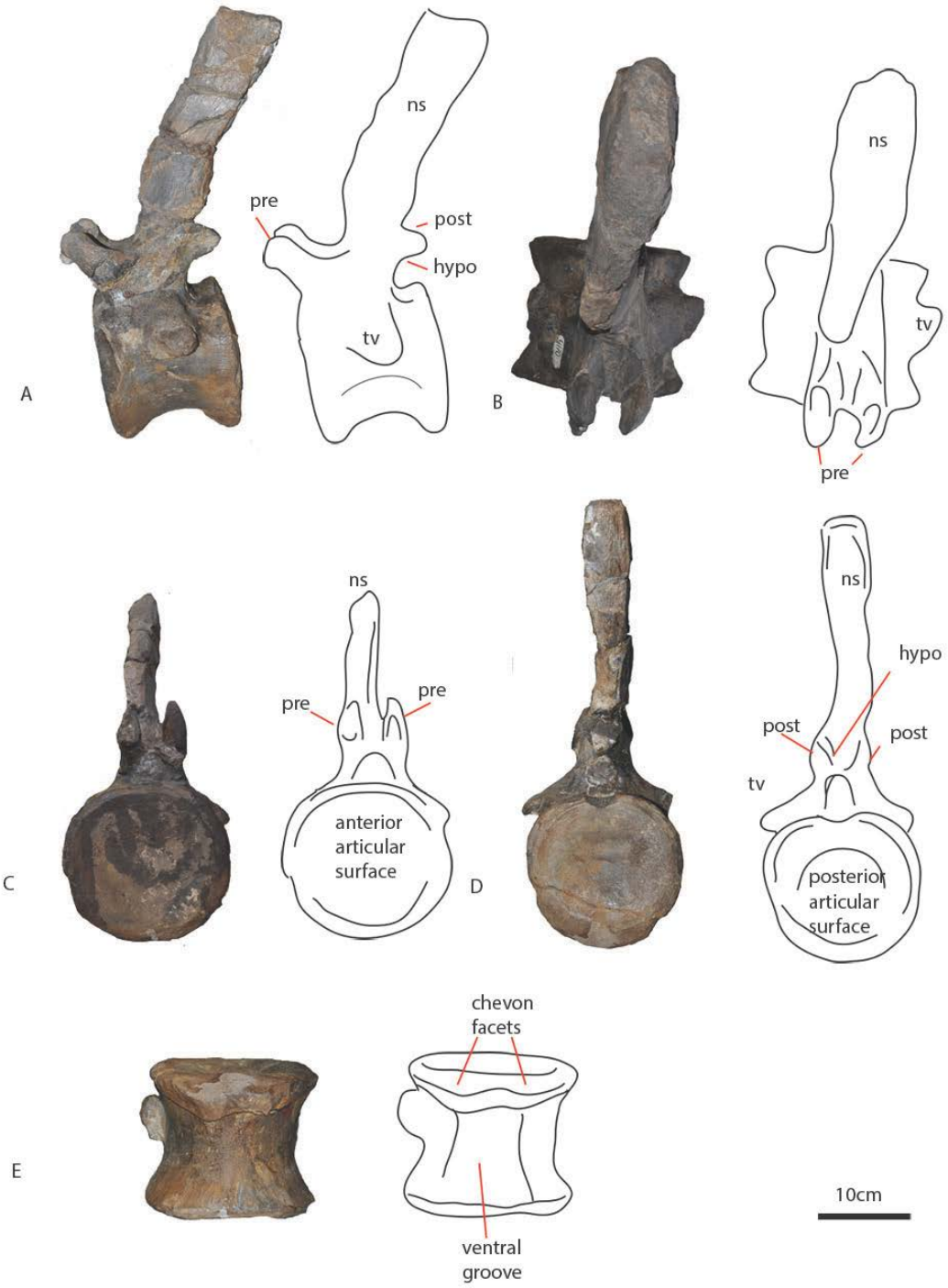

Figure 25: Caudal PVL 4170 (23) in lateral (A), dorsal (B), anterior (C), posterior (D) and ventral (E) views. Abbreviations: hypo = hyposphene, ns = neural spine, post = postzygapophysis, pre = prezygapophysis, tv = transverse process.

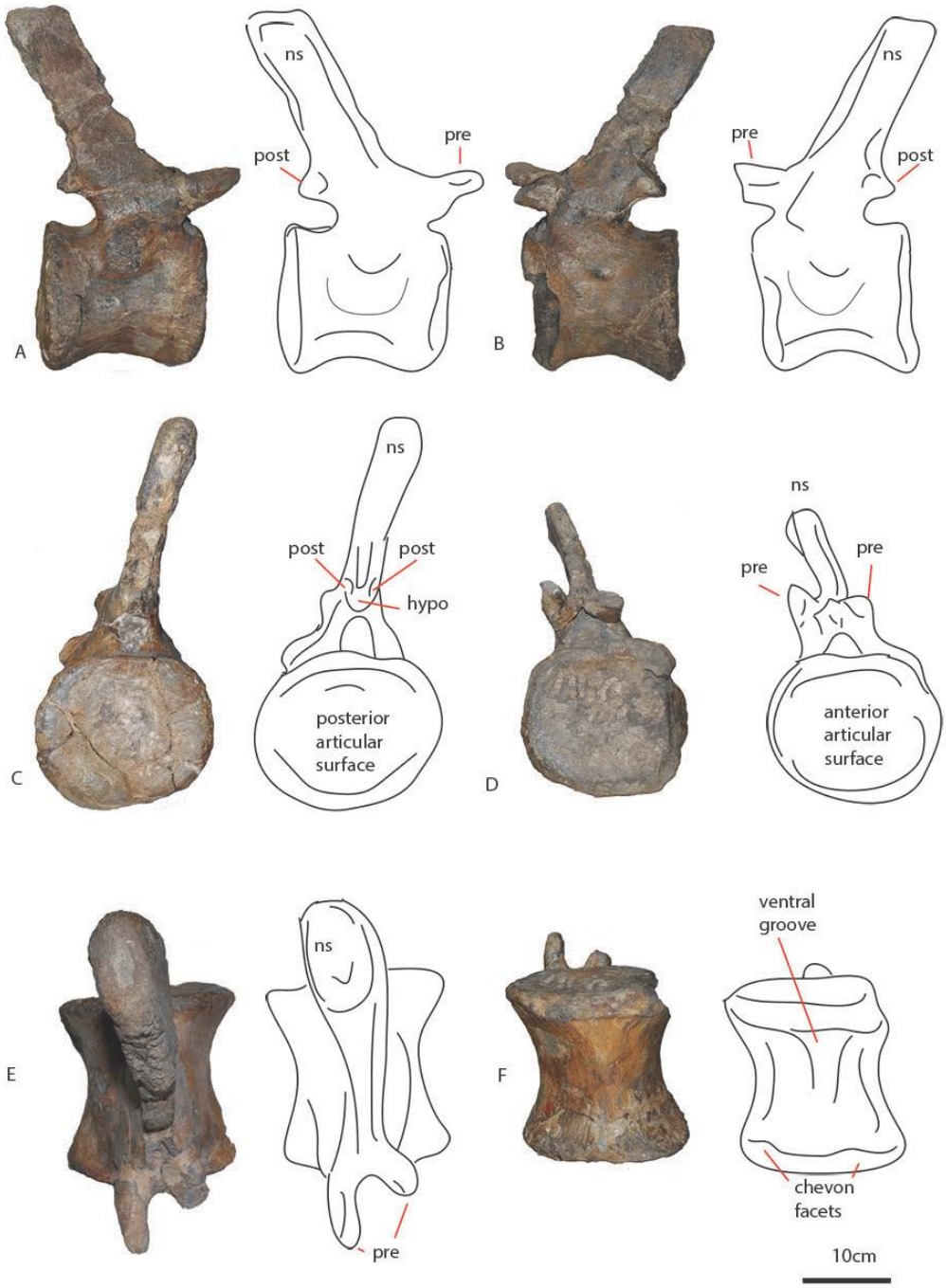

3097
3098 Figure 26: Caudal PVL 4170 (24) in lateral (A,B), posterior(C), anterior (D), dorsal (E) and
3099 ventral (F) views. Abbreviations: hypo = hyposphene, ns = neural spine, post =
3100 postzygapophysis, pre = prezygapophysis, tv = transverse process.
3101

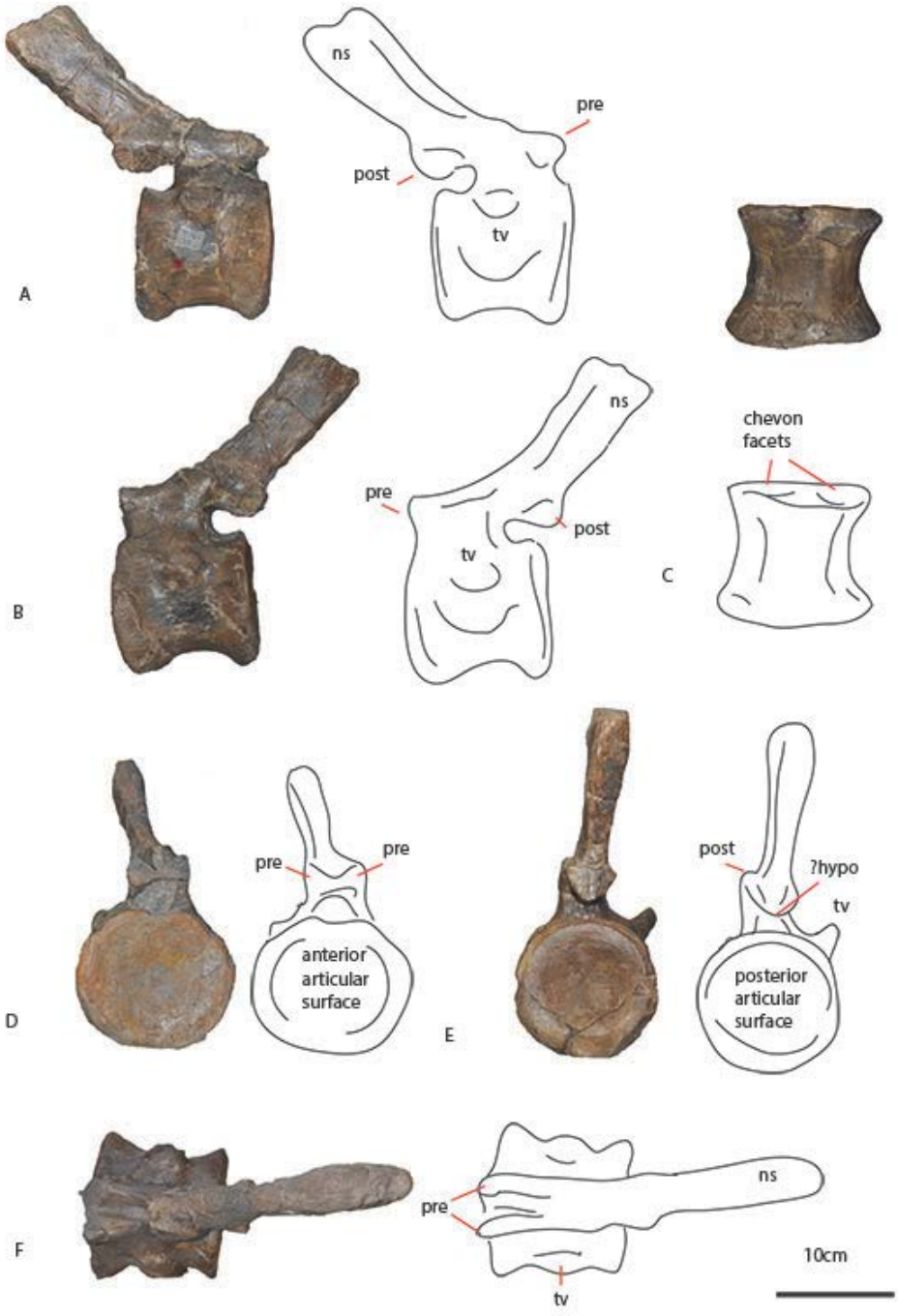

3102
3103 Figure 27: Caudal PVL 4170 (25) in lateral (A,B), ventral (C), anterior (D), posterior (E), and
3104 dorsal (F) views. Abbreviations: hypo = hyposphene, ns = neural spine, post =
3105 postzygapophysis, pre = prezygapophysis, tv = transverse process.
3106

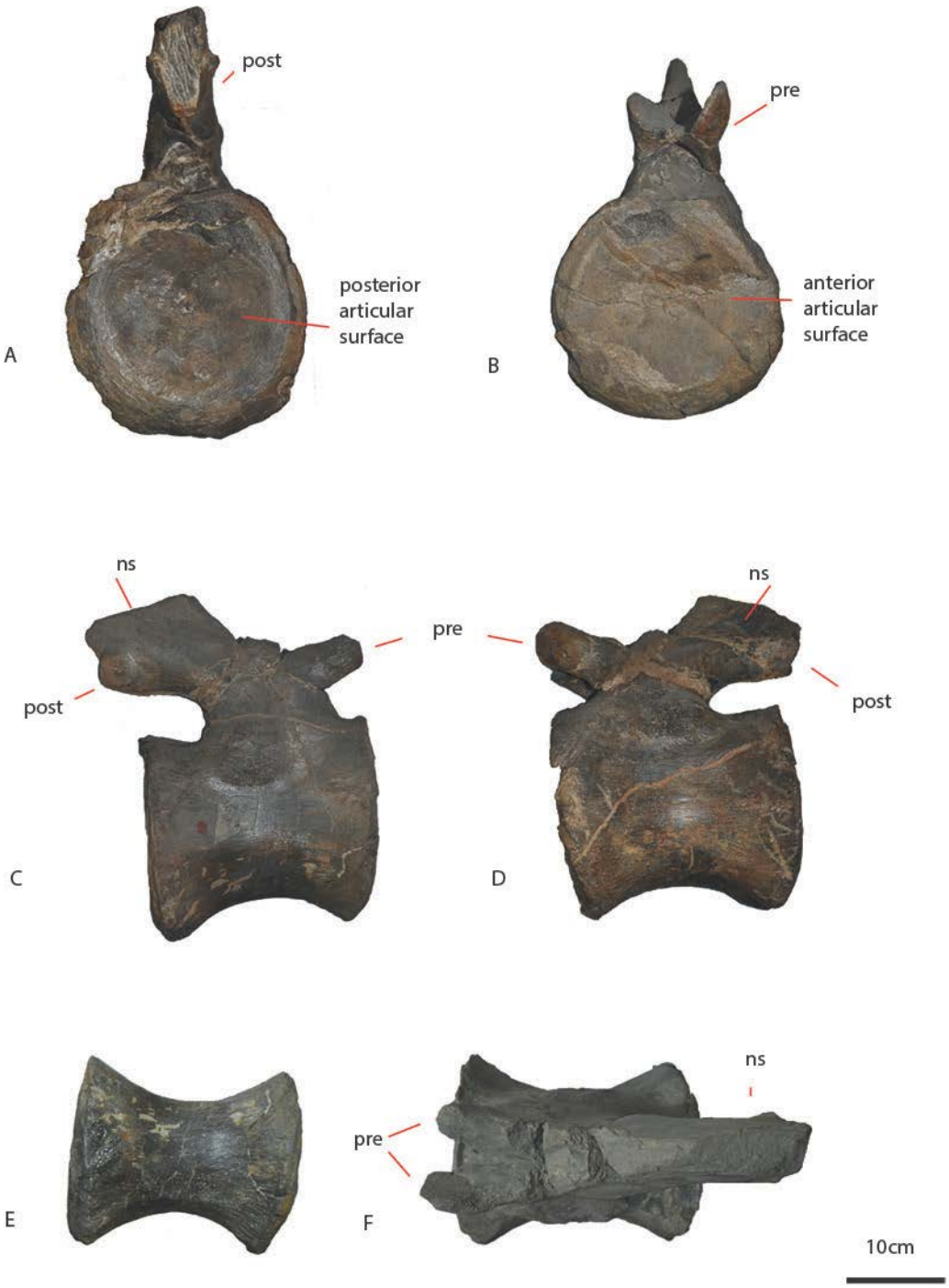

Figure 28: Caudal PVL 4170 (26) in posterior (A), anterior (B), lateral (C,D), ventral (E), and dorsal (F) views. Abbreviations: ns = neural spine, post = postzygapophysis, pre = prezygapophysis, tv = transverse process.

Figure 29: Caudal PVL 4170 (27) in dorsal (A), ventral (B), lateral (C,D), posterior (E), anterior (F) views.

Figure 30: Caudal PVL 4170 (30) in anterior (A), posterior (B), ventral (C), dorsal (D), lateral E,F) views.

3120
3121 Figure 31: PVL 4170 (34) ilium in anterior (A) posterior (B) and lateral (C) view.
3122

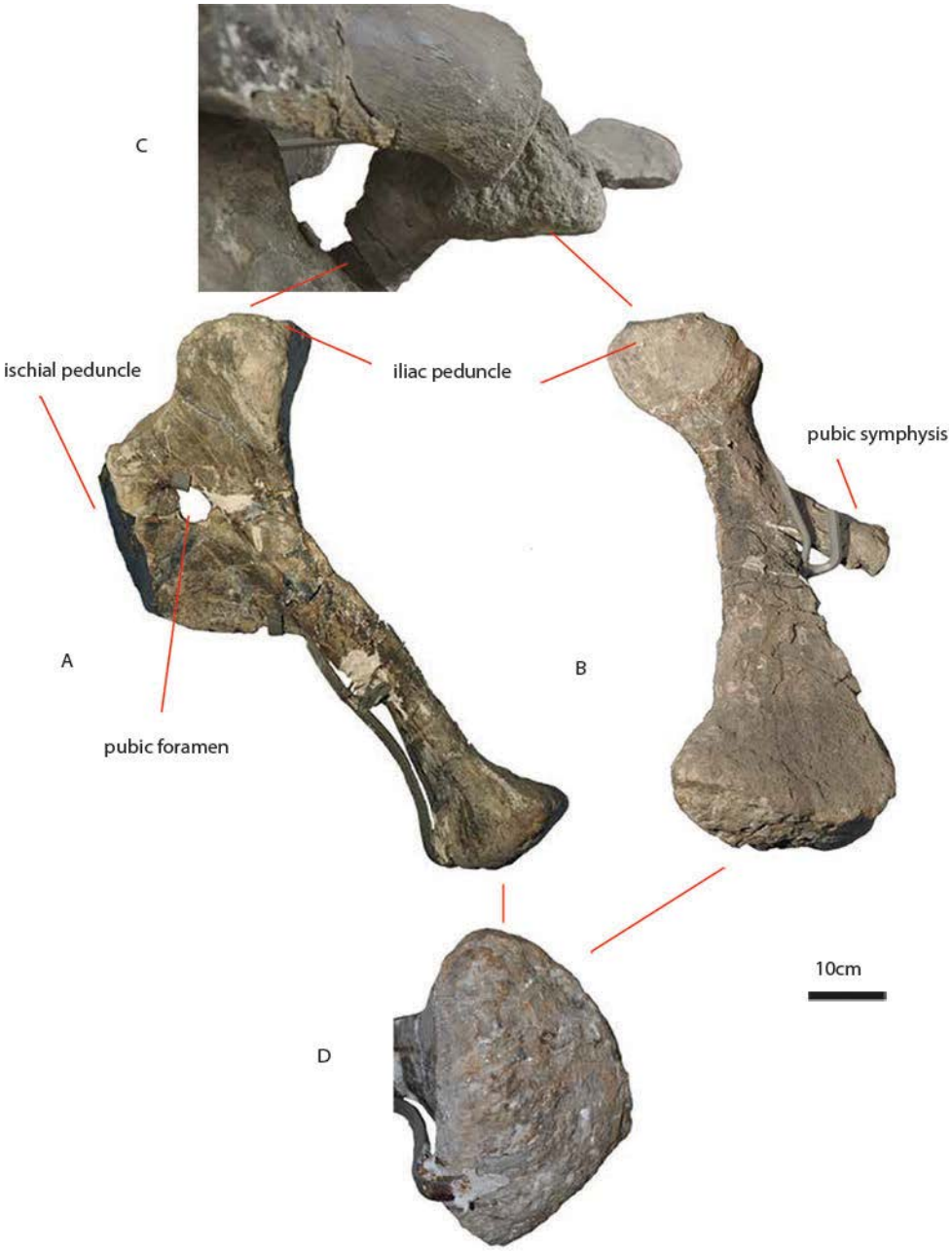

Figure 32: PVL 4170 (35) Pubis in lateral (A), distal (B), dorsal (C) and distal-most (D) view. Note that D is not to scale.

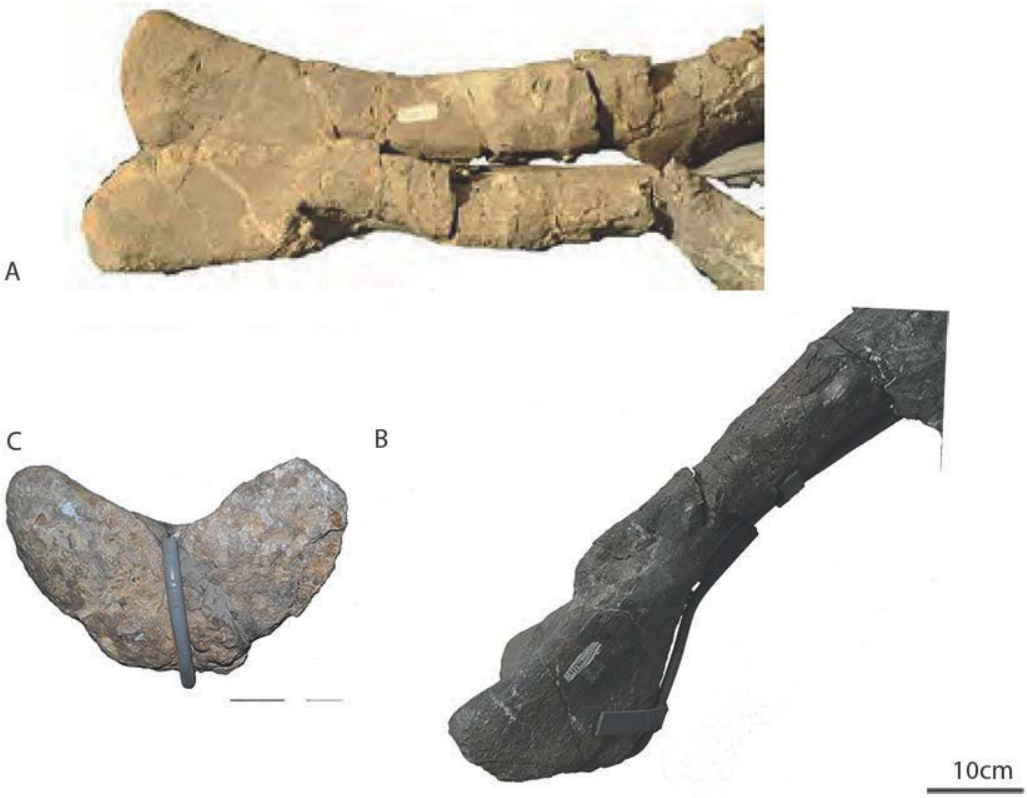

Figure 33: PVL 4170 (36) ischia in dorsal (A) view, distal (B) view, and lateral (C) view.

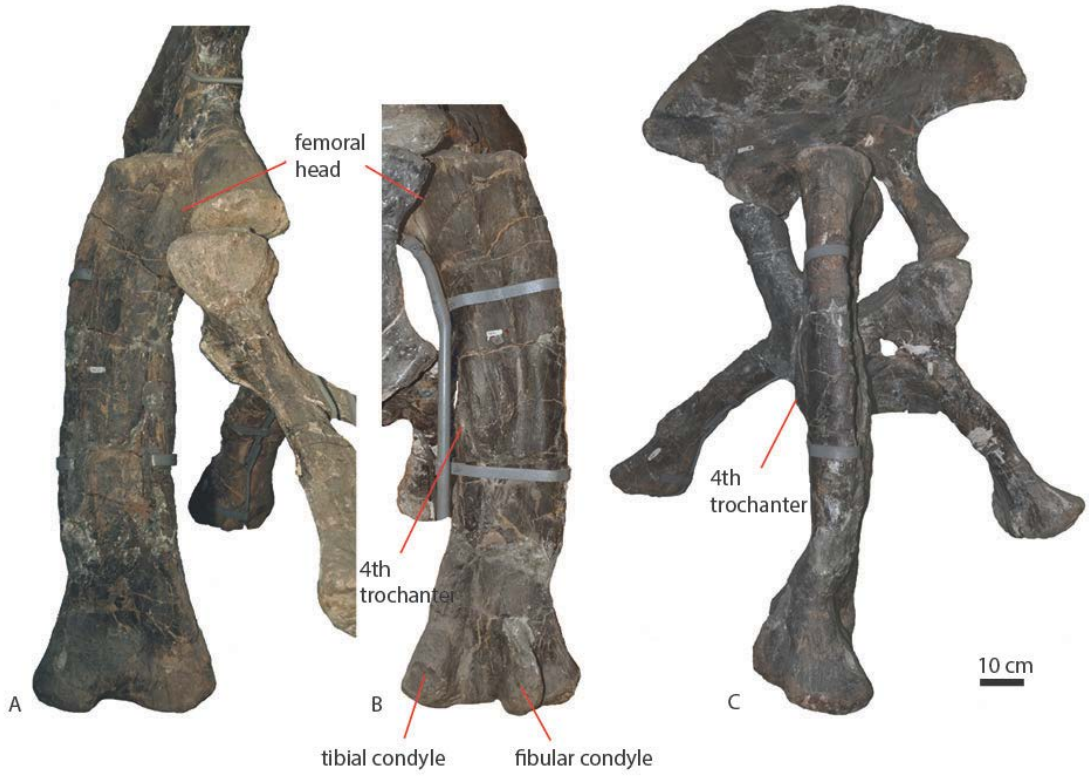

Figure 34: PVL 4170 (37) Femur in (A) posterior, (B) anterior, and (C) lateral view.

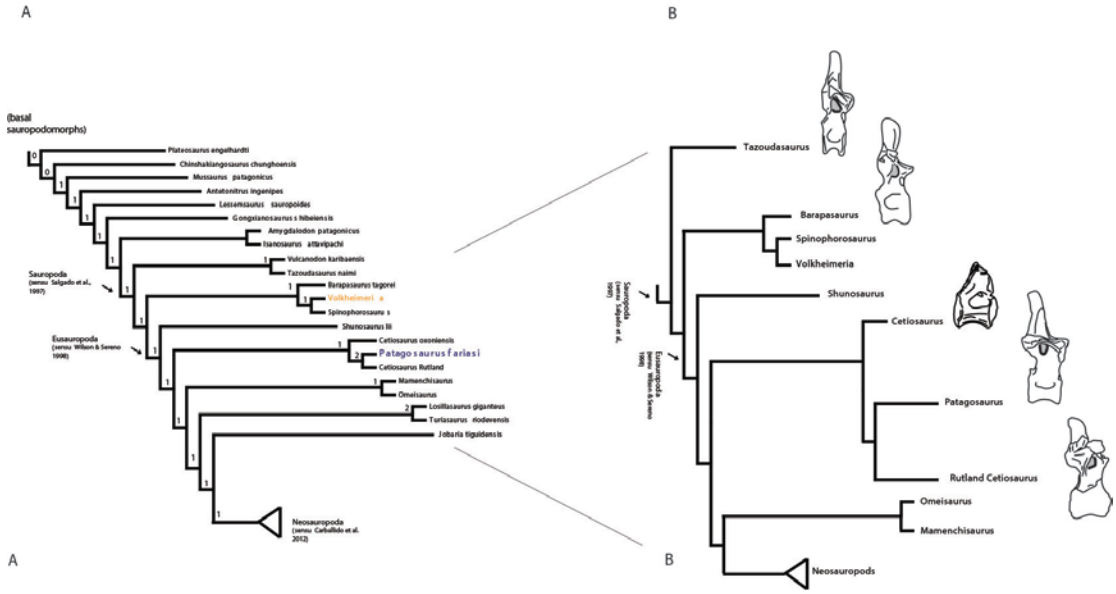

Figure 35: Simplified phylogenetic tree based on Holwerda & Pol, (2018) (A), with posterior dorsal vertebrae of *Tazoudasaurus, Barapasaurus, Cetiosaurus oxoniensis* and the Rutland *Cetiosaurus* showing possible analogous pneumatic features with *Patagosaurus* highlighted in grey (B).

Tables

Table 1: EI and aEI for several sauropod cervicals

Table 2: measurements of all presacral (1-17, blue), sacral (18, red), and caudal (19-30, green) vertebrae.

Table 3: Measurements on appendicular elements of PVL 4170.